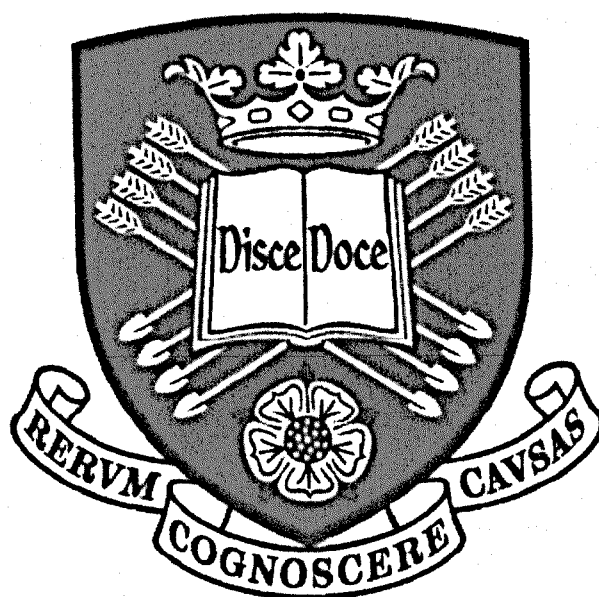# Investigations into the reactivity of thiols and disulfides at membrane interfaces

Alexandre Denis Biojout

Department of Chemistry, University of Sheffield

July 2008

Abstract

The membrane is a key component of cells as it acts as a barrier with the extracellular matrix, preventing alien entities from entering the cell unhindered. It also provides the medium for membrane embedded proteins to bind and react to small molecule messengers and with other cells. The research described in this thesis is focused on the study of the thiol-disulfide reaction at the membrane interfaces in order to understand how this environment affects reactivity and mechanism relative to aqueous solution. This knowledge informs the design of artificial biomimetic systems based on vesicles, which have long been used as the cell membrane model of choice.

Firstly the stability and reactivity of the different thiols and disulfides as well as a water soluble phosphine and potassium ferricyanide were studied in solution. The observed rates for thiol-disulfides exchange reactions in solution were shown to increase with decreasing thiol pK_a. A wide range of reactivity and mechanistic pathways were established.

Thiol-disulfide exchange reactions were then studied at the vesicle interface, with one of the two reactants confined to the vesicle membrane. Conditions were created to study potential intravesicular reaction as well. The membrane interface did not significantly alter the rates of the reactions studied. Studies between embedded molecules suggested that the reaction was not rapid under the conditions used, which is consistent with earlier studies. However, exchange of embedded molecules between interior and exterior surfaces appears to occur which has implications for the utility of these systems.

When reactive components were placed in separate vesicles, rapid changes were observed. These were principally due to electrostatic interactions, generating large aggregates. These aggregates did not appear to be greatly stabilized when covalent connections could also be made.

Declaration

This thesis is a summary of the research work carried out in the Department of Chemistry, University of Sheffield, between March 2003 and February 2007. It is the result of my own work and includes nothing which is the outcome of work done in collaboration. It has not, either in part or as a whole, been submitted for a degree or diploma or other qualification at any other University.

Alexandre Biojout

July 2008

Acknowledgements

Abbreviations

ADP	adenosine diphosphate
ATP	adenosine triphosphate
Boc	*tert*-butyloxycarbonyl
d	doublet
DCC	1, 3-dicyclohexylcarbodiimide
DCM	dichloromethane
DMAP	N,N-dimethyl-4-aminopyridine
DMPC	1,2-dimyristoyl-sn-glycero-3-phosphocholine
DSPC	1,2-distearoyl-sn-glycero-3-phosphocholine
DTT	dithiothreitol
DNA	deoxyribonucleic acid
EDTA	ethylene diamine tetra-acetic acid
Ellman's reagent	5,5-dithiobis(2-nitrobenzoic acid)
ES	electro spray
EYPC	egg yolk phosphatidylcholine
FAB	fast atom bombardment
GDP	guaninediphosphate
GTP	guaninediphosphate
GUV	giant unilamellar vesicle
LG	leaving group
LUV	large unilamellar vesicle
m	multiplet

m	*meta*
MES	2-(*N*-morpholino)ethanesulfonic acid
MS	mass spectrometry
NMR	nuclear magnetic resonance
Nu	nucleophile
o	*ortho*
p	*para*
PPh3	3,3',3''-phosphinidyne-tris(benzenesulfonic acid) trisodium salt
ppm	parts per million
q	quartet
s	singlet
t	triplet
TEM	transmission electron microscopy
TFA	trifluoroacetic acid
TIS	triisopropylsilane
TNB	thionitrobenzoate
Trt	trityl
UV	ultra violet
UV/vis	ultra violet/visible absorption spectroscopy

Table of Contents

Chapter I Introduction

Cells are the principal constituents of all organisms. In order for organisms to function properly the cells need to interact and communicate with each other. This cell-cell communication is a key element for multicellular organisms as it enables cells to effectively interact with each other and the overall organism to work as an discreet entity and not as a collection of cells. In the introduction the different aspects of this mechanism will be analysed. First the cell membrane will be described: its constituents, properties and functions. Following this, we'll talk about the proteins that are part of the membrane and more specifically about the ones that are involved in communication and signalling pathways.

In order to study cells, scientists need a simple model with identical basic properties; vesicle is the system used extensively. The formation, structure of vesicles as well as the various experiments carried out using vesicles will then be described. The main types of experiments will be the signalling systems designed to mimic and study how cells respond to outside stimuli, the use of vesicles in reactions in order to study their influence on the rates and finally cytomimetic studies using vesicles.

I-1 Cell Membrane

I-1-1 Description

The membrane of cells is composed of a bilayer of amphiphilic lipids in which proteins are embedded. One of the main lipid components of the bilayer is phosphatidylcholine that possesses two hydrophobic chains linked to a hydrophilic head by a glycerol molecule. Some other common amphiphilic lipids present in membranes are phosphatidylserine, phosphatidylethanolamine and sphingolipids. The latter differ in

that the alkyl chains are attached with an amide linkage instead of an ester. A proportion of cholesterol of up to 40% [1] of the lipid content is present in the membrane in order to make it more stable and rigid while keeping it fluid. Proteins also are embedded in the membrane in order to modify its properties.
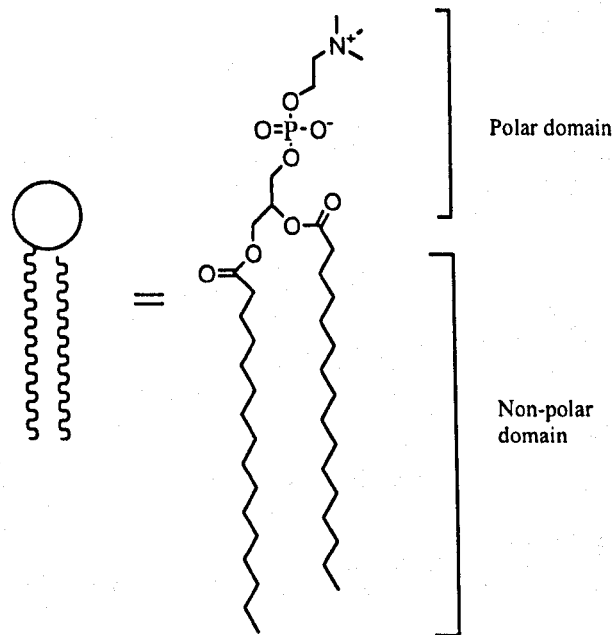
Figure 1. Structure of the main lipid present in natural membranes

Lipids gather in water to form the bilayer that marks the boundary between the cell and the exterior. Their polar domains are in contact internally and externally with water whereas their non polar domains form the hydrophobic interior.
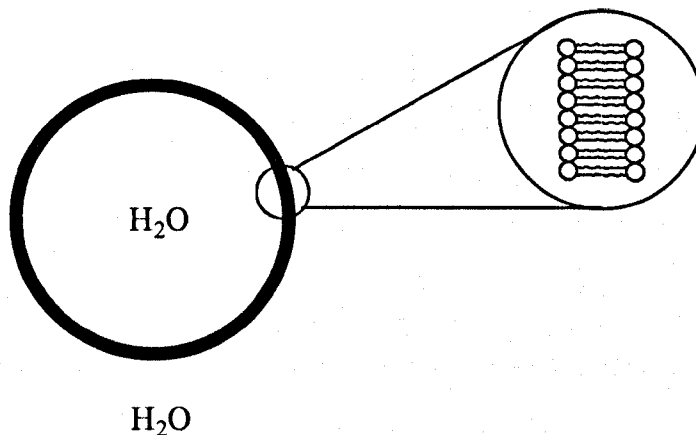
Figure 2. General structure of a vesicle

The widely accepted model for the membrane (proposed in 1972 by Singer and Nicolson [2]) is that of a fluid in which the amphiphilic molecules can move laterally within the membrane and proteins form a fluid mosaic inside the membrane as opposed to previous models where the proteins were believed to stick to the membrane surface. Membranes are highly hydrated, with up to 30 % of the membrane being water [3], and the composition of the dry weight has a ratio of lipid to protein between 4 and 0.5 in animal cells [1]. This composition depends on the function of the cell, with those having only structural functions containing a higher amount of lipids.

I-1-2 Properties

A key feature of the membrane is its fluidity; it enables its constituents to move laterally. The first requirement to obtain a fluid membrane is that the ambient temperature must be higher than the fluid phase transition temperature of the amphiphilic lipids constituting the membrane. Above this transition temperature several other factors affect the fluidity, i.e. the length of the alkyl chains, the degree of unsaturation of those chains and the cholesterol content. The alkyl chains have van der Waals interactions that increase with the number of methylene groups. Hence the longer the chains are, the more it decreases the membrane fluidity. When the alkyl chains contain one or several cis alkenes unsaturations, they possess kinks that decrease the

interactions between adjacent chains and thus increase the membrane fluidity. The cholesterol content in the membrane is the last variable that affects the membrane fluidity. Cholesterol makes hydrogen bonds via its hydroxyl group with the polar head groups of adjacent phosphatidylcholines, resulting in a tighter packing of the non-polar domains of the amphiphilic lipids which decreases the stability of the whole membrane.

Another aspect of the membrane that governs its properties is the movement of a single lipid inside it. Three different movements of lipids exist in the bilayer. The first one is the 'flip-flop' or movement of a lipid from a layer to another. This process is slow: a phospholipid switches layers less than once a week in cells (the process occurs on average every 10^5 s). The two other movements are the rotation of the lipid on its axis and the lateral movement of the lipid in the bilayer. These two processes are very rapid: the rotation occurs every 10^{-9} s and the translation occurs every 10^{-7} s [3].

I-1-3 Functions

The membrane is an essential part of the cell and thus of all living organisms. It maintains the integrity of the cell by keeping all its components together. It also acts as a regulator allowing nutrients to come in and waste to go out of the cell in a controlled manner thanks to its hydrophobic interior that prevents hydrophilic molecules and ions from diffusing into the cell unhindered. It also prevents toxic organisms or substances from pervading the cell. Different types of proteins are embedded in the membrane, regulating the properties described above. The membrane is also responsible for the cell-cell recognition processes that enable different cells to interact with one another. Lastly an essential feature of biological membranes is transmembrane signalling, i.e. the mechanism by which the cell can react to outside stimuli without allowing intracellular penetration.

I-2 Membrane proteins

I-2-1 Transport proteins

Several mechanisms enable molecules or proteins to pervade the cell. The first and simplest one is diffusion through the membrane. However due to its hydrophobicity the membrane prevents ions and most polar molecules from diffusing into the cell. Hydrophobic molecules on the other hand can diffuse in essentially unimpeded. Some proteins embedded in the membrane allow the passage of polar molecules into the cell. The processes by which they fulfil this goal are divided in two: they can be either passive or active. The passive processes do not require the expense of energy. The driving force for those passive processes is the difference in the concentration of the molecule between the inside and the outside of the cell. If the molecule is charged, both the difference in concentration and the membrane potential affect the passive diffusion. Active diffusion, however, requires an energy input in order to work: for example ATP hydrolysis, light, coupled carriage (diffusion of one solute into the membrane as a coupled solute diffuses out) or ion gradient.

Another classification exists for the membrane embedded transport proteins. This differentiates proteins according to their mode of action. The proteins can be divided into carriers or ion channels. Carrier proteins bind the solute and transport it through the membrane by consecutive conformational changes that expose the solute binding site to one side of the membrane and then to the other side. Ion channels on the other hand are proteins with an ion selective pore that is normally closed until a stimulus opens it. The usual stimuli are a change in the voltage across the membrane, external or internal ligand binding or mechanical stress. The actual ion diffusion in ion channels is passive in so far as it is not coupled to an energy source.

I-2-2 Communication, recognition and interaction between cells

I-2-2-1 Communication and interaction mechanisms

Cells need to be able to influence each other in various ways in order for multicellular organisms to function properly. This intercellular interaction can be achieved at different ranges of distances between cells, corresponding to different needs of the organism. The five different types of intercellular signalling are [4]:

- Autocrine signalling: this occurs when cell emits signals for it to respond to. It happens for instance to cells in the development stage who controls their progress and to tumour cells who triggers uncontrolled growth and multiplication via this type of signalling.

- Contact dependent: two cells interact with each other through membrane-membrane contact. This type of interaction is particularly important in the development stage of a multicellular organism and during the immune response.

- Paracrine signalling: these are signal molecules that are released by a cell only to affect cells in its vicinity. The corresponding messengers are usually destroyed by extracellular enzymes or taken up by neighbouring cells in order for them not to diffuse too far away from the emitting cell. This type of signalling is used for example in synapses where neurotransmitters are emitted by neurons or in the immune response.

- Electric signalling: this is performed by neurons transmitting an electrical signal along their axons. It enables information to travel great distance in the body. This type of signalling is linked to the synaptic (paracrine) signalling as it consists of several paracrine signalling in a row along several axons.

- Endocrine signalling: an endocrine cell releases a hormone into the bloodstream in order to affect cells in the entire body.

I-2-2-2 Messengers

Proteins involved in signalling pathways react to stimuli coming from the extracellular medium. Those stimuli or messengers can be of different natures, thus pervading the cell and triggering cell responses in different ways. Hydrophobic messengers such as steroid hormones and certain amines derived from tyrosine (thyroxine for example) can cross the membrane and influence the cell behaviour by activating intracellular proteins. Alternatively hydrophilic messengers such as insulin protein, ADH (antidiuretic hormone) small peptide or hydrophilic amines derived from tyrosine (adrenaline for instance) need to be detected by a membrane embedded protein in order to activate their linked signalling pathway.

I-2-3 Proteins involved in signalling pathways

Two major types of receptor proteins exist in cells, i.e. G-protein-linked receptor and enzyme-linked receptor. They are both transmembrane spanning proteins, possessing a messenger binding site in the extracellular medium. A brief description of the composition, major functions and mode of action of those two types of receptors follows.

I-2-3-1 G-protein-linked receptors

These receptors are found in all eukaryotes and form the largest type of cell-surface receptors. They consist of a receptor and a trimeric GTP binding protein (G-protein) that is associated to it. The receptor is a protein that possesses a messenger binding site protruding outside the cell membrane and a long chain that is folded inside the membrane with exactly six loops (i.e. seven helixes inside the membrane). The G-protein is linked to the receptor protein on one of its inside loops. It is composed of three subunits α, β and γ with α and γ subunits possessing lipid anchors in the membrane. The α subunit binds GDP when the G-protein is not activated. When the

receptor binds the messenger a conformational change induces the release of the α subunit linked GDP that is replaced by a GTP. This then releases the activated α subunit and the activated dimer βγ that can both regulate the activity of intracellular proteins as a consequence.
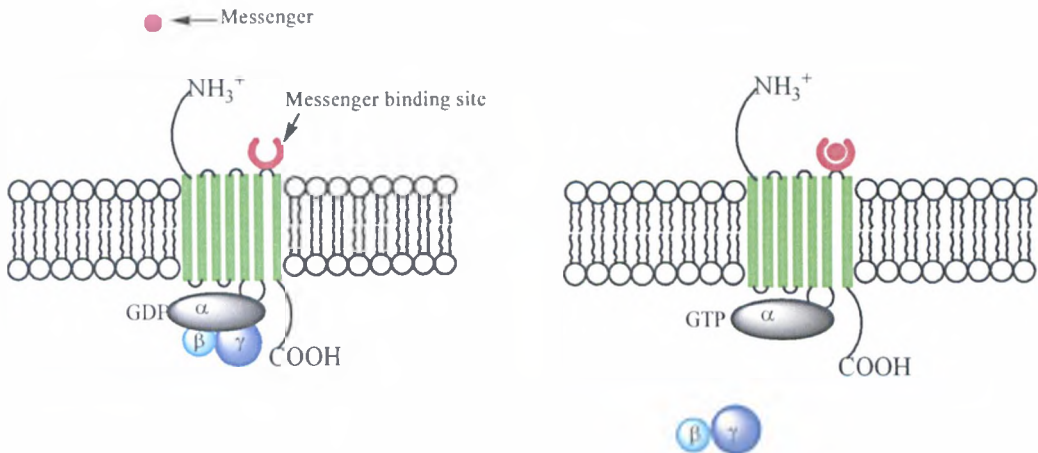
Figure 3. Mechanism of G-protein-linked receptor activation. The trimeric G-protein binds GDP when not activated. Upon extracellular binding of the messenger a conformational change induces the release of the GDP, the binding of a GTP instead and the release of the βγ subunit. The activated α subunit or the βγ dimer can then activate another enzyme or protein.

G-proteins functions are extensive. They are present in every cell and react to a wide range of messengers including neurotransmitters, hormones and local mediators. They are strongly associated with the sense of smell. About half of all known drugs work through G-protein-linked receptors.

I-2-3-2 Enzyme-linked receptors

This type of receptor usually consists of only one transmembrane domain that possesses an intrinsic enzymatic activity or that is directly associated with an enzyme. We will only focus the discussion on the tyrosine kinase associated receptors as they are the most common ones (Figure 4). The mode of action of the other classes of enzyme-linked receptors is similar.
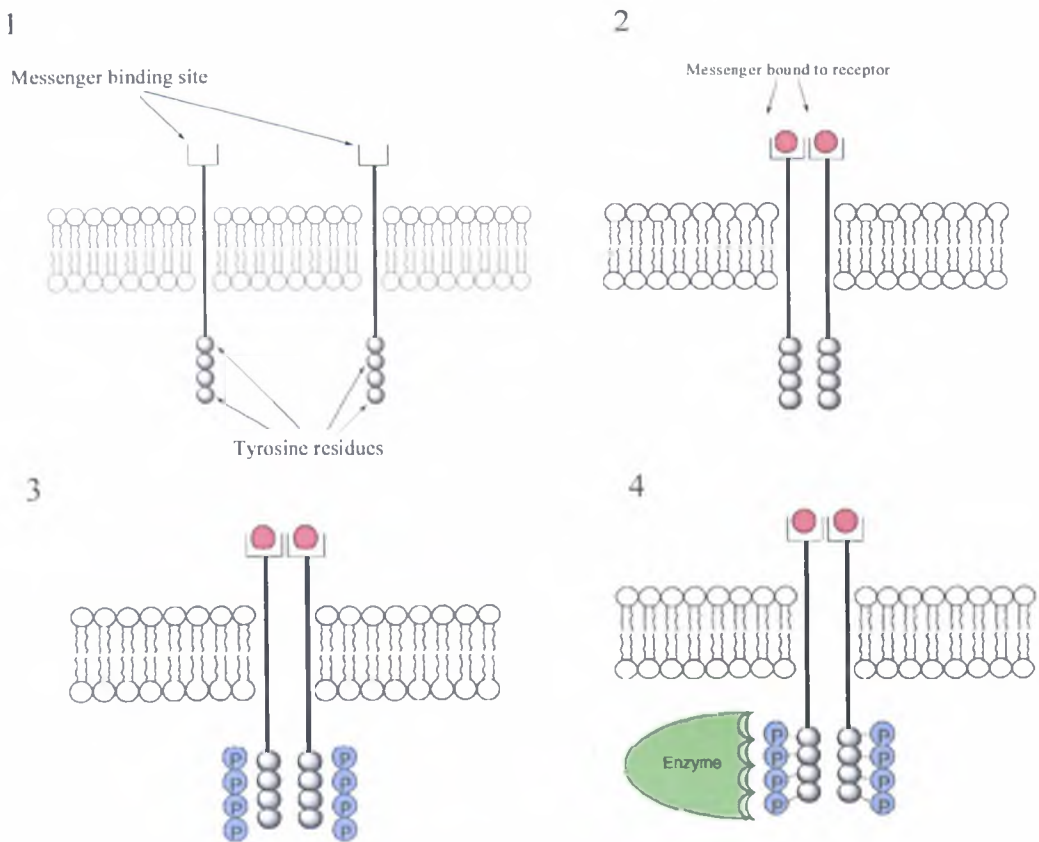
Figure 4. Mechanism of the tyrosine kinase receptor signaling process

Two non-activated tyrosine kinase receptors (1) each bind a messenger and then associate (2). The close proximity thus induced brings the tyrosine residues in the intracellular medium into close contact. This triggers a cross phosphorylation of the tyrosine residues (3), which can subsequently bind a signalling protein or an enzyme (4).

I-3 Vesicles

I-3-1 Formation, structure

The aggregation of lipids is explained by thermodynamic considerations. The two carbon chains of the amphiphilic lipid, when in water, disrupt the water molecules

bulk organisation by forcing them to fit around their hydrophobic parts. This disruption causes a local tighter organisation of the water molecules, i.e. a decrease in entropy. Hence the aggregation of the lipids into vesicles is favourable by allowing water molecules to reorganise into their bulk water network of hydrogen bonds and as a result increasing entropy. Nevertheless, this increase in entropy is opposed by the decrease in entropy that results from the more organised arrangement of molecules in micelles and vesicles. This stems from the decrease in degrees of freedom in their organised state as part of a micelle or vesicle as opposed to their non-aggregated state. The increase or decrease in entropy and therefore the formation of micelles or vesicles depends on the relative strength of both changes in entropy.

In addition to the modification in entropy, the vesicle forming process also decreases the enthalpy of the system. This is due to the formation of van der Waals interactions between the carbon chains of the amphiphiles and the decrease of unfavourable interactions between the carbon chains and water (high interfacial energy) [5].

When put in water above a certain concentration (cmc: critical micellar concentration), synthetic or natural amphiphilic lipids gather to form micelles in order to minimise the unfavourable contact of their hydrophobic domains with water. If the concentration is further increased, above the cvc (critical vesicular concentration), the lipids form a water enclosing bilayer called vesicle or liposome. Not all amphiphiles aggregate in micelles and vesicles; the shape of the aggregate that is favoured depends on the geometry of the amphiphiles. If the amphiphile shape is mostly conical (one carbon chain), micelles are favoured and if the shape is mostly cylindrical (two carbon chains), vesicles are favoured [5].

The vesicle's membrane resembles the cell membrane described earlier. However it is much simpler, as it does not possess bilayer embedded proteins. Depending on the process of formation, lipid composition and temperature, the resulting vesicles can have various sizes and can be either unilamellar (possessing only one bilayer) or multilamellar. Unilamellar vesicles are usually the ones scientists are interested in, as they are the more closely related to cell membranes. The classification

of vesicles is: vesicles 20nm to 50nm in diameter are called small unilamellar vesicles (SUV), vesicles of a few hundreds nanometers in diameter are called large unilamellar vesicles (LUV) and vesicles with a diameter of one to 100 microns are called giant unilamellar vesicles (GUV).

The curvature of SUVs and LUVs is rather high, making them relatively stiff compared with GUVs. Due to their size, which is similar to cells, and the fact that they are readily observable with a simple microscope, GUVs have become popular models for cell membrane studies. However before the development of GUV research, primarily LUVs were used as cell membrane models. Research on vesicles however is not restricted to cell membrane models. The advantages of vesicles for research is that they are stable entities and can withstand chromatography as well as enabling the entrapment of hydrophobic molecules in their bilayer or hydrophilic molecules in the enclosed water pool.

I-3-2 Use

Vesicles have been studied for applications outside of cytomimetic chemistry. However the use of vesicles as microreactors or catalysts has also begun to be studied. In two papers by Tung et al., the use of vesicles as microreactors for the photosensitized oxidation of membrane soluble trans,trans-1,4-diphenyl-1,3-butadiene [6] or α-pinene [7] is described. As regards catalysis, Engberts et al. reported the use of metallo-vesicles formed by a two-tailed phosphate surfactant with a copper(II) counterion as a catalyst for a Diels-Alder reaction in water [8].

Vesicle drug delivery systems on the other hand have been extensively studied; a lot of drugs based on this system have been approved by the FDA for clinical use and clinical trials in recent years [9]. The principle behind these vesicle-formulated drugs is that the actual compound possessing a medical effect is entrapped in a vesicle whose properties are tuned in order for it to release the drug in contact or in the vicinity of the

region to be treated. The properties are tuned by modifying the surface charge, surface hydration, steric effects, fluidity of the bilayer and liposome size.

The following sections are going to develop four cytomimetic aspects of vesicles research, i.e. ion or molecule transport, signalling processes, cytological processes and cell-cell interaction and recognition.

I-3-2-1 Ion or molecule transport

A few different approaches to mimic cell signal transduction by molecule or ion transport through vesicle membranes have been used:
- Synthetic ion channels
- Synthetic molecular transporters
- Synthetic ion carriers

One example of each type of approach will be given in order to exemplify the work in this area.

A lot of work has been carried out to synthesize synthetic ion channels using crown ethers. A nice example of this can be found in the work of Gokel *et al.* [10]. The molecule they designed as the synthetic ion carrier is shown in Figure 5.
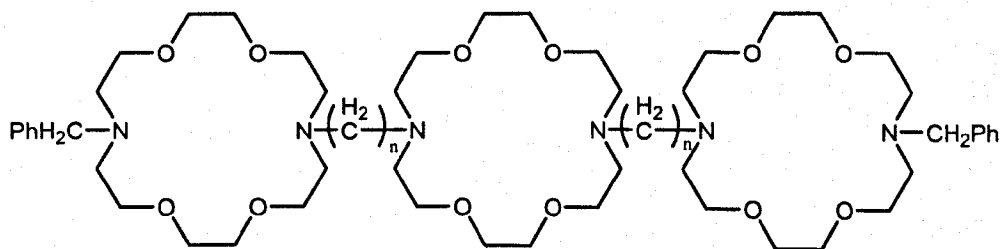
Figure 5. Structure of a synthetic ion channel (n=8, 10, 12, 14 and 16)

The rates with which the molecules with different spacer lengths transport Na^+ ions through the membrane were assessed as well as their antibiotic activity against *Escherichia coli*. It was shown that the molecule with n=12 was the most efficient as an ion transporter and had the highest antibacterial activity. The synthetic ion channel enables ions to diffuse out of the bacteria thus breaking the osmotic equilibrium of the cell and causing its death. However when the central crown ether was not present, the molecule lost its antibacterial activity. This showed that the central crown ether works as a relay between the two others for the ion transport.

Regen *et al.* have used an interesting approach towards molecule transport through membranes [11]. Molecules called 'molecular umbrellas' have been synthesized in order to transport hydrophilic molecules through the hydrophobic vesicle bilayer. The idea is to attach the molecule to be transported through the membrane to several arms (2 to 4) that can adopt two different positions called 'shielded' and 'fully exposed' (Figure 6). The arms are made of sterols that possess both a hydrophobic and a hydrophilic side. The 'shielded' position corresponds to the conformation adopted in hydrophobic medium. The water soluble agent is interacting with the hydrophilic part of the sterols moieties and the hydrophobic parts interact with the hydrophobic medium. Conversely the 'fully exposed' position corresponds to the conformation in hydrophilic medium, i.e. with hydrophilic parts of the sterols exposed to the medium and hydrophobic parts interacting together leaving the hydrophilic agent exposed to the medium (Figure 7).
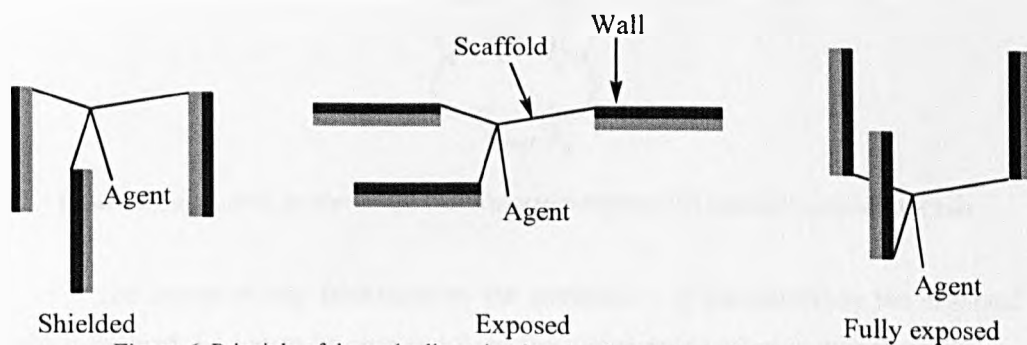
Figure 6. Principle of the umbrella assisted molecular transport through membranes
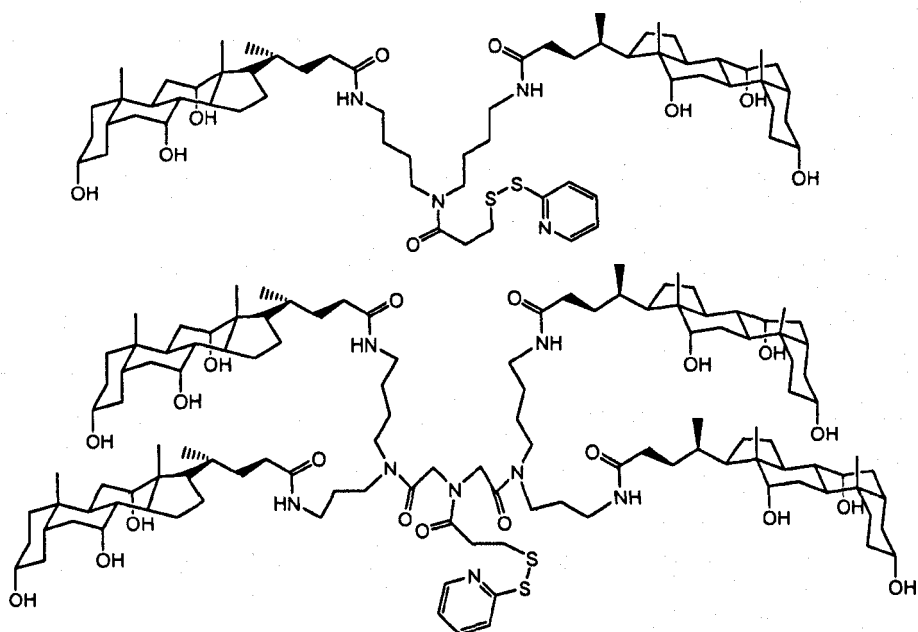
Figure 7. Structures of the molecular umbrellas used by Regen *et al.*

The last example of signal transduction is the use of synthetic ion carriers in order to facilitate ion permeation through vesicle membranes. Lehn *et al.* described the use of molecules called cryptands (Figure 8) in order to enhance ion transport through a membrane [12].
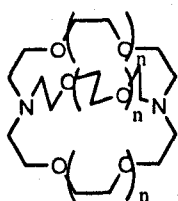
Figure 8. Structure of the crown-ethers used as transmembrane ion transport molecules (n=1,2)

The transport was facilitated by the entrapment of the ion inside the cryptand which enabled the ion to be shielded from the hydrophobic interior of the membrane. By adjusting n the ion selectivity could be tuned. A 20:1 selectivity for Na^+ ions over K^+ ions was obtained with n=1, when n=2 the selectivity was 2:1 for K^+ over Na^+.

I-3-2-2 Signalling processes

The main approaches towards membrane signalling mimic have been the use of fluorescent lipids, conjugated lipid polymer vesicles or carotenoids. The monomer and excimer of lipid linked fluorescent moieties possess different fluorescence emissions. Arnold *et al.* have published several papers making use of this fact to mimic membrane signalling [13, 14]. Lipids containing a metal-chelating part and a fluorescent moiety have been synthesized. When they are put in a vesicle membrane, they dimerize, and the excimer emission of the fluorescent moiety can be observed. Upon addition of metal the dimer is disrupted, and the monomer emission replaces the excimer one. When a two-histidine-tagged protein or molecule is added to the solution it binds two metal-chelated fluorescent lipids, giving back the excimer emission (Figure 9).
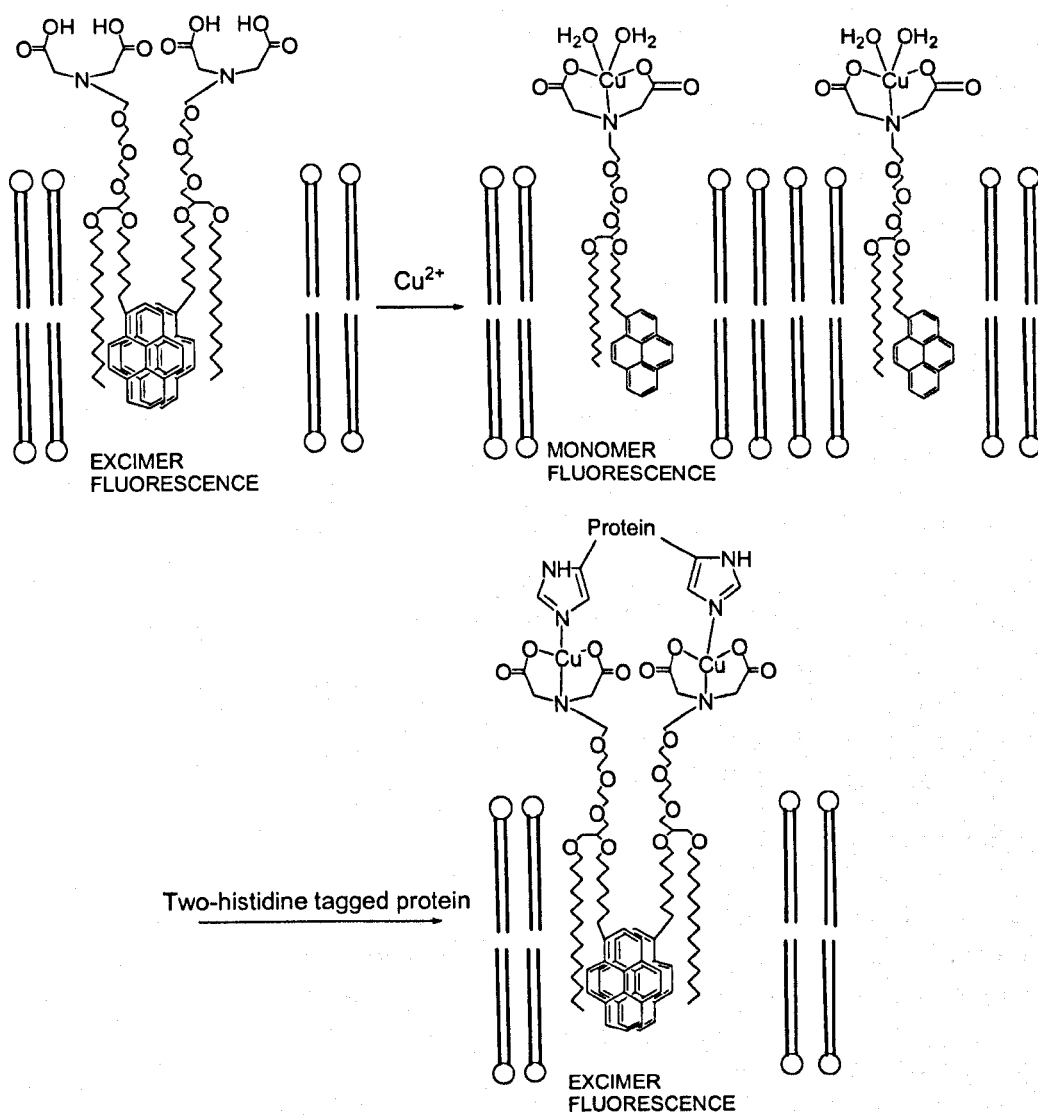
Figure 9. Scheme of the signaling process designed by Arnold et al. using lipids bearing a metal-chelating part and a fluorescent moiety, pyrene that possesses both monomer and excimer fluorescences. When put in a lipid bilayer they dimerize, giving an excimer emission; upon addition of copper ions, the dimers are disrupted, which gives a momomer emission. Finally when two-hystidine tagged proteins are added to the solution, dimers are reformed, giving back the excimer emission.

A similar approach has been used by Song *et al.* with a pentasaccharide (ganglioside GM1) as the receptor anchored on a fluorescein bearing lipid and cholera toxin as the messenger [15]. The high affinity of cholera toxin for GM1 makes it one of the most extensively studied bacteria toxin oligosaccharide recognition pairs. Similarly

16

Sasaki *et al.* synthesized a fluorescent lipid that possessed a crown ether as the recognition site [16]. When put in a vesicle membrane, the lipids aggregate, and the excimer emission is observed. When metal ions are added to the vesicle solution, the aggregates are disrupted by crown ether metal binding, and the monomer emission replaces the excimer one (Figure 10). Removal of the ions by EDTA gave the excimer emission back.
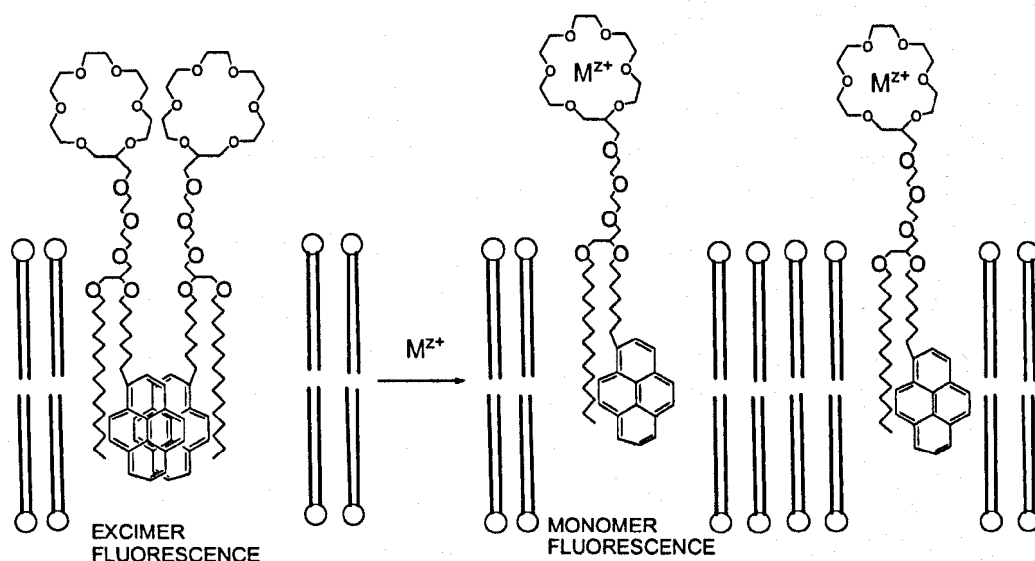
Figure 10. Scheme of the experiment designed by Sasaki *et al.* using lipids bearing a crown-ether and a fluorescent moiety. When put in a lipid bilayer they dimerize, giving an excimer emission, upon addition of metal M^{z+} (Cadmium (II), lead (II), mercury (II) or strontium (II)), the dimers are disrupted, which gives a momomer emission.

Several papers [17-19] reported the use of conjugated lipid polymers (poly(diacetylene)) (Figure 11). The colour of this type of polymer depends on the conformation of the conjugated (ene-yne) backbone.
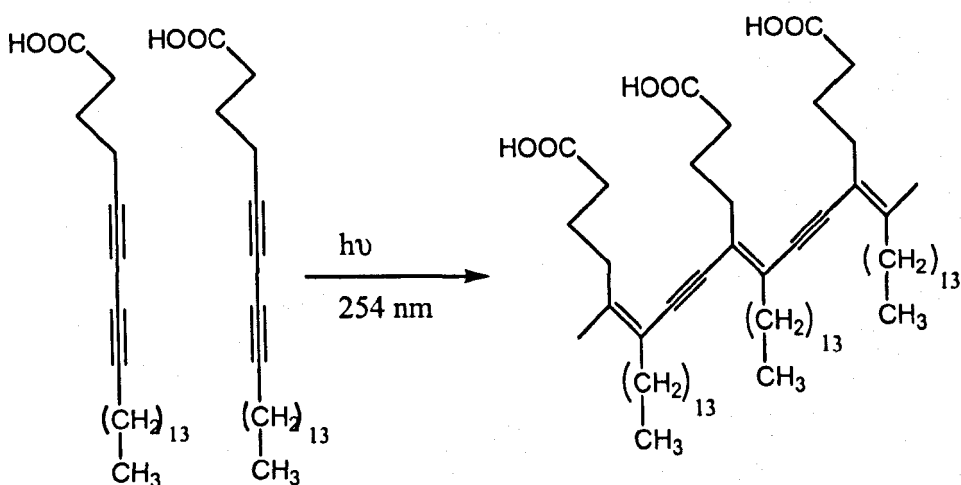
Figure 11. Structures of the polymerizable lipids and the resulting oligomer

When a lipid equipped with a recognition site is inserted into vesicles formed with this polymer, a certain colour is observed. Upon addition of the substance recognized by the binding site, a conformational change occurs in the polymer and a colour shift is triggered. The different recognition pairs that cause the colour shift described in the literature are:

- GM1 linked lipid and cholera toxin
- phospholipid and phospholipase
- ionophore and metal ion.

Another approach is the one published by Lehn *et al.* [20], in which a carotene derivative was used as vesicle membrane spanning electron wire. The efficiency of this system was checked using vesicle entrapped reduction of ferricyanide by dithionite. This reaction was enhanced by a factor of 8 times when the carotenoid was inserted in the vesicle membrane (Figure 12).

Intravesicular medium: Ferricyanide

Figure 12. Use of a molecular wire to enhance the reduction rate of vesicle entrapped ferricyanide by dithionite

As has been shown, systems that mimic membrane signalling have been studied, but a new development would be to design a system that mimics transmembrane signalling, i.e. a system that would react to an extravesicular messenger and trigger the release of an intravesicular response without a physical transport of the messenger across the membrane. Barton *et al.* have reported such as system [21]. Two types of membrane spanning molecules bearing complementary reactive chemical groups were inserted in vesicles. Upon successive addition of a reductant and an oxidant, a signal was released on the inside of the vesicle as a response to the message (reductant and oxidant additions). The molecules used and the scheme are shown in Figures 13 and 14.
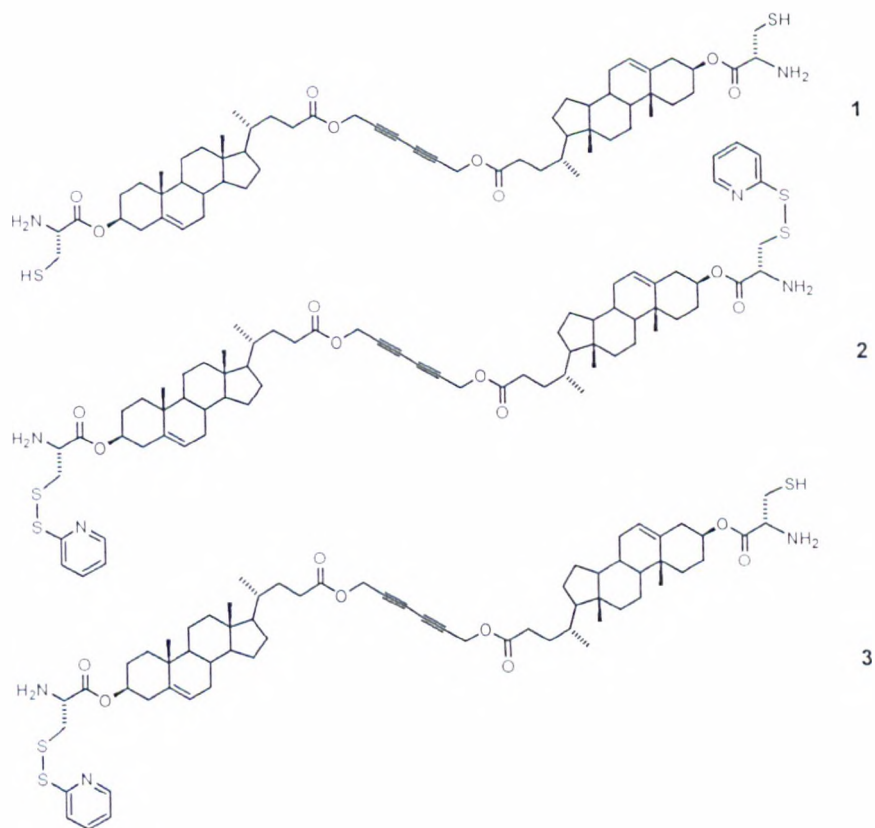
Figure 13. Membrane spanning molecules
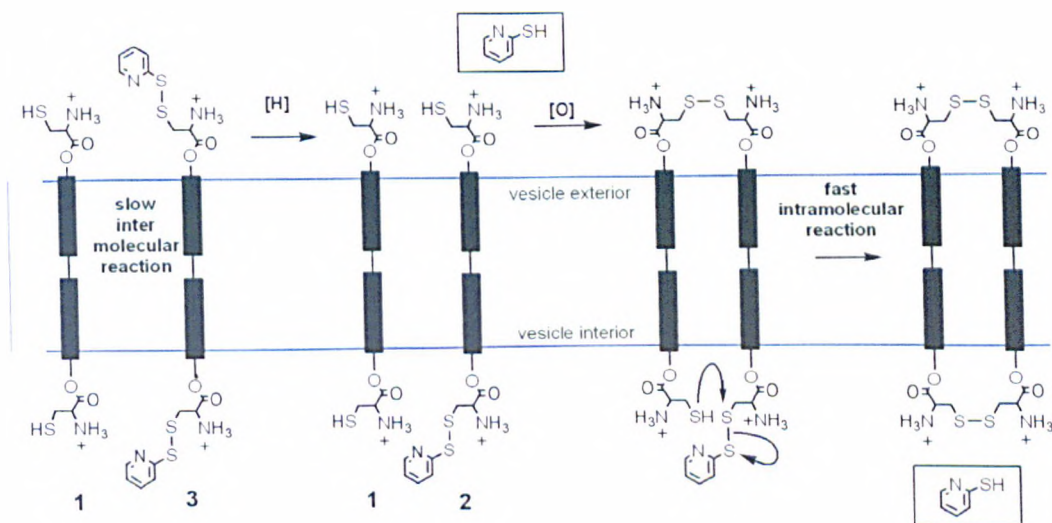
Figure 14. Principle of the transmembrane signalling system : [H] is the reductant (3,3',3''-phosphinidyne-tris(benzenesulfonic acid) trisodium salt) and [O] the oxidant (potassium ferrocyanide)

I-3-2-3 Reactions in vesicles

The following is a summary of the research carried out on how vesicular media influence the behaviour of chemical reactions.
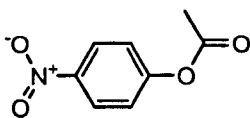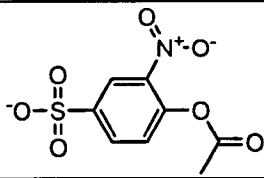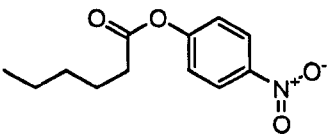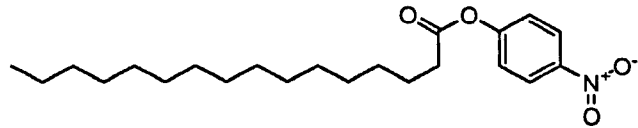
Bizzigotti [22] looked at the reaction of a thiol-functionalised lipid ($(nC_{16}H_{33})_2(CH_3)N^+(CH_2CH_2SH)$, Cl^-), embedded in dipalmityl dimethyl amino chloride vesicles, with Ellman's reagent (5,5'-dithio-bis(2-nitrobenzoic acid)). The reaction rates obtained were compared with thiol-disulfide reactions in solution. The usual mechanism for this reaction is the following:

$$R-S^- + R'-SS-R' \xrightarrow{k_1} R-SS-R' + R'-S^-$$

$$R-SS-R' + R-S^- \xrightarrow{k_2} R-SS-R + R'-S^-$$
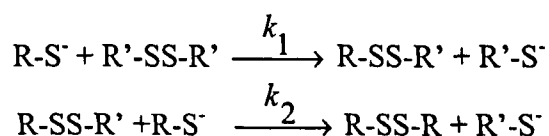
In this study R'-SS-R' is Ellman's reagent and R-SH is the thiol-functionalised lipid. The results found by Bizzigotti are that k_2, which represents the intravesicular thiol disulfide exchange, is 10 times slower than the slowest thiol-disulfide reaction measured in solution (with 2-thioacetic acid).

Moss et al.[23] also investigated the esterolytic activity of vesicles composed solely of the same thiol-functionalised lipid as used by Bizzigotti. The different substrates used and their pseudo first order rate constant (k_ψ^{max}) are shown in the table below (Table 1).

Table 1. Pseudo first order rates for the cleavage of the different esters in the presence of vesicles composed uniquely of thiol-functionalised lipid

Substrate	k_ψ^{max} (s^{-1})
(4-nitrophenyl acetate structure)	4.9
(2-nitro-4-sulfonatophenyl acetate structure)	7.3
(4-nitrophenyl hexanoate structure)	13.4
(4-nitrophenyl long-chain ester structure)	21.7

The small differences in reactivity between the esters are attributed to their different hydrophobicity, hence to a difference in binding with the reactive vesicles.

Moss *et al.*[24] carried out research to study the reactivity of thiols of different hydrophobicity with Ellman's reagent in pH 8 buffer, cetyltrimethylammonium bromide micelles or dioctadecyldimethylammonium chloride vesicles containing solutions. The ratio of pseudo-first order rate constants obtained in the presence of micelles in pH 8 buffer over the one measured in pH 8 buffer is between 400 and 4000 for the thiols studied, i.e. DL-cysteine, glutathione, thiophenol and 2-thionaphthol. This acceleration can be explained by the fact that the rate constants are calculated taking into account the bulk concentration whereas the microscopic concentrations are higher in the micelles due to the interactions between micelles and reagents. Among structurally similar

reagents, the more hydrophobic ones show a higher acceleration due their stronger interaction with micelles, hence their higher microscopic local concentration.

García-Río et al.[25] studied the transfer of nitroso group from N-methyl-N-nitroso-p-toluenesulfonamide to a range of secondary amines that possessed different hydrophibicity and basicity in three different colloidal aggregates: dodecyltrimethylammonium bromide micelles, didodecyldimethylammonium chloride vesicles and microemulsions of sodium bis(2-ethylhexyl)sulfosuccinate/isooctane/water. The amines were always in large excess compared to the N-methyl-N-nitroso-p-toluenesulfonamide, hence the study was under pseudo-first order conditions. The results indicate that the reactivity depends on the hydrophobicity of the interface between water and the colloidal aggregate. By applying a pseudo phase model, i.e. the colloidal aggregate is considered a different and separate phase than water, they found that the more hydrophobic the amine, the more reactive it is to nitrosation. The different aggregates are classified by their interface with water hydrophobicity: micelles < microemulsions < vesicles.

Fendler et al.[26] studied the base-catalysed hydrolysis of Ellman's reagent in water, micellar (hexadecyltrimethylammonium bromide) and vesicular (dioctadecyldimethylammonium chloride) media. The presence of micelles or vesicles respectively increased the rate of reaction by a factor of 15 and 1500 as compared to the reaction in water. In this study as well, the increases in rates due to the presence of lipids aggregates are attributed to the increased local concentrations of reactants in the colloidal pseudo-phases, i.e. micelles and vesicles.

Cuccovia et al.[27] studied the alkaline hydrolysis of the two drugs indomethacin and acemetacin shown below (Figure 15) in the presence of zwitterionic hexadecylphosphocholine micelles and zwitterionic phosphatidylcholine vesicles. The rate of hydrolysis was also measured in the presence of cationic micelles or vesicles.
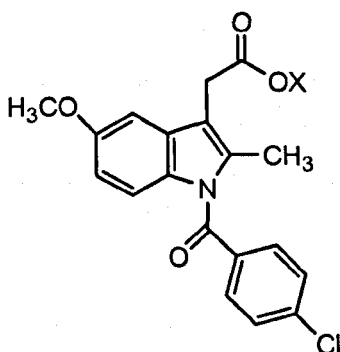
X= H, indomethacin
X=CH₂CH₂OH, acemetacin

Figure 15. Structure of the molecules studied by Cuccovia *et al.*

It was found that zwitterionic micelles and vesicles slowed the rate of reaction compared with the same reaction carried out in water. On the other hand cationic ones increased the rate, which was explained by the pseudo-phase model and ionic exchange of the lipid counterion (i.e. bromide or chloride) with hydroxide. By varying the ratio of zwitterionic and cationic lipids and choosing judicious pH and ionic strength the rate of reaction could be tuned.

Cuccovia *et al.*[28] also investigated the ester thiolysis of p-nitrophenyl octanoate by n-heptyl mercaptan in presence of cationic vesicles. It was found that at pH 4 the reaction was accelerated by a factor higher than 10^6 in presence of vesicles made of dioctadecyldimethylammonium chloride. This remarkable enhancement in reactivity is attributed to the higher local concentration of reagents in the dimensionally restricted lipid bilayer and to the modified dissociation and reactivity of the reagents in this environment. A parallel is drawn with the enzyme kinetics and attention is brought on the importance of entropic factors in both vesicle mediated and enzyme catalysis.

Cuccovia *et al.*[29] also studied the influence of the vesicle size on the alkaline hydrolysis and thiolysis (using heptyl mercaptan) of p-nitrophenyl octanoate. They showed that small vesicles (radius ranging from 11 to 10 nm) were 2 to 5 times more

effective as catalysts than larger vesicles (ca. 140 nm). Analysis of the kinetics results indicate that this effect is due to differences in ion dissociation, intrinsic reactivities and substrate binding constants, the latter having been measured by fluorescence quenching methods. The smaller the vesicles, the higher the binding constant was for heptyl mercaptan. ·

Kunitake *et al.*[30] in an early study on reactions in vesicles investigated the difference between intra- and intervesicular catalytic hydrolysis of phenyl esters. The two substrates and the catalysts are shown below (Figure 16).
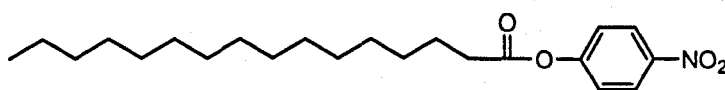
p-nitrophenyl palmitate (PNPP)
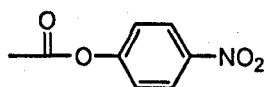
p-nitrophenyl acetate (PNPA)
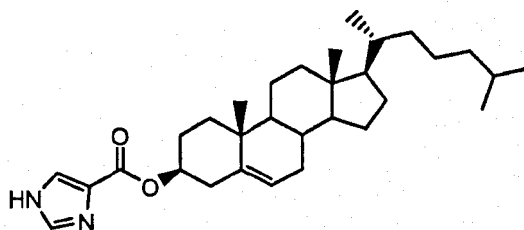
catalyst

Figure 16. Molecules used in the studies by Kunitake *et al.*

The vesicles used for the studies are made with dodecyldimethylammonium bromide. When the catalyst and PNPP were embedded in different set of vesicles (intervesicular reaction), the reaction was slower than when both the catalyst and PNPP were in the same vesicle (intravesicular reaction). However, the intervesicular and intravesicular reactions of PNPA have a similar rate, around 15 times faster than the intervesicular reaction of PNPP. This is explained by the localisation of both the reagent

and PNPP almost entirely in the vesicles bilayers and not in solution like PNPA. The localisation restricts their mobility in three dimensions but when both molecules are embedded in the same vesicle, they "find" each other more easily, hence the higher rate. In summary the rates are as follows: PNPP intravesicular > PNPA > PNPP intervesicular.

Menger *et al.* studied the recognition of two vesicles through chemical reaction [31]. One vesicle contained cholesterols attached to an electrophilic chemical group and the other one lipids attached to a nucleophilic group (Figure 17).
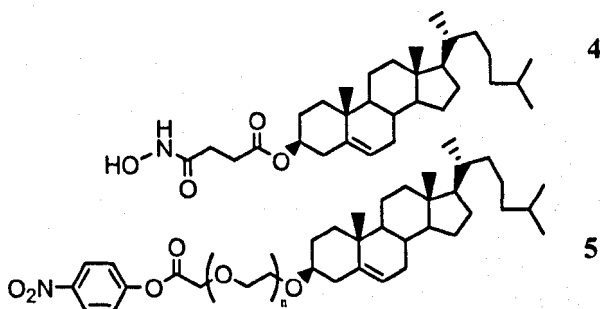
Figure 17. Molecules used in the recognition studies by Menger *et al.* [31] (n=1,2,3)

The kinetics of the reaction between the nucleophile bearing vesicle and electrophile bearing vesicle have been determined and compared to different reactions using acetohydroxamate and p-nitrophenolacetate as the water soluble equivalents of 4 and 5 respectively. The rate of reaction decreases in the order: intravesicular, solution/solution, solution/vesicle and intervesicular.

From all those studies opposite conclusions have been reached as regards the influence of colloidal pseudo-phases (micelles and vesicles) over the rate of reactions. The vesicles and micelles are in certain studies reported to increase the rate of reactions whereas in other studies they are reported to decrease the rate of reactions. A key distinction needs to be made between the actual rate of reaction and the observed rate of reaction. The difference in rate constants reported due to the presence of micelles or vesicles range from several units to several thousands. Several factors play a part in

determining whether the presence of micelles or vesicles will increase or decrease the rate of a reaction compared to its equivalent in solution. Those factors are the lipids forming the colloids, the reactive lipids, the structural and chemical relationships between the non-reactive lipids and the reactive lipids, the ionic strength of the solution, the pH of the reaction, local pH effects at the vesicle interface with the bulk medium. The effects of those different factors have been studied in the publications mentioned above. Even though a full understanding of the effect of all those factors has not yet been gained, increased microscopic concentrations is the main explanation for the increase in observed rate in the presence of micelles and vesicles.

I-3-2-4 Cytological processes

In several papers [32-37], Menger *et al.* have reported the study of cytological processes such as budding, growth, fusion, endocytosis, fission, birthing, foraging, wounding and healing with the use of giant vesicles which enabled them to directly observe the processes. With the use of biological instruments such as micropipette, phase contrast and dark field microscopy and chemicals they managed to artificially reproduce the transformations that cells usually undergo. They induced the aggregation of positively charged giant vesicles using sulphate ions [35]. The attraction between vesicles is explained by the electrostatic neutralization of the repulsion between negatively charged giant vesicles that takes place thanks to the sulphate ions. They reported the fusion of positively charged vesicles induced by acetate provided the temperature was above the lipid phase transition temperature [35]. Fusion of positively charged giant vesicles was also induced when a dipicolinic acid (DPA) solution was added to giant vesicles. They achieved endocytosis-like processes when giant vesicles were put in contact with a DPA solution [38]. The fission of giant vesicles was obtained through mechanical agitation and dilution [37]. The birthing of a smaller vesicle entrapped in the water pool of a bigger one through the addition of octyl glucoside solution to the giant vesicle vicinity was observed [39]. The addition of a relatively high concentration sodium cholate solution to a giant vesicle solution triggered the rapid fusion process of the giant vesicles leading to a massive one which then disappeared in

a process called foraging [39]. The last cytomimetic process studied is the wounding and healing capacity of giant vesicles [32]. The addition of a low concentration solution of sodium cholate gave birth to holes in the giant vesicles that healed automatically after a few seconds.
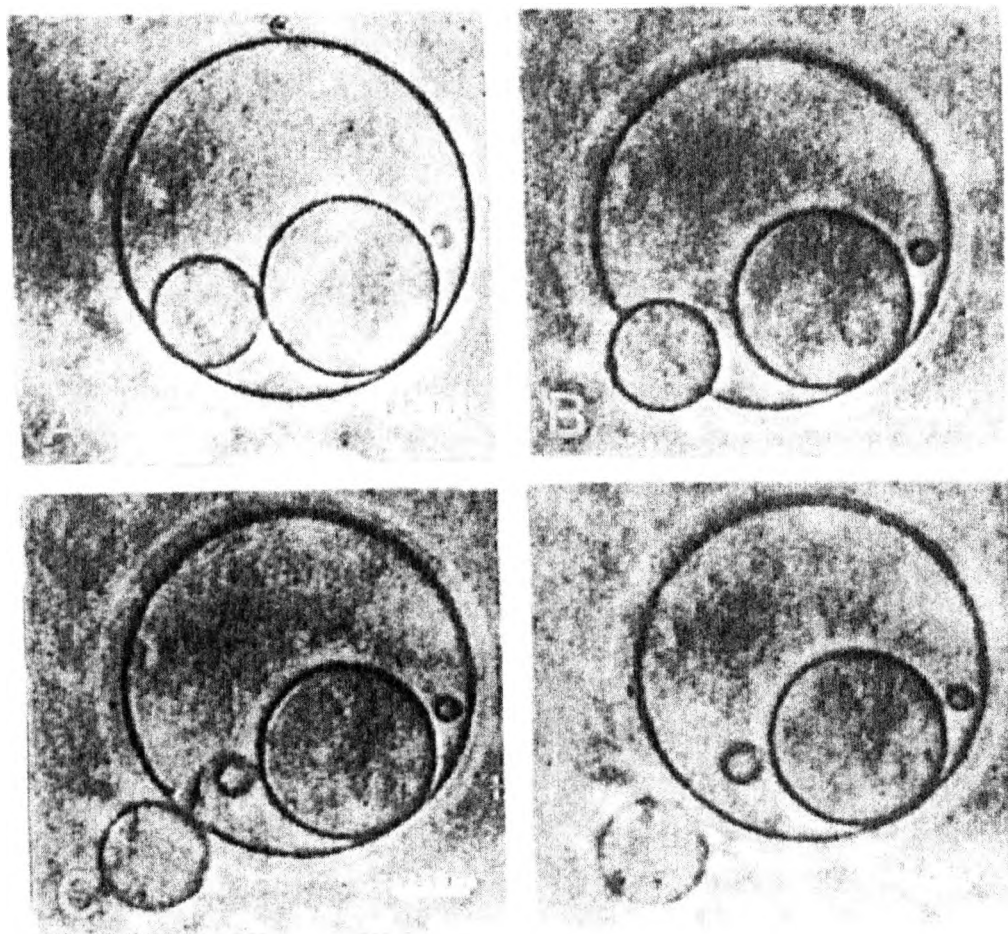
Figure 18. Example of a cytomimetic process induced by octyl glucoside on giant vesicles: "birthing" i.e. the release of a vesicle entrapped in a bigger one [34]

Vesicles have been studied as biochemical compartments in an attempt to get a better understanding of the origin of life. The reactions that were carried out inside the vesicles were the polymerase chain reaction (PCR) [40], mRNA synthesis [41], protein

expression [42] and synthesis of functional proteins [43], all of which correspond to processes happening within cells.

I-3-2-5 Cell-cell recognition and interaction

Mimicking the cell-cell interaction requires vesicles to be brought into close contact by way of membrane embedded chemicals that recognize each other. A few systems have been reported.

Lehn *et al.* have achieved vesicle recognition by inserting lipids bearing complementary hydrogen bonding head-groups in two different sets of vesicles [44, 45]. After mixing of the two sets of vesicles, observation with freeze-fracture electron micrographs and dynamic light scattering showed the presence of approximately ten times larger entities. Those entities were cluster of vesicles and even big vesicles resulting from the fusion of smaller ones brought into contact by the recognition process.

TAP lipid (TAP: 2,4,6 triaminopyrimidine)

BAR lipid (BAR: barbituric acid)
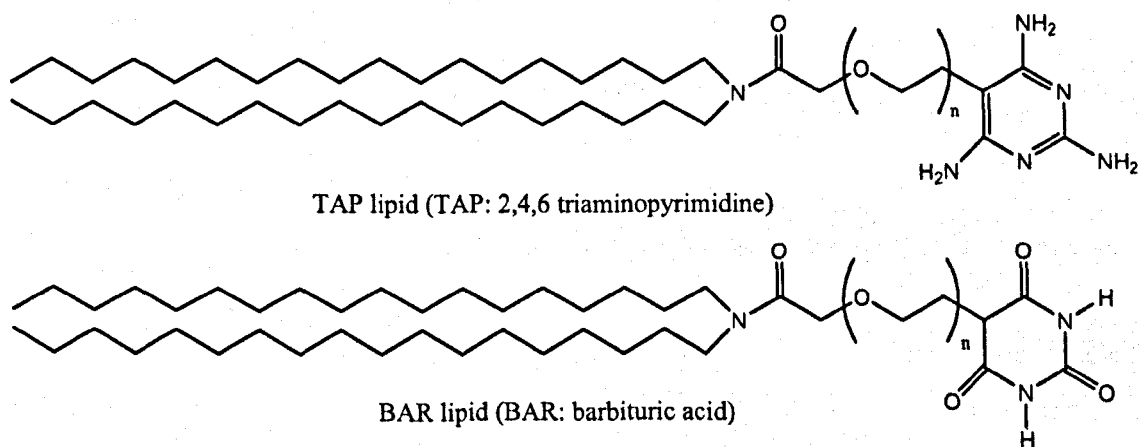
Figure 19. Lipids used by Lehn *et al.* [44, 45] in their recognition studies (n=4)

Chiruvolu *et al.* have used biotin and streptavidin in the design of their system. Their mutual strong affinity is known and has been studied extensively. The binding constant is of the order of 10^{15} M^{-1} [46]. Streptavidin linked lipids were inserted in

vesicles and upon addition of biotin to the solution, liposome aggregation was observed followed by precipitation.

A similar approach towards vesicle-vesicle recognition has been used by Sideratou et al. [47]. Two sets of vesicles were prepared, each one containing one of two lipids bearing complementary hydrogen bonding head groups (Figure 20). Upon mixing, turbidity measurements, phase-contrast microscopy and AFM images showed the aggregation of vesicles. A study of the effect of vesicle cholesterol content on molecular recognition was carried out showing that at a certain cholesterol concentration, recognition is enhanced.

1-(4-(Dihexadecylcarbamoyl)butyl)guanidinium p-toluene sulfonate

Dihexadecylphosphate
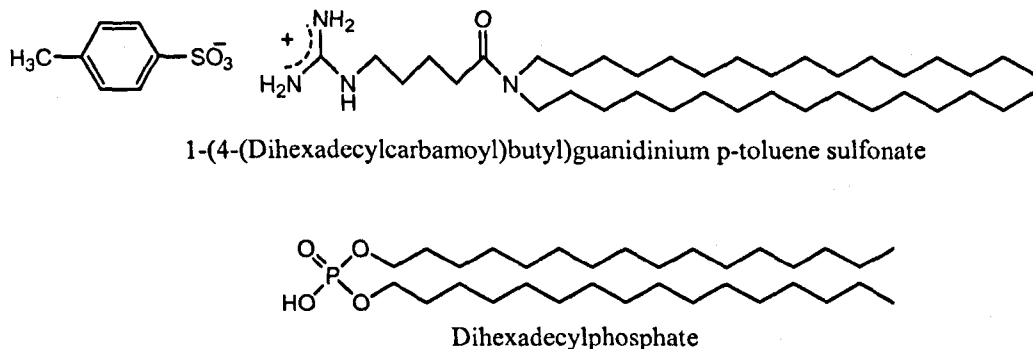
Figure 20. Molecules used by Sideratou et al. [47]

Constable et al. used metals in order to design a system with reversible aggregation [48]. A 2,2':6',2"-terpyridine (terpy) motif was attached to a phospholipid and then inserted in vesicles (Figure 21). When iron(II) ions were added to the vesicle solution, freeze fracture electron micrographs and dynamic light scattering measurements indicated that clusters of vesicles were formed through complexation of iron(II) by terpy motifs belonging to different vesicles. Those clusters could be disrupted by addition of a solution of $Na_2(H_2EDTA)$. The EDTA having a stronger affinity for iron(II) than the terpy motif, the driving force for aggregation was removed.
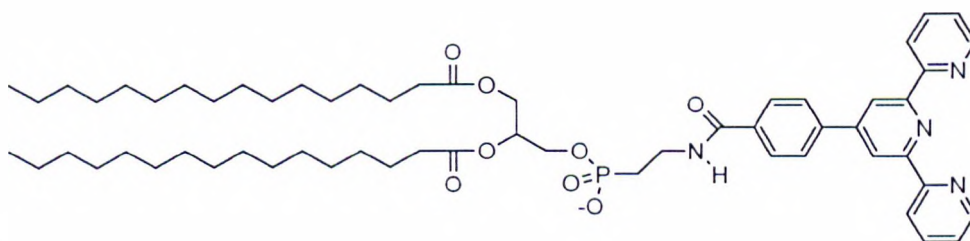
Figure 21. Molecule used by Constable *et al.* as the vesicle embedded lipid bearing inducing aggregation upon addition of iron(II) ions [18]

The last approach, developed by Lehn *et al.* [49] and Menger *et al.*, [50] is the electrostatic interactions that exist between oppositely charged vesicles. Both studies found that vesicles are brought into contact due to electrostatic interactions, followed by lipid exchange between the oppositely charged vesicles leading to a charge neutralisation and consequently to the breaking of the interaction without fusion of the enclosed pools. Lehn *et al.* moreover studied the effect of vesicle size on such interactions. Giant vesicles lead to aggregates that could be observed for several minutes, whereas LUV did not lead to such observable clusters. Menger *et al.* showed that a positively charged vesicle could adhere to a negatively charged vesicle already in contact with a positively charged one, if the two points of contact were far apart, showing that the lipid exchange was confined to the area of contact (Figure 22).
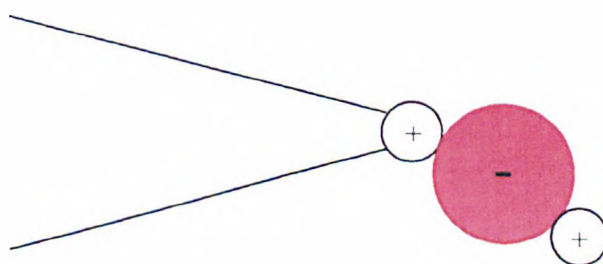
Figure 22. Scheme of the experiment with charged vesicles designed by Menger *et al.* A positively charged vesicle is held in place by suction. A negatively charged one comes into contact due to the electrostatic forces in play, and lipid exchange takes place between the first two vesicles. Another positively charged vesicle can adhere to the negatively charged one at a different point on its surface, which shows that the lipid exchange is confined to the area of contact.

Overall, we have seen the different uses of vesicles as reaction media and cell mimics for the study of transport across the membrane, signaling and cell-cell interaction. However it is clear that further research is still required to better understand the mechanisms at play when those processes are involved. This study is a small step towards this goal.

Chapter II Aims/Design

The system designed by Barton *et al.*[21] for the mimic of transmembrane signaling is the basis for the research carried out in this thesis. The main idea is to identify if this system can be used as a tool for intervesicular studies, i.e. to study the reaction between vesicles that possess complementary molecules. However instead of membrane spanning molecules similar to the ones used in the transmembrane signaling experiment, half spanning molecules (with only one cholesterol unit) will be used.

The system had not been fully characterized and in order to use it for the purpose of our research a better understanding is required. We will try and gain a better understanding using membrane anchored molecules bearing a single cholesterol unit.

The reaction rate between the embedded thiol and the embedded disulfides is a key factor in this system as this limits its potential. Depending on the speed of the reaction, the system might be tailored by varying the reactants concentrations in the vesicles.

Several species may interact in the conditions used for the experiment: the released signal molecule (pyridinethiol), the embedded thiol and the water soluble phosphine. Their interactions in the conditions used for the system need to be determined (see Figure 14 above).

The last potential interaction to be studied is between vesicles containing complementary functions, i.e. thiols and disulfides being embedded in different vesicles, therefore enabling a thiol-disulfide exchange reaction intervesicularly.

Hence, to arrive at a complete understanding of the system the following studies need to be carried out:

We need to fully characterize all the possible solution reactions between each reductant and each oxidant involved in this system.

We need to fully characterize all the possible reactions that can occur at the vesicle interface between each reductant and each oxidant involved in this system.

Finally we need to explore the use of the system for intervesicular reactivities.

Chapter III Solution studies

Before studying the reactivity of the molecules embedded in vesicles we need as a comparison to determine the mechanism and the rates of the same reactions in solution. In order to achieve this, water soluble model molecules with identical reactive chemical groups were used.

III-1 Design:

The molecules used in the vesicle studies consist of a cysteine or cysteine derivative linked to a cholesterol unit via an ester or a carbamate linkage. The water soluble equivalent molecules have been designed by replacing the cholesterol moiety by an ethyl group. The following figure shows the correspondence between the amphiphilic molecules used in the vesicles studies and the water soluble ones along with the other molecules used in the study.

For the solution kinetic studies, apart from the solution analogues of the membrane anchored molecules, the other thiol studied is DTT (shown below), it is included in the study as it crosses the vesicle membrane and it will be used in vesicle experiments, control studies and titrations of disulfides. Hence its reactivity towards disulfides needs to be well characterized. In addition to this, the study of the reactivity of the three thiols will enable us to assess the influence of the thiol pK_a in thiol-disulfide reactions. The last reductant studied was a water soluble phopshine (PPh3 shown below) known not to cross phospholipid membranes[51] and is the reductant used by Barton *et al.* in their signaling experiment.

Four disulfides were used for the studies, the two asymmetric ones shown in figure and two symmetric ones, Ellman's reagent and 2,2'-dithiodipyridine (both shown below).

The last molecule used is potassium ferricyanide $(K_3Fe(CN)_6)$, this is the oxidant used by Barton *et al.* in their signaling experiment.
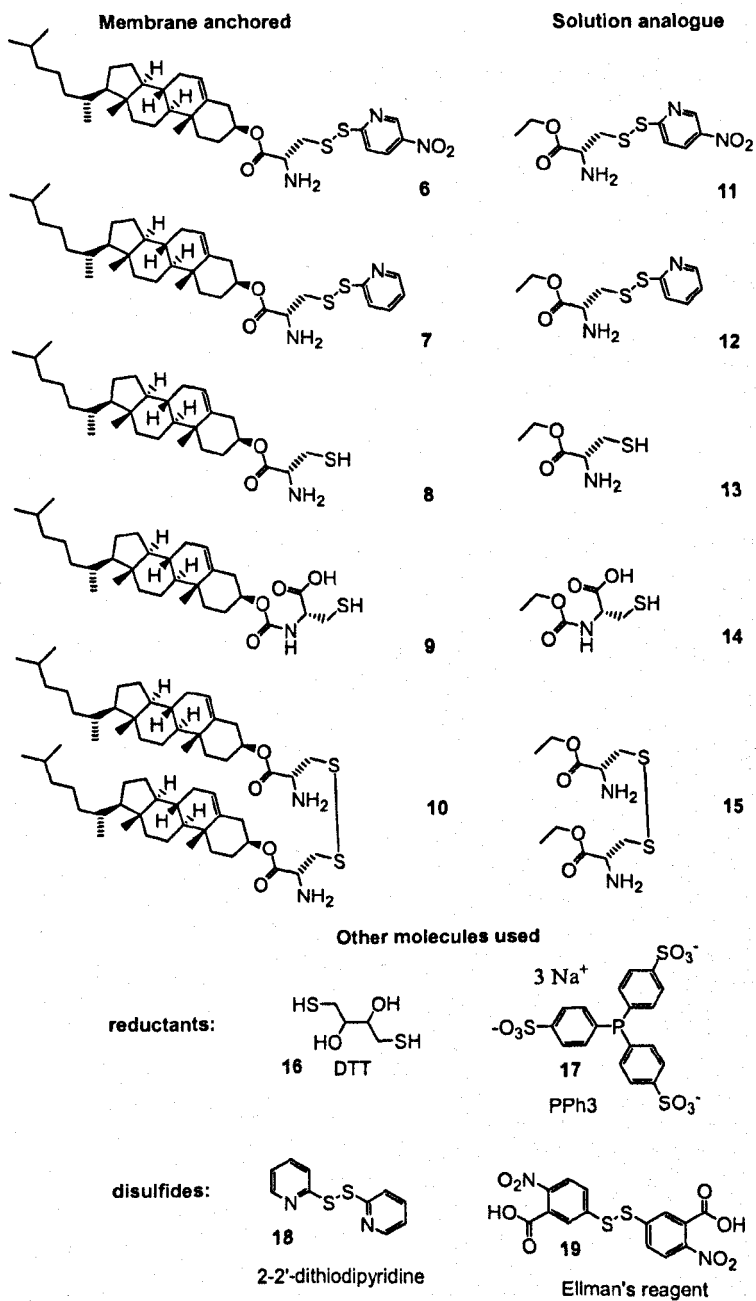
Figure 23. Organic molecules used in this study.

The conditions used for the kinetic studies in solution are the ones from the system designed by Barton *et al.* [21] . The kinetics were carried out in MES buffer at pH 5.5, at 25 degrees Celsius. The kinetics traces are obtained by following the appearance or disappearance of the chromophore, depending on the reaction studied, at the relevant wavelength. The different chromophores are pyridinethiol, 4-nitro-pyridinethiol, phosphine and potassium ferricyanide.

III-2 Results:

All the different couples of reductant and oxidant described above have been studied kinetically by following the appearance or disappearance of the relevant chromophore at its maximum absorption wavelength. The experiments have resulted in five different analyses of the data depending on the underlying reaction mechanism between the two reactants and the amount of chromophore released. The five types of analysis will be discussed in turn using an example. The corresponding reaction mechanism will be looked at in conjunction with the data analysis.

III-2-1 Single step reaction mechanism

This analysis corresponds to a reaction with the following simple one step mechanism:

Mechanism 1:

Reactant 1   +   Reactant 2 $\xrightarrow{k}$ Chromophore   +   Product
|
Chromophore
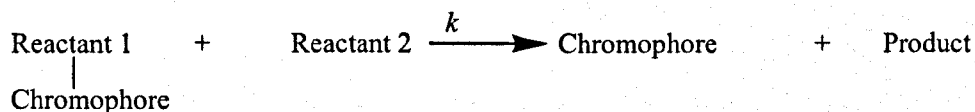
Figure 24. Single step reaction mechanism.

By forcing the non chromophore containing reactant's concentration to be almost constant over the course of the reaction, i.e. [reactant 2] > 10 × [reactant 1], the data obtained fits a simple exponential curve for all concentration ranges following the rule given above. This simple exponential curve corresponds to a first order kinetics and the k obtained when fitting the data is a pseudo first order rate constant.

An example of the types of curve obtained is shown in the figure below.
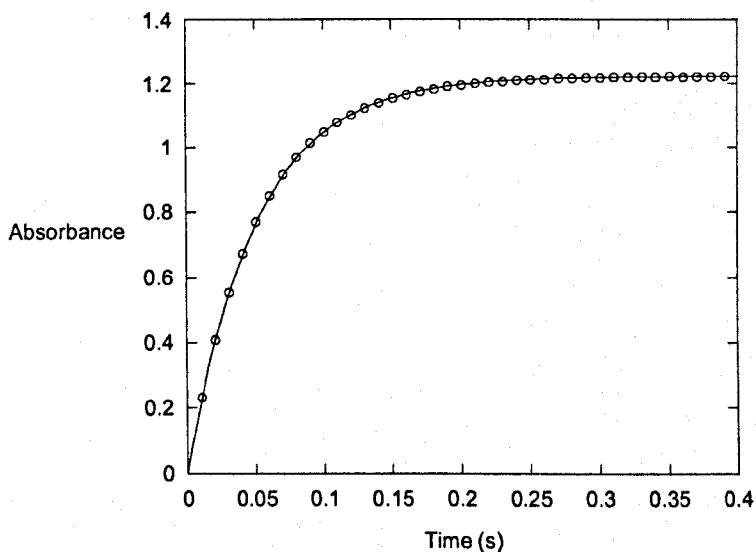
Figure 25. First type of curve obtained from the solution studies experiments. The reaction represented here is between 10.75 mM of **13** and 48 μM of **11**. The open circle indicates the actual data point (5% of them) and the line represents a single exponential fit with a k_{obs} of 19.3 ± 0.1 s^{-1}.

In order to determine the value of the second order rate constant, data are gathered at different concentrations of the reactant in excess. All obtained curves are then fit via a single exponential as shown above and the pseudo first order rate constants are plotted against the concentration of the reactant in excess as is shown in Figure 26 below for the same reaction whose data are shown on Figure 25 above.
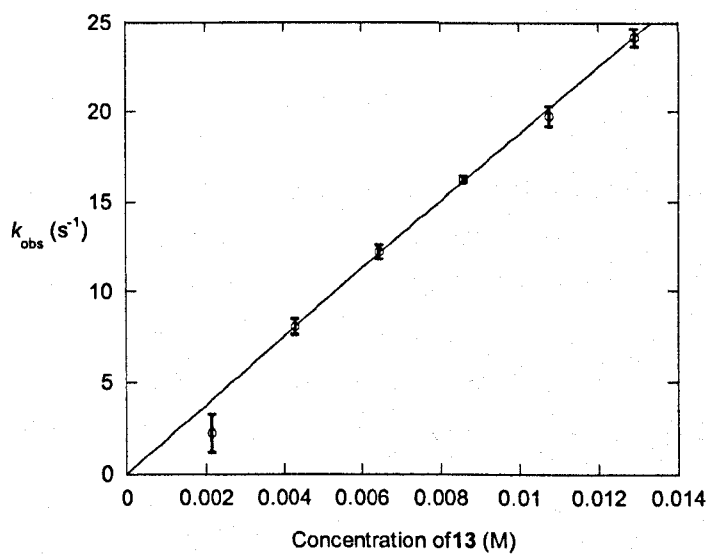
Figure 26. Plot of the pseudo first order rate for the reaction of **13** with **11** against the concentration of **13**, the data points are given by the open circles and the solid line is the linear fit through the origin. The second order rate constant obtained (slope of the curve) is 1880 ± 20 M^{-1} s^{-1}.

The straight line through the data indicates that the reaction is second order, i.e. first order in each reactant. The slope of the line gives the second order rate constant for the studied reaction.

III-2-2 Two steps reaction mechanism

For certain reactions, the curves obtained could not be fit to a single exponential as explained above due to the fact that the reaction mechanism involved more than one step. In this case, the data obtained were fit to two single exponentials, each representing a distinct step in the reaction mechanism. This is only possible if the two steps have significantly different rate constants, otherwise the two steps of the reaction mechanism will not be distinguishable and the data will fit a single exponential.

This situation occurred only for symmetrical disulfides made of two chromophores, i.e. Ellman's reagent and molecule **18**, with reactants **13** and molecule **18** with reactant **14**.

The following figure gives the general reaction mechanism, which gives kinetics data that can only be fitted to two single exponential. This is the case when k_1 and k_2 differs significantly:

Mechanism 2:

Chromophore + Reactant 2 $\xrightarrow{k_1}$ Chromophore + Product
| |
Chromophore   Chromophore

Product + Reactant 2 $\xrightarrow{k_2}$ Chromophore + Product
|
Chromophore

Figure 27. Two steps reaction mechanism.

The following figure gives an example of curve obtained when following the kinetics using the stopped flow apparatus:

Figure 28. Second type of kinetic curve obtained when 4.0 mM of molecule **13** reacts with 0.053 mM of molecule **18**. Only 50 data points are represented, which represents 2.3% of the total data recorded. The line is the two exponentials fit with $k_{1obs} = 3.37 \pm 0.01$ s^{-1} and $k_{2obs} = 0.50 \pm 0.01$ s^{-1}.

Once the values of the pseudo first order rate constants k_{1obs} and k_{2obs} have been determined at the various concentration of the reactant in excess, they are both respectively plotted against that concentration as shown in Figure 25 above.

The slope of each plots provide the values of the second order rate constant corresponding to each step in the reaction mechanism shown above in Figure 27.

III-2-3 Single step reaction mechanism with weak interaction between the reactants

The third type of kinetic curve obtained corresponds to the following mechanism, which is the equivalent of the mechanism described in Figure 24 above with a weak interaction between the reactants.

Mechanism 3:

$$\text{Reactant 1} + \text{Reactant 2} \underset{}{\overset{K}{\rightleftharpoons}} \left[\text{Reactant 1} + \text{Reactant 2} \right]$$

(Reactant 1 | Chromophore) + Reactant 2 ⇌ [Reactant 1 (| Chromophore) + Reactant 2]

$$\left[\text{Reactant 1} + \text{Reactant 2} \atop | \atop \text{Chromophore} \right] \xrightarrow{k} \text{Chromophore} + \text{Product}$$
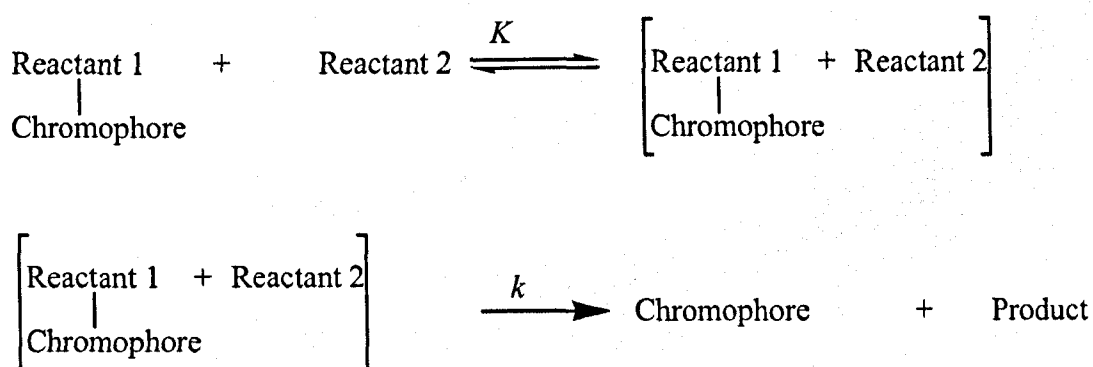
Figure 29. Single step reaction mechanism with a weak interaction between the reactant.

When compared with reaction mechanism 1 with only a single step, this mechanism has an added equilibrium prior to the reaction between the reactants. For this type of reaction mechanism, the kinetic data can be fit to a single exponential as for mechanism 1 above. This is due to the fact that the step producing the chromophore, the reaction of the complex, follows a simple first order kinetic. However in this case, when plotting the pseudo first order rate constant against the concentration of the reactant in excess, another equation is required to characterise the system.

The equation is as follows and is identical to a Michaelis-Menten equation for substrate binding to an enzyme and subsequent reaction:

$$v = \frac{k \times [reagent]}{K + [reagent]}$$

where v is the pseudo first order rate of the reaction, k is the maximum pseudo first order rate for the studied reaction, K is the equilibrium constant for the weak interaction between the reactants and [*reagent*] is the concentration of reactant in excess.

In order to obtain an approximation of the second order rate constant, we use the tangent of the curve at a concentration of reactant in excess equals to zero, i.e. at a concentration where the weak interaction is removed. The derivation is given in Appendix I. The second order rate constant is given by k/K.
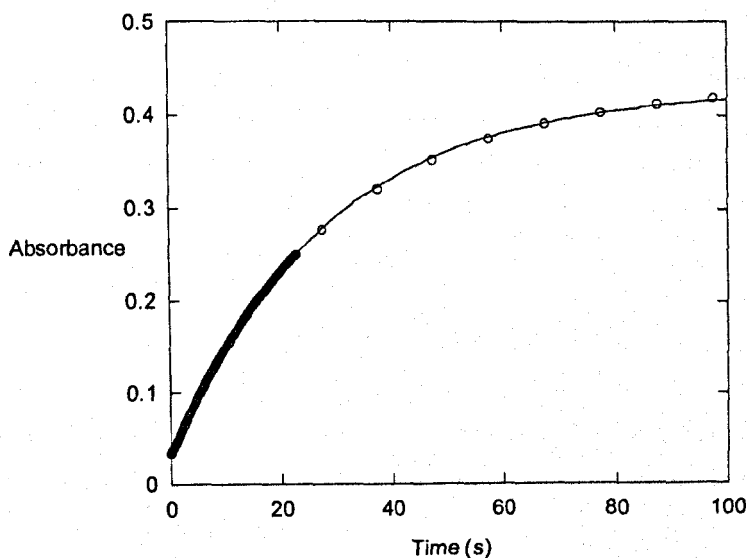
Figure 30. Third type of kinetic curve obtained when 1.525 mM of molecule **14** reacts with 0.10 mM of molecule **12**. Only 10% of the data points are represented. The line is a single exponential fit with k_{obs} = 0.035 ± 0.001 s^{-1}.

After obtaining all the pseudo first order rate constants (k_{obs}) for the different concentrations of the reactant in excess, k_{obs} is plotted against the concentration in order to derive the second order rate constant from the slope. As mentioned above for certain couple of reactants, a weak interaction exists between the two molecules before they react together. This leads to a curve with characteristics similar to the ones on the following graph (Figure 31).
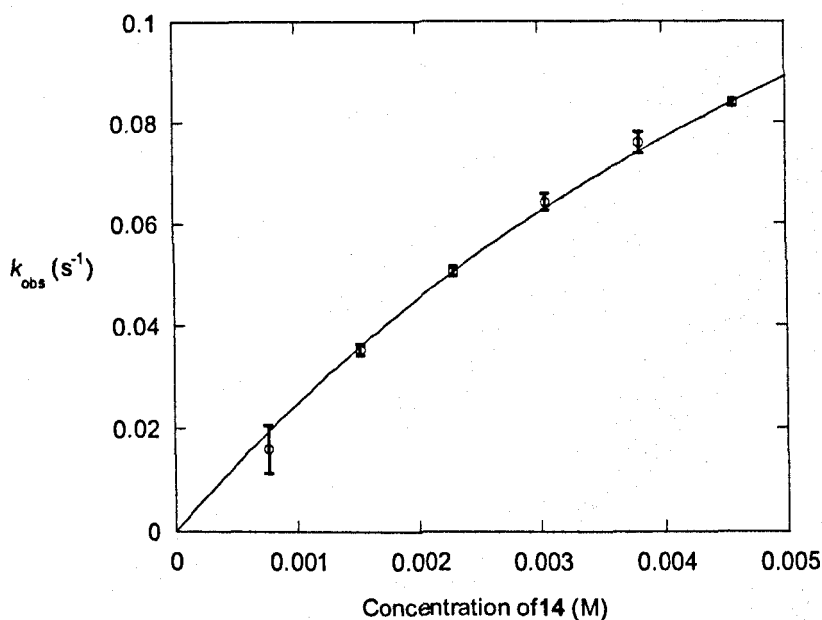
Figure 31. Plot of the pseudo first order rate constants against the concentration of **14** for the reaction between **12** and **14**. The fit corresponds to the equation for the weak interaction between the reactants with $k = 0.25 \pm 0.02$ s^{-1} and $K = 0.0091 \pm 0.001$ M, hence the second order rate constant is $k/K = 27.5 \pm 3.8$ M^{-1}.s^{-1}.

This method provides a second order rate constant at a concentration where the molecule do not interact with each other, since it is the tangent of the curve at a concentration of reactant in excess equals to zero. Therefore the rate constant thus obtained can be used for comparison with the rate constants computed from other methods described above and below.

III-2-4 Two steps mechanism with weak interactions between the reactants in both steps

The reaction between molecule **14** and molecule **19** (Ellman's reagent) gave rise to kinetic curves that could only be fitted with two single exponentials as described above in section III-2-2. When k_{1obs} and k_{2obs} are plotted against the concentration of **14**, the two following curves are obtained (Figures 32 and 33).
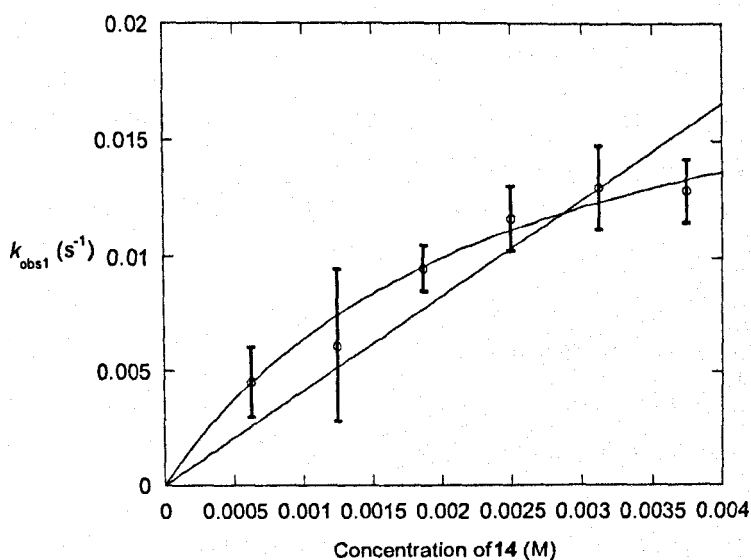
Figure 32. Plot of k_{obs1} against the concentration of **14** for the reaction of **14** with **19**. The straight line is the linear fit through the origin with a slope that gives the second order rate constant of 4.2 ± 0.2 s^{-1}. The curve is the weak interaction fit with $k = 0.022 \pm 0.007$ s^{-1} and $K = 0.0024 \pm 0.0015$ M, therefore a second order rate constant of 9.2 ± 6.4 M^{-1}.s^{-1}.
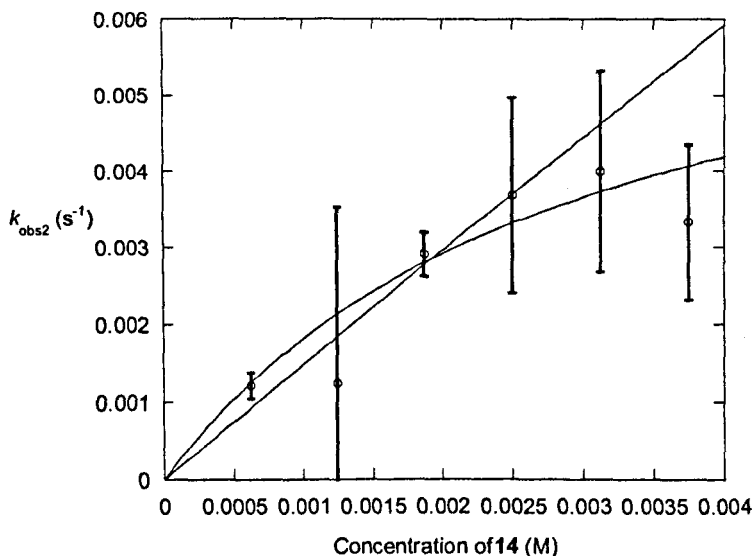
Figure 33. Plot of k_{obs2} against the concentration of **14**. The straight line is the linear fit through the origin with a slope that gives the second order rate constant of 1.5 ± 0.1 s^{-1}. The curve is the weak interaction fit with $k = 0.0074 \pm 0.003$ s^{-1} and $K = 0.0031 \pm 0.0019$ M, therefore a second order rate constant of 2.4 ± 1.8 M^{-1}.s^{-1}.

Both molecule **19** and molecule **14** possess negatively charged carboxylate groups and are therefore overall negatively charged. As a result it seems highly unlikely that a weak interaction between the two molecules would occur since they should repel each other electrostatically. Hence the second order rate constant taken to characterise the reaction described between **19** and **14** is the slope of the linear fit through the origin. The fact that the weak interaction model fits the data better is assumed to be a result of significant errors in the measurements.

III-2-5 Complex reaction mechanism

The last type of curve obtained from the experiments is a double exponential as shown on the figure below (Figure 34). It is obtained only for the reaction between molecules **17** and **18**. For this type of curve instead of fitting it to a single exponential, two exponentials were used to fit the data as explained in section II-2-2.
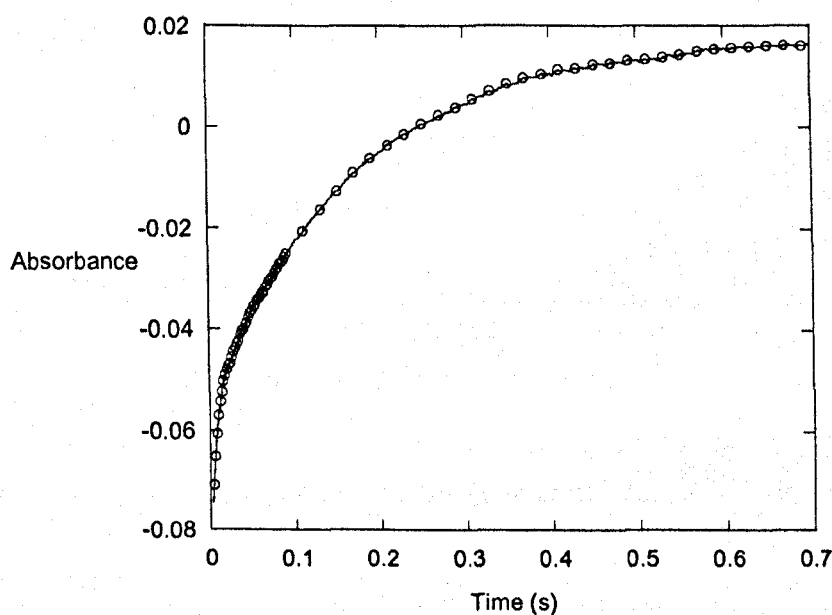
Figure 34. Fifth type of curve obtained from the solution studies experiments. The reaction represented here is between 15.7 mM of **17** and 50 μM of **18**. The open circle indicates the actual data point (5% of them) and the line represents a double exponential fit with a k_1 of 170 ± 1 s^{-1} and a k_2 of 5.82 ± 0.01 s^{-1}.

In a manner similar to the treatment of the data obtained from single exponential fits, k_{obs1} and k_{obs2} are then plotted against the concentration of **17**, i.e. the water soluble phosphine. The first dataset provides a second order rate constant using a weak interaction fit as described earlier (Figure 35). The difference with other computations is that when k_{obs2} is plotted against the concentration of **17**, it is constant across the range of **17** concentrations (figure 37). This indicates that k_{obs2} is zero order in **17**. In

pseudo first order conditions, the concentration of one of the reactant is in excess and remains largely constant over the course of the reaction.
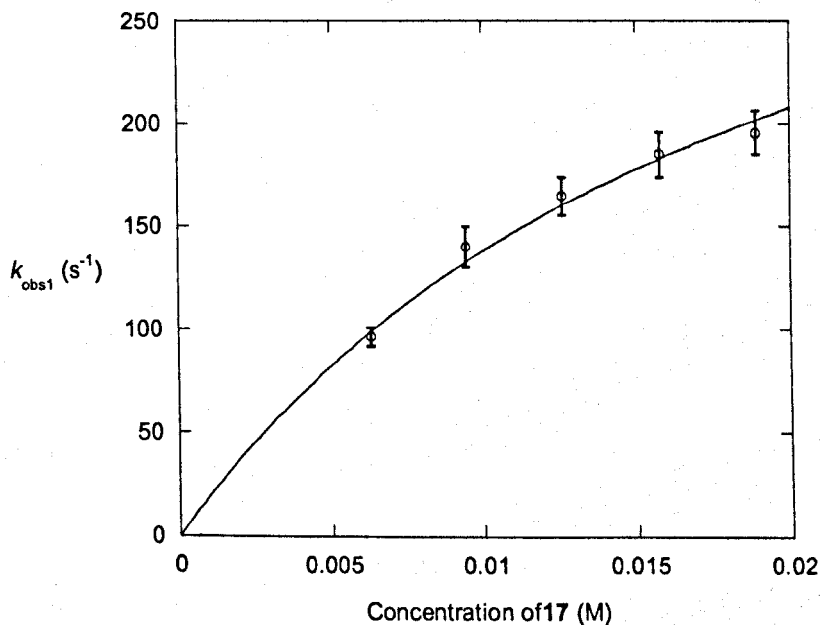
Figure 35. Data obtained for the reaction between **18** and **17** in pseudo first order conditions, i.e. [**17**] > 50 times [**18**], when plotting k_{obs1} against the concentration of **17**. The fitted line corresponds to a weak interaction between reactants using the following equation: $k_{obs1}=k\times[17]/(K+[17])$. The equation was fitted to the data using the following values for $k = 419 \pm 71$ s^{-1} and $K = 0.02 \pm 0.005$ M, therefore the second order rate constant is $k/K = 21000 \pm 6300$ M^{-1}.s^{-1}.

Mechanism 4:

Chromophore $+$ Reactant 2 $\xrightleftharpoons{K}$ $\begin{bmatrix} \text{Chromophore} + \text{Reactant 2} \\ | \\ \text{Chromophore} \end{bmatrix}$

Chromophore

$\begin{bmatrix} \text{Chromophore} + \text{Reactant 2} \\ | \\ \text{Chromophore} \end{bmatrix}$ $\xrightarrow{k_1}$ Chromophore $+$ Reactant 2

Chromophore

Reactant 2 $+$ H_2O $\xrightarrow{k_2}$ Product $+$ Chromophore

Chromophore
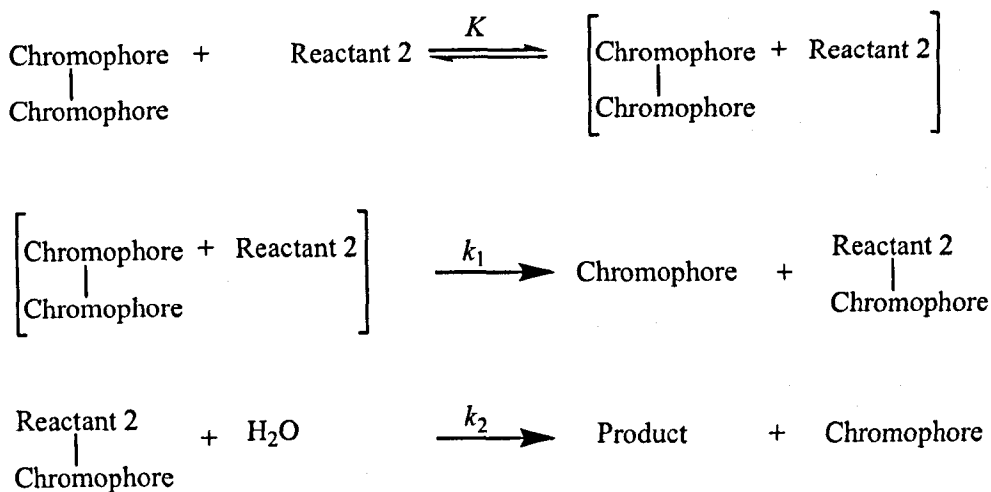
Figure 36. Reaction mechanism with a first order second step.
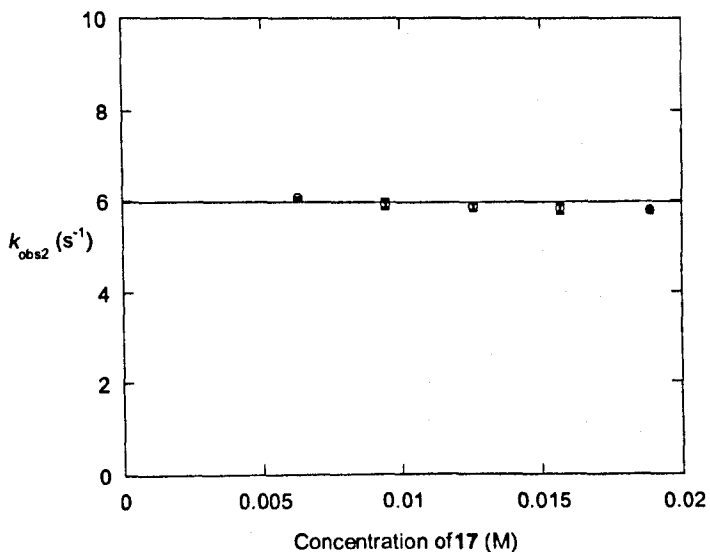
Figure 37. Data obtained for the reaction between 18 and 17 in pseudo first order conditions, i.e. [17] > 50 times [18], when plotting k_{obs2} against the concentration of 17. The rate constant is independent of the concentration of 17. Therefore $k_{obs2} = 5.98 \pm 0.02$ s^{-1}.

Therefore the mechanism for the reaction is as shown in Figure 36 above. It involves a first weak interaction between molecules **17** and **18** followed by a reaction which produces a chromophore containing intermediate. The last reaction is the reaction of the intermediate with water to produce the product and the second equivalent of the chromophore. This reaction is first order due to the fact that one of the reactant is the solvent, i.e. water, and hence has a constant concentration over the course of the reaction. This mechanism is consistent with the mechanism proposed by Overman *et al.* for the cleavage of aryl disulfide bonds by phosphine in water dioxane medium [52].

III-2-6 The oxidation of thiols and water soluble phosphine by potassium ferricyanide

The phosphine and ferricyanide do not react together on the time scale we are interested in (a few hours maximum) as was determined by following the absorption peak of the ferricyanide in UV at 420 nm, when both reactants were mixed in equimolar quantities.

Regarding the reactions of ferricyanide with DTT, ethyl ester cysteine hydrochloride and 2-ethoxycarbonylamino-3-mercapto-propionic acid, the kinetic traces were gathered in pseudo first order conditions with a large excess of the thiols over the ferricyanide. The data on each of the following graphs (Figures 38, 39 and 40) were obtained by fitting the kinetic traces to a single exponential. However the mechanism of oxidation by potassium ferricyanide is complex at the pH we worked at (pH=5.5)[53-58], this is evidenced by the fact that there does not seem to be any easy rationale for the influence of the concentration of ferricyanide and of the thiols on the speed of the reaction.
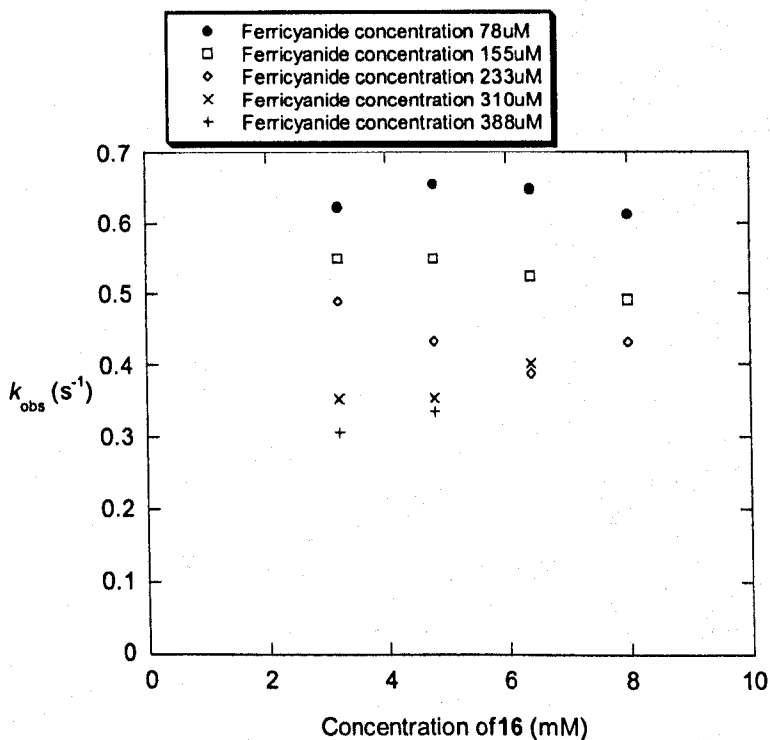
Figure 38. Oxidation of **16** by potassium ferricyanide.
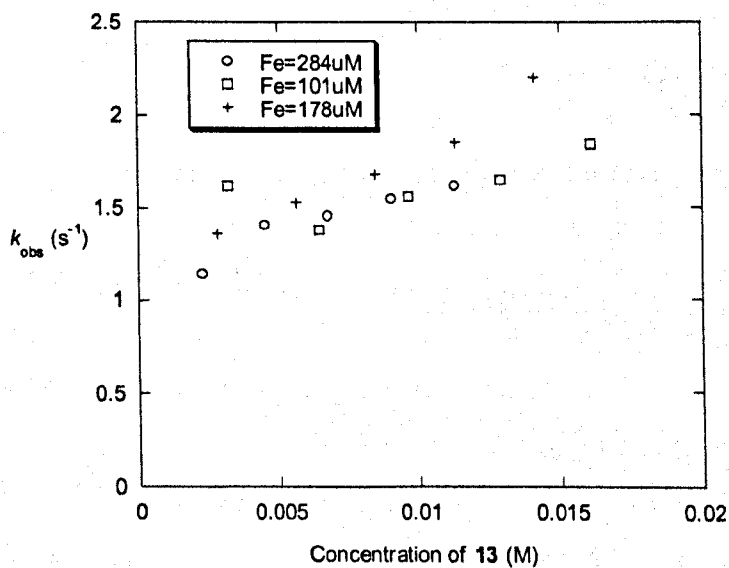
Figure 39. Oxidation of **13** by potassium ferricyanide.
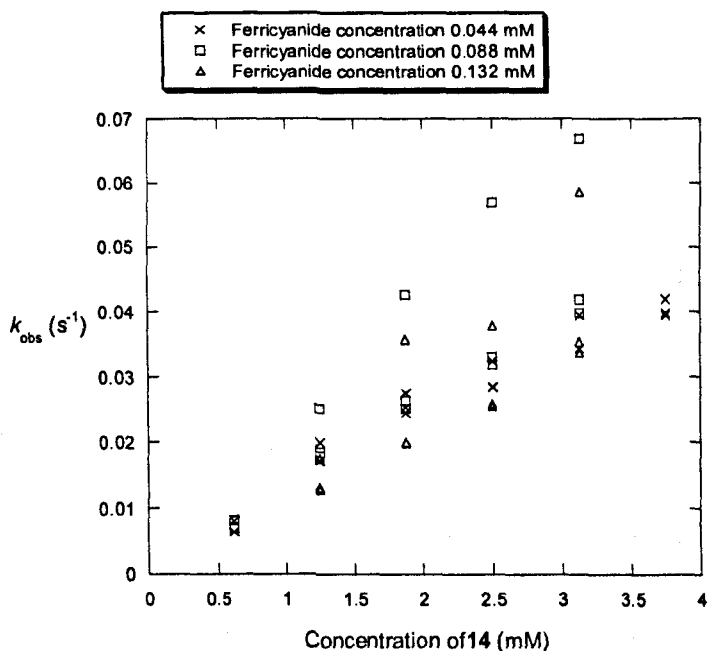
Figure 40. Oxidation of 14 by potassium ferricyanide.

Nevertheless from the data gathered it is obvious that the thiols can be classified as follows in order of increasing ease of oxidation by ferricyanide: 2-ethoxycarbonylamino-3-mercapto-propionic acid < DTT < ethyl ester cysteine hydrochloride. This is likely to be related to their decreasing pKa and hence a higher concentration of thiolate at pH 5.5, the thiolate being the molecule oxidized.

Ethyl ester cysteine hydrochloride has a microscopic pK_a for the thiol of 7.30 as reported by Reuben *et al.* [59] in water at 30 °C, Patel *et al.* [60] reported 7.45 for the same ionization in water at 25 °C. We worked at 25 °C in 50 mM MES buffer in deionised water so for this study we assume the pK_a of this thiol to be 7.45. Whitesides *et al.* have reported a pK_a in water at 25 °C of 9.26 for DTT[61]. Patel *et al.* [60]have reported a pK_a of 9.60 for the thiol of N-acetyl-L-cysteine. 2-ethoxycarbonylamino-3-mercapto-propionic acid is very similar in structure to N-acetyl –L-cysteine, hence 9.60 was used as the pK_a of 2-ethoxycarbonylamino-3-mercapto-propionic acid for the purpose of discussion. Those three pK_a confirm that the ease of oxidation is linked to

54

the availability of thiolate, since the easier thiol to oxidize is the one with the lower pKa and as a consequence with the higher concentration of thiolate.

III-2-7 Test for the disproportionation of asymmetric disulfides

The asymmetric disulfides have been reported in two studies to be rather unstable molecules[62, 63], Khim *et al.* studied the effect of neighboring group such as acid on the disproportionation reaction whereas Kice *et al.* studied the acid catalysed disproportionation.

In order to assess the stability of 2-amino-3-(pyridin-2-yldisulfanyl)-propionic acid ethyl ester in the conditions used in the kinetic studies, a solution of this asymmetric disulfide at a concentration of 0.63 mM was prepared. Two experiments were carried out, in one UV cell a few microliters of a solution of pyridinethiol were added to the disulfide solution to obtain a concentration of 56 mM of pyridinethiol in the cell. In the other cell no pyridinethiol was added. The evolution of the absorption of both cells was followed at 341 nm. The two figures below show the results obtained.
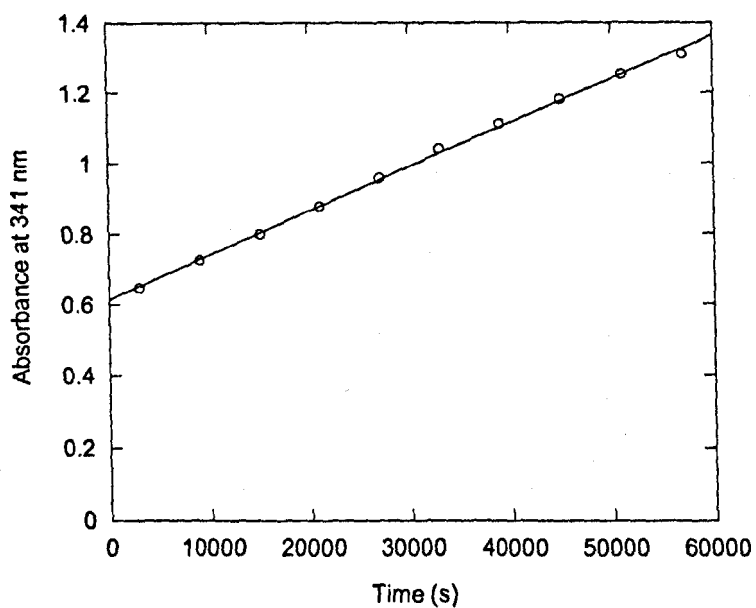
Figure 41. Evolution of the absorbance of a mixture of **12** (0.63 mM) and pyridinethiol (56 μM) at 341 nm. The open circle represents 2 % the gathered data and the solid line is the linear fit with a slope of 1.2 × 10⁻⁵ Abs.s⁻¹.
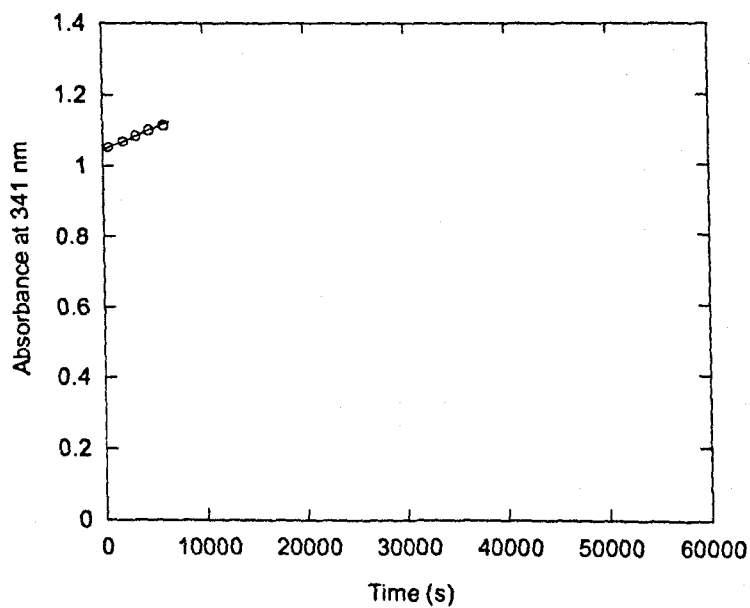
Figure 42. Evolution of the absorbance of **12** (0.63 mM) at 341 nm. The open circle represents 20 % the gathered data and the solid line is the linear fit with a slope of 1.2 × 10⁻⁵ Abs.s⁻¹.

The results shown on Figures 41 and 42 indicate that the asymmetric disulfide disproportionates in the conditions of the experiment, since the increase in absorption can only be accounted for by a release in pyridinethiol from the disulfide. This effect takes place whether pyridinethiol is already present or not, however some minute amounts of pyridinethiol could be present in the asymmetric disulfide solution as impurities. Hence we cannot conclude definitely on the reason for the disproportionation, nevertheless this result confirms the relative instability of asymmetric disulfide in acidic media. The reaction that causes this instability could be the hydrolysis of the disulfide bond that links the cysteine moiety to the chromophore. Kice et al. [62] have reported similar disproportionation in acidic medium of asymmetric disulfides.

III-3 Discussion:

The reactivity of the thiols in the thiol-disulfide exchange reaction is linked with their pKa, i.e. the lower the pK_a the more reactive the thiol is. This is due to the fact that the first step in the thiol-disulfide exchange is the deprotonation of the thiol to form the thiolate. The thiolate is the reactive species that then attacks the disulfide. The following table summarises the observed rate constants obtained. Those are the rate constants computed with the concentration of thiol, determined using the methods described earlier in sections III-2-1 to III-2-5.

Table 2. Observed rate constants

All rate constants are in $M^{-1} s^{-1}$		Reductants			
		Thiol **13**	Thiol **14**	DTT **16**	PPh3 **17**
Oxidants	2,2'-dithiodipyridine **18**	k_1=900 ± 11 k_2=130 ± 2.0	k_1=26 ± 0.4 k_2=4.8 ± 0.3	53 ± 1.0	20600 ± 6300
	Disulfide **12**	144 ± 2.0	27 ± 4	29 ± 0.7	320 ± 110
	Disulfide **11**	1880 ± 20	290 ± 54	300 ± 2.0	1200 ± 140
	Ellman's reagent **19**	k_1=73 ± 1.7 k_2=26 ± 0.3	k_1=9.2 ± 6.4 k_2=2.4 ± 1.8	19 ± 1.0	450 ± 4.0
	Symmetrical disulfide **15**				25 ± 0.5

The first observation that can be made when analysing those data is that all other factors being equal, disulfide **11** is more reactive than disulfide **12** towards thiol-disulfide exchange. This is due to the fact that the chromophore in disulfide **11** has an added nitro group on the pyridine ring. The electron-withdrawing character of this group reduces the electron density on the sulphurs of the disulfide bond in **11** when compared with **12**. This effect has been reported by Narisada et al. [64].

The second observation is related to the symmetrical disulfides **18** and **19**. They both have similar patterns of reactivity as is evidenced by the fact that they have similar reactions mechanisms when reacting with the same thiol. However **18** is an order of magnitude more reactive than **19** across the range of thiols used. This difference in reactivity between Ellman's reagent (**19**) and 2,2'-dithiodipyridine (**18**) is explained by the difference in the electron density on the disulfide bond. The nitrogen atom in ortho position on the pyridine ring in molecule **18** decreases the electron density on the sulphurs in the disulfide bond when compared to the identical bond in molecule **19**. This is due to the increased electronegativity of the nitrogen in **18** over the carbon atom in the identical position on the aromatic ring in **19**. This appears to overcome the electron withdrawing character of the nitro group present in **19**, which would also reduce the electron density on the sulphur atoms.

The rate constants obtained for the different thiols can be linked with their respective pK_a. The observed reactivity of thiol in thiol-disulfide exchange reactions is linked to the concentration of thiolate at the pH of the reaction. Thiol **13** (cysteine ethyl ester hydrochloride) has a lower pK_a (7.45) than the two other thiols **14** and **16** (9.26 and 9.60 respectively), which explains why its observed rate constant is higher. The two other thiols both have similar pK_as and observed reactivities, which confirms the influence of the pK_a on the observed rate constants.

The exact concentration of thiolate in the solution can be calculated using the pK_a of each thiols at the pH used for all experiments, 5.5. The rate constants calculated using the thiolate concentrations present in solution for each thiol are given in Table 3 below. Those constants have been computed by replacing the concentration of thiol by the concentration of thiolate and then fitted to the identical equations required to obtained the observed rate constants given in Table 2 above.

Table 3. Rate constants

All rate constants are in $M^{-1}s^{-1}$		Reductants		
		Thiol 13	Thiol 14	DTT 16
Oxidants	2,2'-dithiodipyridine 18	k_1=82000 ± 1100 k_2=12000 ± 130	k_1=330000 ± 4700 k_2=60500 ± 4400	310000 ± 5800
	Disulfide 12	13000 ± 150	304000 ± 61000	170000 ± 3900
	Disulfide 11	170000 ± 1600	3630000 ± 690000	1700000 ± 10000
	Ellman's reagent 19	k_1=67000 ± 1600 k_2=24000 ± 280	k_1=116000 ± 81000 k_2=30400 ± 22000	110000 ± 550

When comparing the rate constants in Table 3 with their equivalents in Table 2 it appears that the disulfides 11 and 12 still follow the same pattern where disulfide 11 is one order of magnitude more reactive than 12. The difference between the reactivity of 18 and 19 are similar. However the rate constants in Table 3 indicates that step 2 of the two steps reaction mechanism for the thiol-disulfide exchange of symmetrical disulfides (18 and 19) with thiol 13 is faster for 19 than for 18. This departs from the patterns found in Table 2 regarding the rate constants of thiol-disulfide reactions. It indicates that the intermediate asymmetric disulfide with the TNB chromophore reacts more rapidly with the thiolate resulting form the deprotonation of thiol 13 than the one containing 2-pyridinethiol. In this case it appears that the electron-withdrawing effect of the nitro group in para to the disulfide bond is stronger than the electron-withdrawing effect of the nitrogen atom in ortho. There is evidence that the second step of the reaction between 12 and 13 is between disulfide 11 and thiol 13 since the rate constant for both reactions are very similar at 12000 ± 130 $M^{-1}.s^{-1}$ and 13000 ± 150 $M^{-1}.s^{-1}$

respectively. Overall in the asymmetric disulfides studied, the electron-withdrawing effect due to increased resonances forms, induced by the nitro group in para, is stronger than the same effect induced by increased electronegativity of an atom on the aromatic ring, here the nitrogen atom in ortho to the disulfide bond.

In addition to those observations, the reactivity order of the thiols has been modified when looking at the rate constants (Table 3) and not the observed rate constants (Table 2). This is due to the fact that the higher observed rate constants for thiol **13** stemmed from higher thiolate concentrations at the pH used for the experiments. Since the pK_a of thiol **13** is approximately two points lower than the other two thiols, the concentration of thiolate would be two orders of magnitude higher in reactions involving **13**. Therefore when analysing the reactivities of the different using the thiolate concentrations, the difference in reactivity can be appropriately assessed. Evaluating the Brønsted coefficients β for the reactions studied will provide us with another insight into the thiol-disulfide exchange reaction mechanism and an explanation as to why the thiols with higher pK_as are the most reactive ones.

Low β value:

$$R_1\text{-}S^{\ominus} \quad + \quad R_2\text{-}S\text{-}S\text{-}R_2 \quad \longrightarrow \quad \left[R_1\text{-}S^{\ominus} \text{-----} \underset{\overset{|}{R_2}}{S}\text{-}S\text{-}R_2 \right]^{\ddagger}$$

High β value:

$$R_1\text{-}S^{\ominus} \quad + \quad R_2\text{-}S\text{-}S\text{-}R_2 \quad \longrightarrow \quad \left[R_1\text{-}S\text{-}\underset{\overset{|}{R_2}}{S} \text{-----} S^{\ominus}\text{-}R_2 \right]^{\ddagger}$$
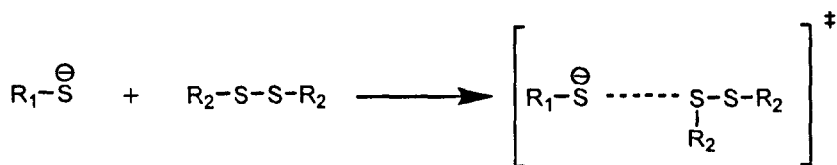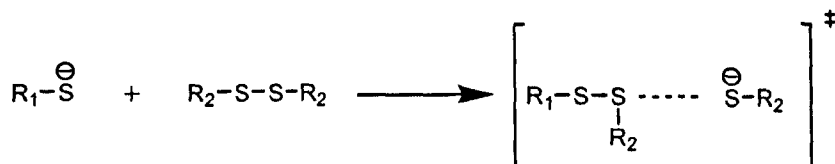
Figure 43. Different transition states depending on the value of the β determined by the Brønsted equation: $\log(k) = \beta \times pK_a + C$.

61

By plotting the logarithms of the rate constants obtained in Table 3 against the pK_a of the thiolate, Brønsted coefficients β can be calculated for the thiol-disulfide exchanges studied. The following figures show those plots for the different disulfides. The Brønsted equation used to fit the data is: $\log(k) = β \times pK_a + C$. Since the reactive species is the deprotonated thiol (thiolate), if a low β value is computed, it indicates that the rate of the reaction is not dependent on the pK_a of the attacking species (thiol). Therefore for low values of β the transition state of the reaction is closer to the original state of the molecules, i.e. where the bond between the attacking thiol and the disulfide is hardly formed (Figure 43). High β value on the other hand indicates that the rate of the reaction is strongly dependent on the pK_a of the thiol. This corresponds to a transition state of the reaction, closer to the final state of the molecules, where the bond between the attacking thiol and the disulfide is mostly formed (Figure 43).
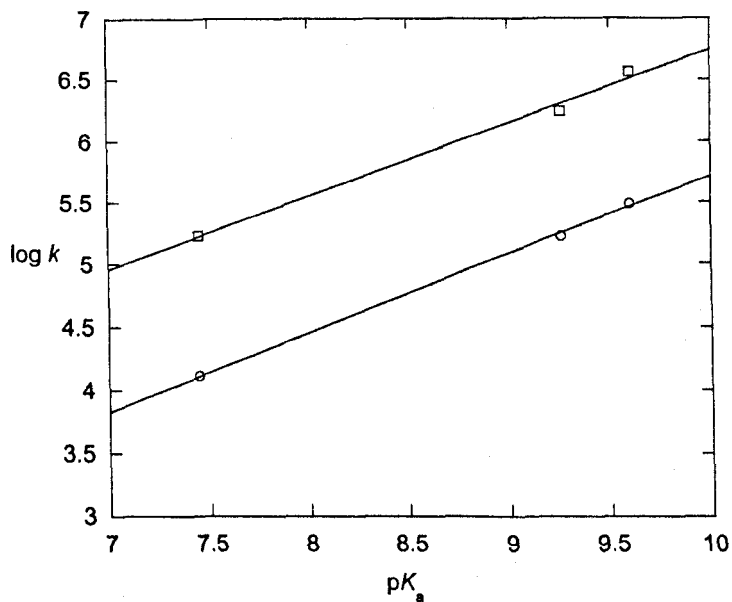
Figure 44. Plot of log$k$ against the pK_as of the three thiols studied for **12** (open circles) and **11** (open squares). The respective β coefficients obtained are 0.63 (R^2=0.999) and 0.60 (R^2=0.997).

Figure 45. Plot of log$k$ against the pK_as of the three thiols for 2,2'-dithiodipyridine **18** (open squares) and Ellman's reagent **19** (open circles). The respective β coefficients obtained are 0.29 (R^2=0.993) and 0.11 (R^2=0.999).
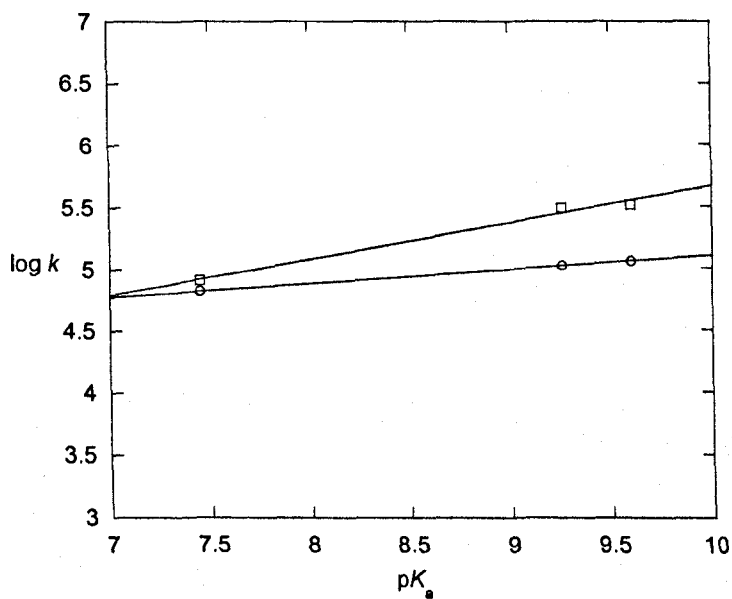
There is a significant distinction between the thiol-disulfide reactions involving symmetrical disulfides and those involving asymmetrical disulfides. This is evident when comparing the results on Figure 44 with those on Figure 45 above. The Brønsted coefficients for the thiol-disulfide exchange reaction involving the symmetrical disulfides are in the 0.1-0.3 range whereas those for the asymmetrical disulfides are in the 0.6-0.65 range. This indicates that the transition state has a strongly formed between the attacking thiol and the disulfide when asymmetric disulfides are the reactants. This is due to the fact that the asymmetry in the disulfide bond creates a polarisation where one sulphur becomes more electron deficient than the other. This facilitates the attack of the charged thiolate on the disulfide bond, which corresponds to the second step of the thiol-disulfide mechanism as reported in the literature [65], [66]. Figure 46 below gives the different disulfides used in the present studies.
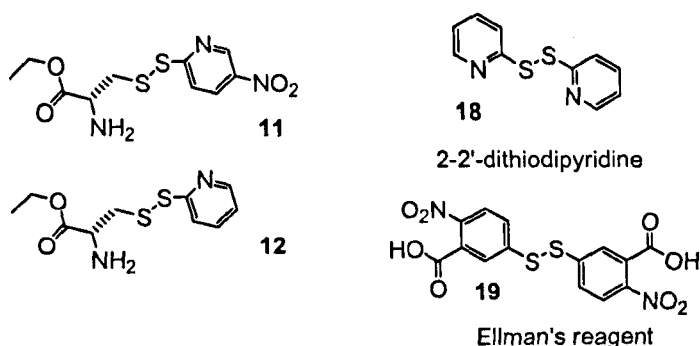
Figure 46. Disulfides molecules studied.

Those results regarding the thiol-disulfide exchange reaction are in line with the results reported by Whitesides *et al.* [66] and Hupe *et al.* [67]. Whitesides *et al.* reported a β of 0.36 for the reaction of Ellman's reagent with thiols in pH 7.0 phosphate buffer at 30.0°C. In our studies we found a β of 0.11 for the reaction of Ellman's reagent with thiols. This is significantly lower than the value reported by Whitesides *et al.*, however our studies are carried out in MES buffer pH 5.5 at 25°C as opposed to phosphate buffer pH 7.0 at 30.0°C for the β of 0.36. Our result is based only on three thiols, whereas Whitesides' computation is based on 19 thiols and the temperature is different by 5°C. This would explain some of the discrepancy between the two values. Nevertheless both

values are approximations, especially ours which is derived from three points, and the are in relative agreement since they both indicate that the transition state is similar the original state of the molecules (Figure 43).

Hupe *et al.* reported a β of 0.5 for the reaction of asymmetric disulfide with aromatic moiety (p-nitrothiophenol) with thiols in imidazole buffer pH 6.0 at 25°C. Th temperature is identical to the one used in our studies and for this type of reaction those involving asymmetric disulfides, the β calculated in our studies agree well wi the one from Hupe *et al.* A β of 0.62 and 0.65 was reported for the two asymmetr disulfides studied in this thesis. This is in agreement with the 0.5 reported as it mea that the transition involves a stronger bond between the attacking thiolate and th disulfide where asymmetric disulfides are involved instead of symmetric ones.

III-4 Conclusion:

Thanks to the solution studies carried out, a better understanding of the reactivities of the reactants involved in the system designed by Barton *et al.* has been achieved. The different reactants have been classified according to their reactivity towards the disulfides. The rate constant of the reaction will increase with a higher pK_a of the thiol since it is a better nucleophile for the attack on the disulfide bond. However, when dealing with observed rate constant, the pH of the reaction medium might counter this effect. This is due to the fact that thiolate resulting from thiol with lower pK_a will be present in much higher proportion than thiolate from higher pK_a thiol if the pH is relatively low. This is the fact in our studies, where the pH used is 5.5 which is approximately 4 pK points lower than the two best thiols' pKa, i.e. thiols **14** and **16**. This explains why thiol **13** appears to be the most reactive when analysing the observed rate constants (Table 2 above), when it is in fact the least reactive when comparing rate constant (Table 3 above).

In addition it was found that asymmetric disulfides reaction mechanism has a transition state that involves a stronger bond between the attacking thiolate and the difulfide than for reactions involving symmetric disulfides.

The oxidation of thiols by ferricyanide and the disproportionation of disulfides remain areas where more research needs to be carried out. However as regards the oxidation of thiols, a link between the reactivity and the pK_a of the thiol was established.

The next step is now to embed one of the reactant in vesicles and assess whether the reactivity is modified or not.

Chapter IV Interface reactions studies

Compared with the reaction in solution, is the rate modified if one of the two reactants is embedded in a vesicle bilayer?

IV-1 Design:

Amphiphilic molecules are synthesized in order to be embedded in vesicle bilayers and to possess the identical chemical group as their water soluble counterpart used in the solution studies. The membrane anchor used to embed the molecule in the vesicles bilayer was cholesterol. As seen in the introduction it is a natural part of the cell membrane in living organisms and its hydroxyl group facilitates the addition of other molecules to the main cholesterol unit via ester or carbamate linkages for instance.

For the reaction studies one of the amphiphilic molecules is embedded in vesicle in a bulk concentration of around 50 µM (similar to the concentration used in the buffer experiments). Then the other reactant is added in the bulk solution to obtain a similar concentration. The appearance or disappearance of one of the reactant is then followed by UV at the relevant wavelength.

In order to complete those studies at the vesicle membrane interface, molecules **7** and **8** were synthesized according to the reaction scheme shown below in Figure 47.
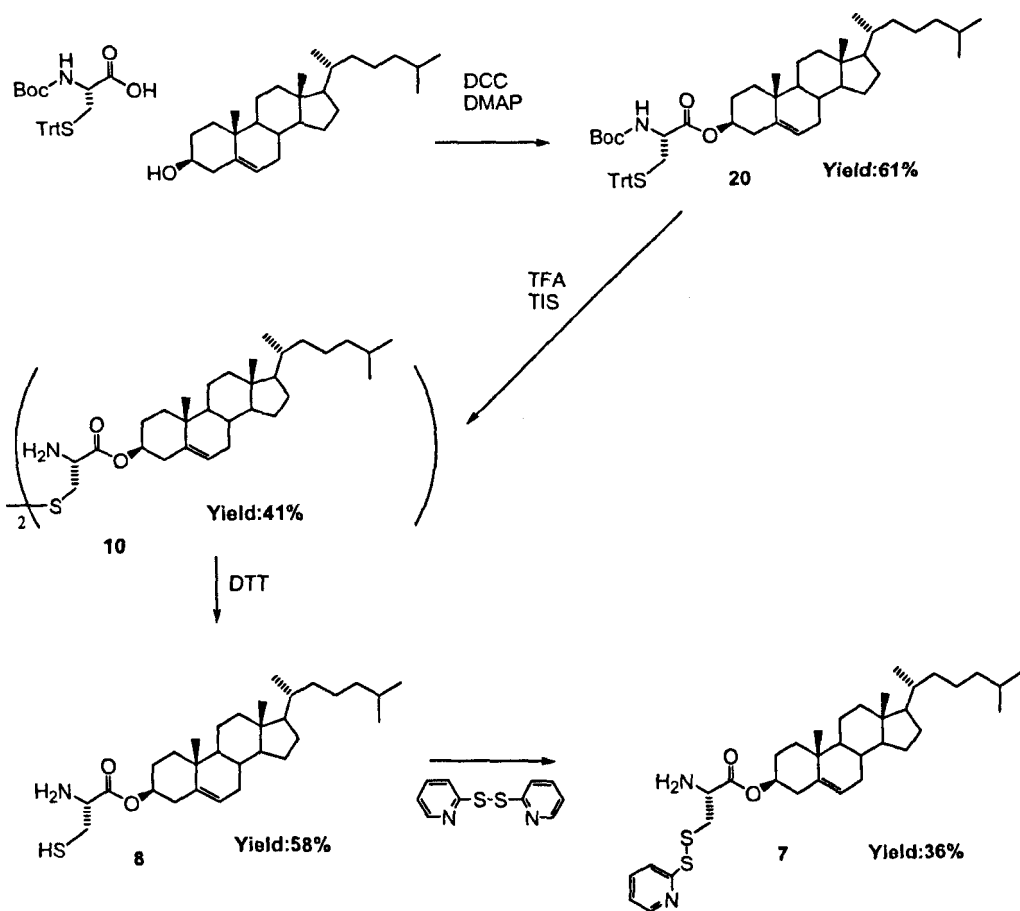
Figure 47. Reaction scheme for the synthesis of the membrane anchored thiol **8** and asymmetric disulfide **7**.

Care should was taken when manipulating the mixed disulfide as it tends to disproportionate over time back to the symmetrical disulfides.

Thiol **8** presented a problem as it seems to oxidize quickly at room temperature and when it is embedded in vesicles it needs to be stable for at least a few hours at room temperature to allow for the time it takes to process the vesicles and for the experiments to be run.

This has lead to a slight change in design in which the cysteine is attached through a carbamate linkeage. The following scheme shows how this new thiol (**9**) is

obtained. After having been through the vesicle making process it retained most of its activity (around 70%), as was determined by reaction with Ellman's reagent.

Figure 48. Reaction scheme for the synthesis of the carbamate linked thiol **9**.

IV-2 Experiments for the reactions at the interface

First the method used to determine the concentration of the embedded molecules will be discussed. Given that thiols **8** and **9** and disulfide **7** are likely to be as unstable as their water soluble equivalents due to oxidation and disproportionation respectively, the final amount of embedded molecules needs to be determined after the vesicles have been prepared.

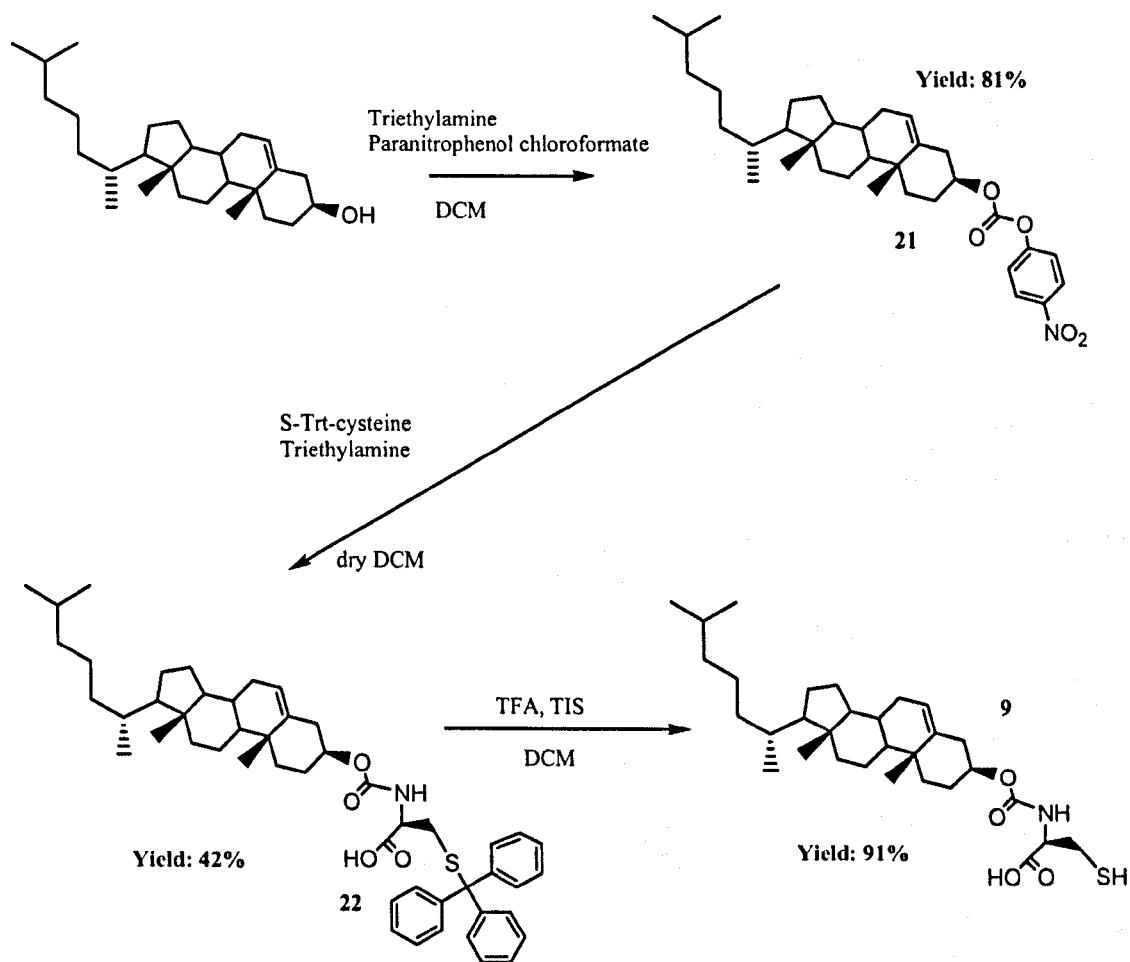250 μL of the vesicles solution containing disulfide was mixed with 750 μL of MES buffer. Then 10 μL of a concentrated solution of DTT were added to the vesicle solution. The increase in absorbance at 341 nm corresponds to the amount of pyridinethiol released. Each disulfide releases one pyridinethiol molecule so with the absorbance of the pyridinethiol at 341 nm being 8220 M.cm^{-1} we can calculate the amount of disulfide present.

250 μL of the vesicle solution containing thiol was mixed with 750 μL of MES buffer. Then 200 μL of a saturated solution of Ellman's reagent was added to the solution. The increases in absorbance at 420 and 600 nm are monitored. One TNB molecule is released for each thiol and absorbs at 420 nm. Due to the large amount of solution added we use the difference in increase in absorbance between 420 nm and 600 nm to determine the amount of thiol present.

IV-2-1 Reaction of 2,2'-dithiodipyridine (18) in a solution containing blank vesicles with an excess of phosphine (17)

The aim of this experiment is to determine the effect the presence of blank vesicles has on the reaction between 2,2'-dithiodipyridine **18** and water soluble phosphine **17**. We can then compare the kinetic data calculated to the ones obtained in the solution studies (chapter 3). The issue here is that 2,2'-dithiodipyridine **18** could partition between the solution and the vesicles membrane.

In order to prepare the vesicles needed for this study, a stock solution of 2,2'-dithiodipyridine **18** was prepared by dissolving an amount of the symmetric disulfide measured by weight in a known amount of MES buffer: 47 mg in 4 mL which gives a concentration of 53.2 mM. The volume required of the latter solution was added to the EYPC in order to obtain a concentration of 0.2 mM of the disulfide and 4 mM in lipid in the stock vesicle solution. This solution is then used in the stopped flow as the oxidant solution that reacts with the reductant, i.e. the water soluble phosphine.

The following graph (Figure 49) shows an example of a curve obtained from the stopped flow and the two exponentials curve fit associated.
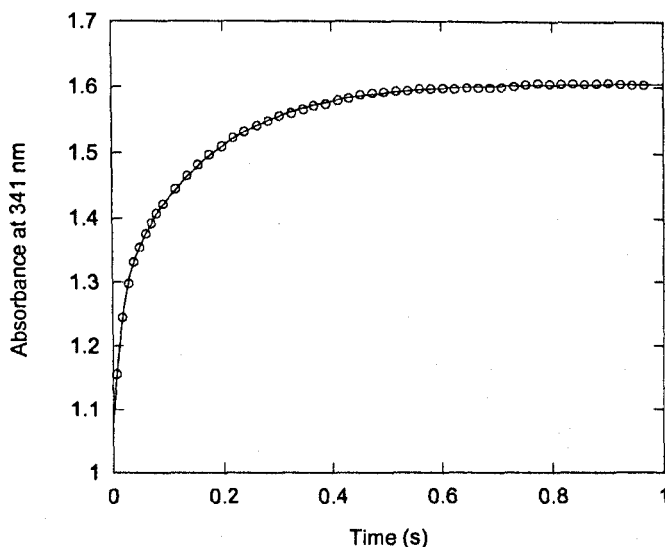
Figure 49. Stopped flow data (open circles) of which only a fraction is represented for readability and the curve fit (solid line) which corresponds to two consecutive first order reaction with $k_1 = 65.2 \pm 0.3$ s^{-1} and $k_2 = 6.07 \pm 0.01$ s^{-1}.

The different rate constants are then plotted against the concentration of the reactant in excess, in this case the phosphine. The slope of the latter gives the second order rate constant for the studies reaction. The results obtained are given in the two graphs below (Figures 50 and 51).

71
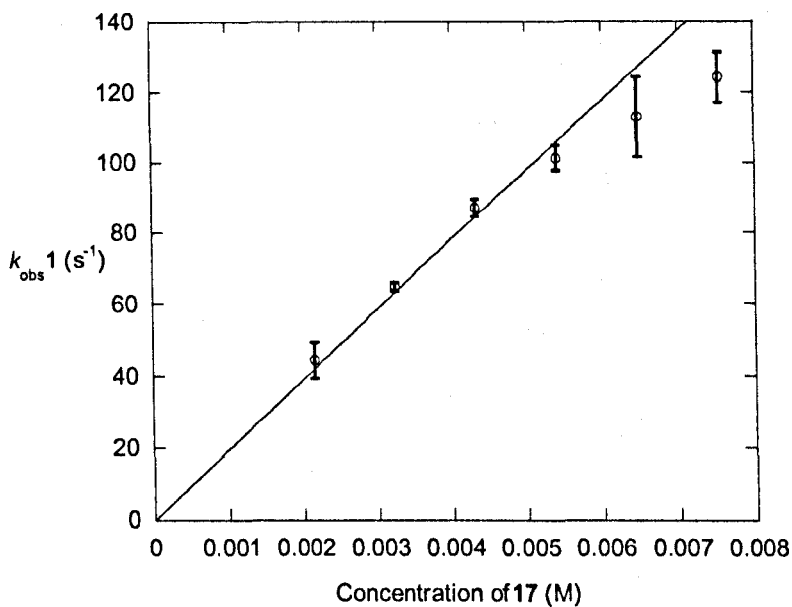
Figure 50. This graph represents the data for the first rate constant (open circles) and the fit corresponds to a linear fit through the origin. The second order rate constant obtained is $k = 19600 \pm 260 \ M^{-1} \ s^{-1}$.
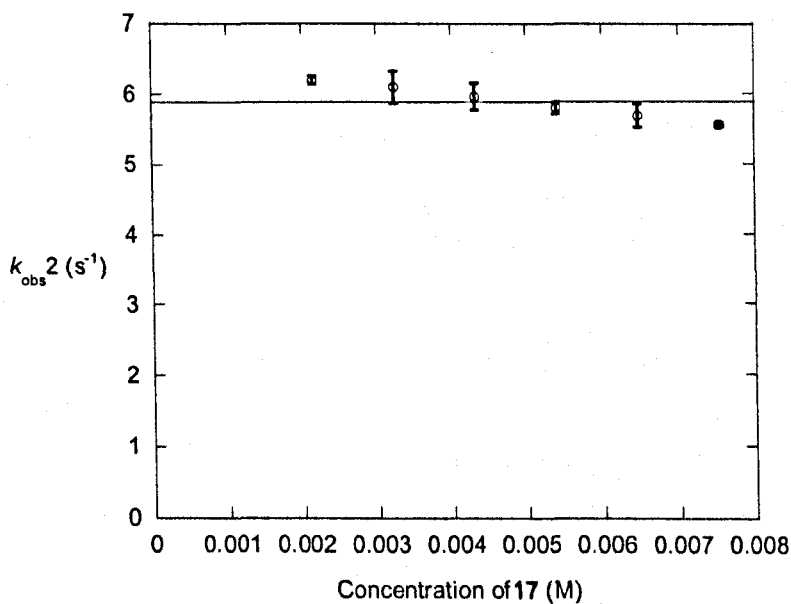
Figure 51. This graph represents the data for the second rate constant obtained from the fit as given in example in Figure 90 (open circles), the solid line is the fit to a constant. The first order rate constant calculated is $5.9 \pm 0.1 \ s^{-1}$.

The second order rate constant ($20000 \ M^{-1} \ s^{-1}$) and the first order one ($5.9 \ s^{-1}$) obtained are in very good agreement with the ones obtained in solution ($21000 \ M^{-1} \ s^{-1}$ and $5.9 \ s^{-1}$). Moreover the facts that the first rate constant is a second order one and that the second rate constant is first order are consistent with the results obtained in solution. This strongly indicates that the vesicles do not influence the reactivity of the symmetrical disulfide with the water soluble phosphine 17. This indicates that there is no partitioning of 2,2'-dithiodipyridine or at least that the partitioning of the disulfide does not significantly modify the rate of its reaction with the phosphine 17.

IV-2-2 Reaction of disulfide (7) embedded within vesicles with an excess of phosphine (17)

The aim of this experiment is to determine to the influence of the vesicles on the reaction between the water soluble phosphine 17 and disulfide 7 when the latter is embedded in the vesicle membrane via a cholesterol moiety.

Vesicles have been prepared as described in the experimental section. Disulfide was embedded in the vesicles so as to obtain a concentration of 4mM of lipid and 200 μM of disulfides. The amount of disulfide was calibrated using an excess of dithiothreitol and was found to be 189 μM. The vesicle solution was then reacted with different amount of phosphine 17 in excess in stopped flow covering the range of concentration from 0.69 mM to 4.11 mM for a disulfide concentration of 50 μM (lipid 1 mM) and 25 μM (lipid 0.5 mM).

The following graph gives an example of the curve obtained. It is clear from the shape of the curve that a complex set of reactions is happening. At least two stages can be clearly seen on the graph: a rapid phase that accounts for approximately a third of the increase in absorbance and a slow phase that accounts for approximately two thirds of the increase (see Figure 52 below). The phosphine 17 in excess increases the absorption over the whole range of wavelengths and hence is added to the increase due to the release of pyridinethiol.
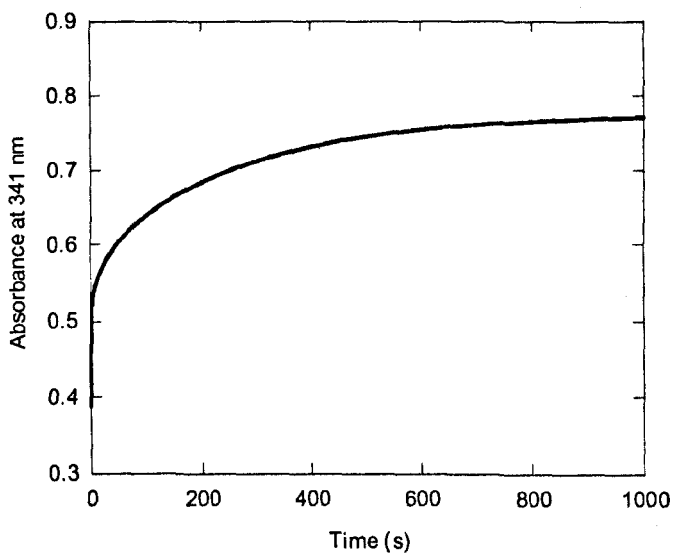
Figure 52. Typical curve for the reaction between disulfide **7** embedded vesicles and an excess of water soluble phosphine. Here the concentrations are the following: 1 mM of lipid with 50 μM of disulfide plus 1.37 mM of phosphine **17**.

If the two processes (rapid and slow) are separated, the curve can be fitted to exponentials and an indication of the rates for the reactions involved is thus obtained. The curve obtained can be divided into four steps, each of which can be fitted to a single exponential.
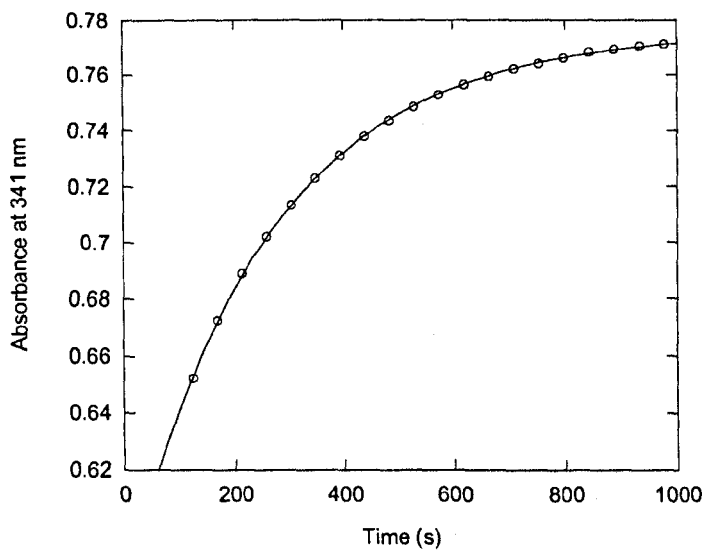
Figure 53. This graph gives an example of first order fit (solid line, $k = 3.7 \times 10^{-3} \pm 0.1 \times 10^{-3} \text{ s}^{-1}$) for the last part of the curve given in graph 11 (open circles).

On Figure 53 the fit for the last part of the curve is shown, other earlier parts of the curves can also be fitted to a first order mechanism. Each rate constant is then plotted against the concentration of the reactant in excess, in this case the water soluble phosphine **17**. The following four Figures (54, 55, 56 and 57) give the results obtained for the four rate constants calculated versus the concentration of phosphine **17**.
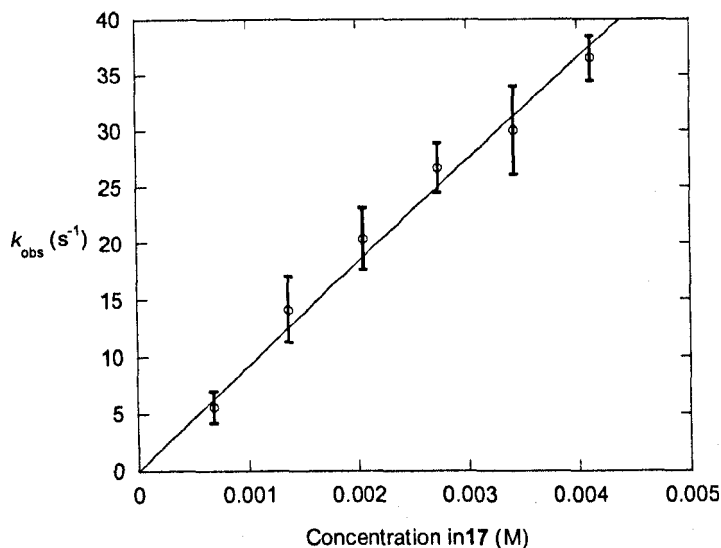
Figure 54. Relation between the first order rate constant and the concentration of phosphine **17** for the earliest part of the reaction. The solid line is the linear fit with a slope of $9140 \pm 190 \text{ M}^{-1} \text{ s}^{-1}$, which gives the second order rate constant for this step.
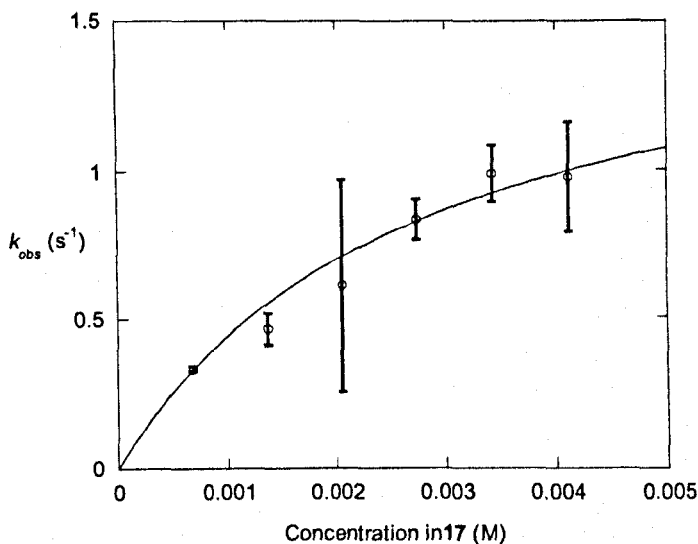
Figure 55. Relation between the first order rate constant and the concentration of phosphine **17** for the second part of the reaction. The fit (solid line) corresponds to a saturation curve, i.e. there is a non reactive interaction between the reactants ($k=1.7 \pm 0.3 \text{ s}^{-1}$ and $K=2.8 \pm 0.5$ mM), with a second order rate constant of $600 \pm 150 \text{ M}^{-1} \text{ s}^{-1}$.

Figure 56. Relation between the first order rate constant calculated from the fit and the concentration of phosphine **17** for the third part of the reaction.

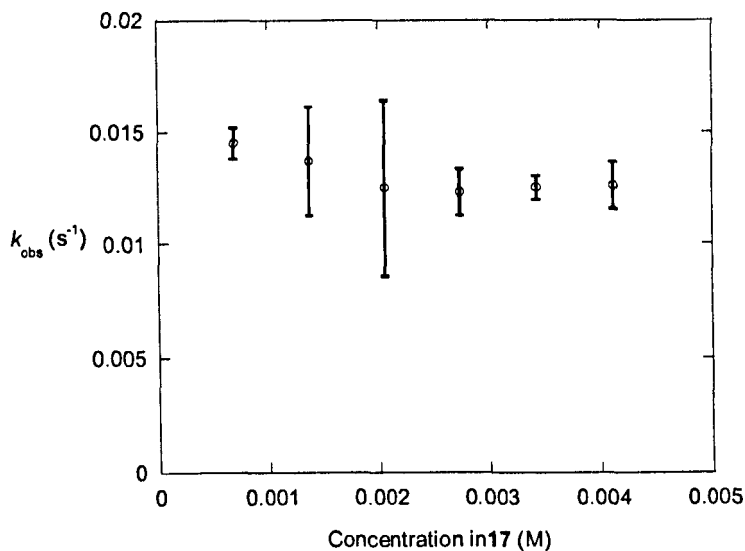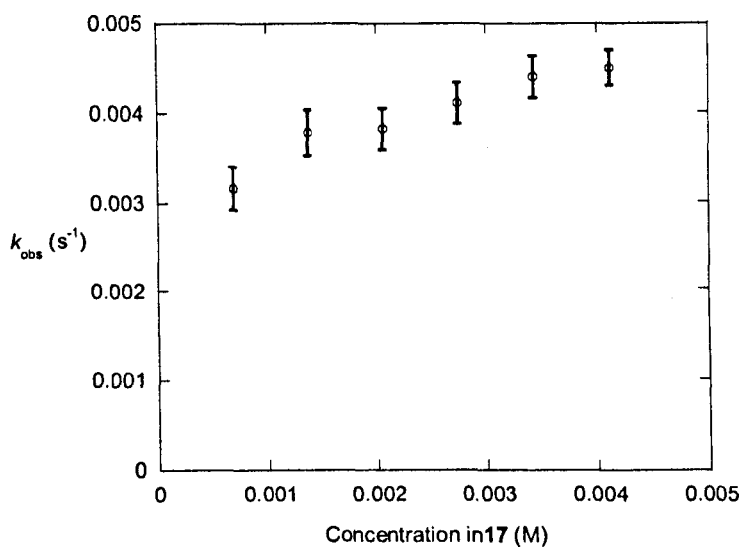**Figure 57.** Relation between the first order rate constant calculated from the fit and the concentration of phosphine **17** for the last part of the reaction.

The relation between the rates and the phosphine concentration offers an insight into the mechanism and the species involved in the different steps.

The first reaction represented by the relation in Figure 54 seems to be the reaction between 2,2'-dithiodipyridine **18** with the phosphine **17**. The rate calculated is very similar to the ones obtained for the reaction between this symmetrical disulfide and the phosphine in solution and for the same disulfide with phosphine in a suspension of vesicles.

The second reaction seems to be the reaction between the embedded asymmetric disulfide with the phosphine (Figure 55). The rate is comparable to the one calculated for the similar reaction in solution. Moreover the fact that the relation between the rate and the concentration of phosphine reaches a maximum indicates an interaction between the two reactants. This is a pattern we saw previously for the reaction between the positively charged asymmetric disulfide and the negatively charged phosphine.

The third and fourth reactions are less clear (Figures 56 and 57). The rate constants are more or less constants over the range of phosphine concentration used. Several reaction steps could account for the rates obtained. The first one is the reaction of the phosphonium adduct, from the reaction with the symmetrical disulfide, with water. It was shown in chapter 3 that this reaction is independent of the concentration of the phosphine. This phosphonium could also come from the reaction between the phosphine and the asymmetric disulfide (Figure 58 below). The increase in absorbance could also be due to the effect the phosphine in excess has on the vesicles, as will be described below in the next experiment.
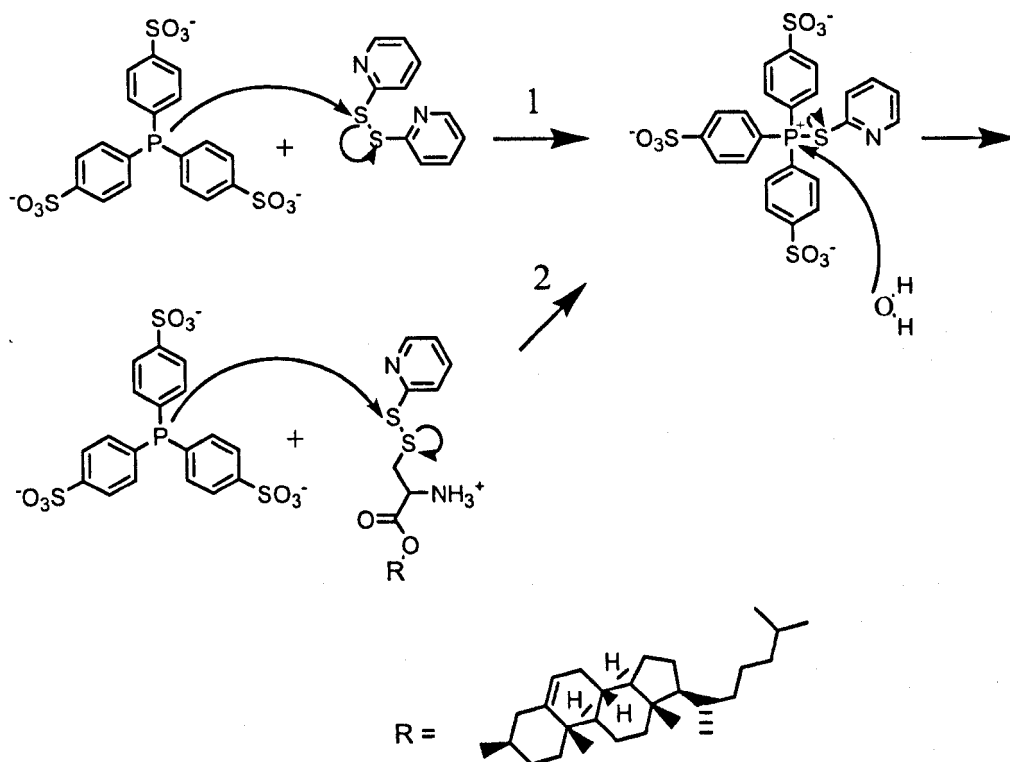
Figure 58. The above scheme represents the two routes that can lead to the formation of the phosphonium.

IV-2-3 Mixture of blank vesicles with high concentration of phosphine (17)

To assess the effect of the phosphine on the vesicles, the following experiments were carried out. Blank vesicles, i.e. vesicles without any embedded molecules, were prepared using the standard method. Several equivalent of phosphine as compared to the amount of phosphatidylcholine were subsequently added to the vesicles. The results obtained are shown in the graph below (Figure 59).
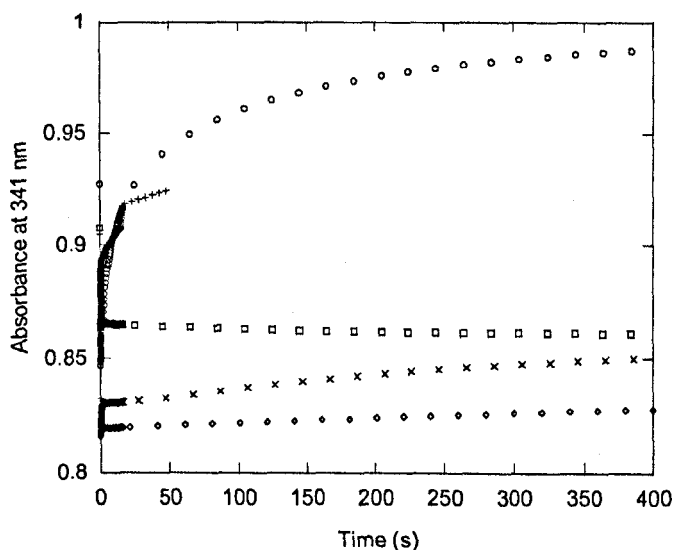
Figure 59. Changes in absorbance when phosphine **17** is added to a 1 mM solution of lipids. The different concentrations of phosphine are: 0 (open circles), 1.2 mM (open squares), 2.3 mM (open losanges), 4.7 mM (diagonal crosses) and 5.8 mM (vertical crosses). Only 5% of the data gathered are shown, except for the data related to the phosphine concentration of 5.8 mM for which 20% of the data are shown. Each data shown is the average of three gathered at identical concentrations of phosphine and lipids.

From the results shown above in Figure 59, no obvious explanations can be found to explain the behaviour observed. However it seems that upon closer examination a pattern evolves. The absorbance of the vesicles increases when they are diluted with buffer (open circles data on Figure 59), however this effect is not observed when approximately an equivalent of phosphine is added as compared to the amount of phosphatidylcholine. When the amount of phosphine is further increased the increase in absorbance appears again.

This is probably due to the negatively charged phosphine interacting with the outer layer of lipids on the vesicles. First the phosphine might act as a repulsive counter ion, hence keeping the vesicles stable and preventing interactions and fusions between each other. When more equivalents of phosphine are added to the system, this might

disrupt the stability of the vesicles and allow them to interact with each other, thus modifying the absorption.

IV-2-4 Reaction of disulfide (7) embedded within vesicles with an excess of DTT (16)

The aim of this experiment is to continue the previous experiment about the influence of the vesicles on the reduction of disulfide 7, this time the reductant being dithiothreitol 16.

The vesicles containing the asymmetric disulfide with the cholesterol moiety are prepared as described before. The amount of disulfide is calibrated using an excess of dithiothreitol 16 and was found to be 197 μM in the stock solution with a concentration of 4 mM of lipid.

The solution is then reacted with an excess of dithiothreitol 16 in the stopped flow with various ratio of dithiothreitol 16 to disulfide. The curves are then analysed as is shown on Figure 60 below. By fitting the curve to a first order mechanism a first order rate constant is obtained.
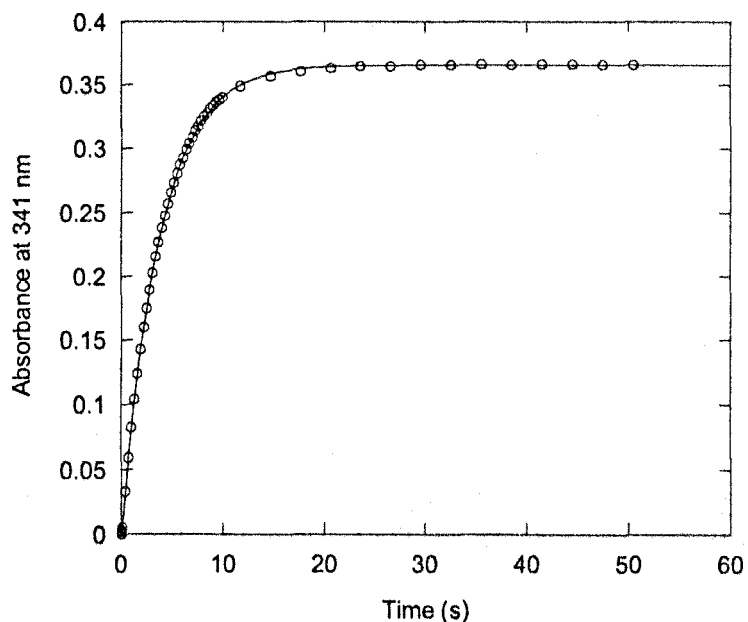
Figure 60. Curve obtained for a concentration of dithiothreitol **16** of 14.5 mM reacting with a vesicle solution (1mM lipid) containing 49 µM of asymmetric disulfide embedded within (open circles). The first order fit is represented by the solid line and corresponds to a rate constant of 0.27 ± 0.01 s^{-1}.

All the rates are then plotted against the concentration of dithiothreitol **16** since it is the reactant in excess. The following graph (Figure 61) sums up all the data obtained and the second order rate constant calculated from the fit of the curve following a non reactive interaction between the reactants.

Figure 61. This graph presents all the data obtained for the reaction between the dithiothreitol and the embedded disulfide (open circles). The fit (solid line) corresponds to a non reactive interaction between the reactant before the reaction occurs and gives a second order rate constant of k = 24 ± 2 M^{-1} s^{-1}.

The value obtained, k = 24 ± 2 M^{-1} s^{-1}, is very similar to the one obtained in solution with the water soluble asymmetric disulfide with a second order rate of 29 ± 2 M^{-1} s^{-1}. Hence the presence of the vesicles does not seem to significantly influence the rate of the reaction.

IV-2-5 Reaction of disulfide (7) embedded within vesicles with an excess of cysteine ethyl ester hydrochloride (13)

The aim of this experiment is to continue the previous experiment about the influence of the vesicle on the reduction of disulfide **7**, this time the reductant being cysteine ethyl ester hydrochloride **13**.

The vesicles containing the asymmetric disulfide with the cholesterol moiety are prepared as described before. The amount of disulfide is calibrated using an excess of dithiothreitol **16** and was found to be 177 µM in the stock solution with a concentration of 4 mM of lipid.

The solution is then reacted with an excess of cysteine ethyl ester hydrochloride **13** in the stopped flow with various ratio of **13** to disulfide. The curves are then analysed as is shown on Figure 62. By fitting the curve to a two exponentials fit, two first order rate constants are obtained.
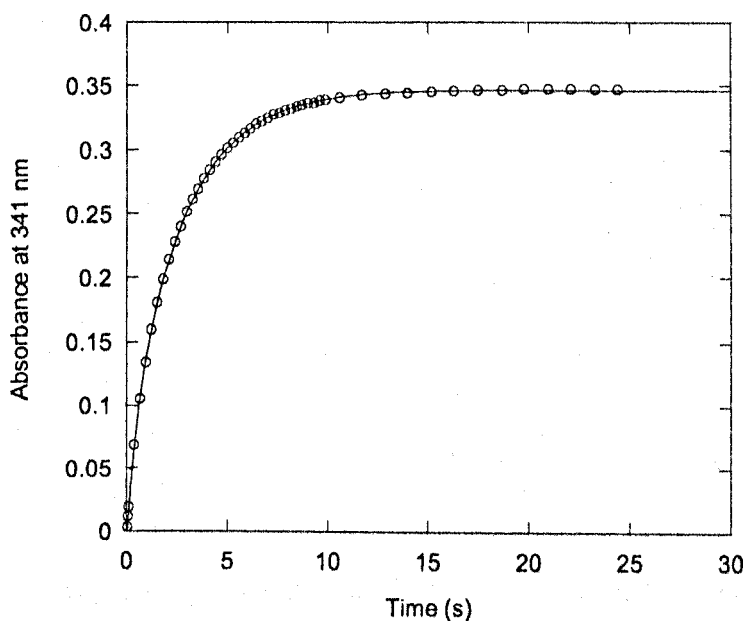
Figure 62. Data (open circles) obtained from the reaction between 9.975 mM of **13** and 44 μM of asymmetric disulfide **7** in 1 mM of lipid. The fit (solid line) corresponds to two consecutive first order reactions with rate constants of 2.19 ± 0.01 s^{-1} and 0.37 ± 0.01 s^{-1}.

All the rates are then plotted against the concentration of cysteine ethyl ester hydrochloride **13** since it is the reactant in excess. The following graphs (Figures 63 and 64) sum up all the data obtained and the second order rate constants calculated from the fit of the curve following a non reactive interaction between the reactants.
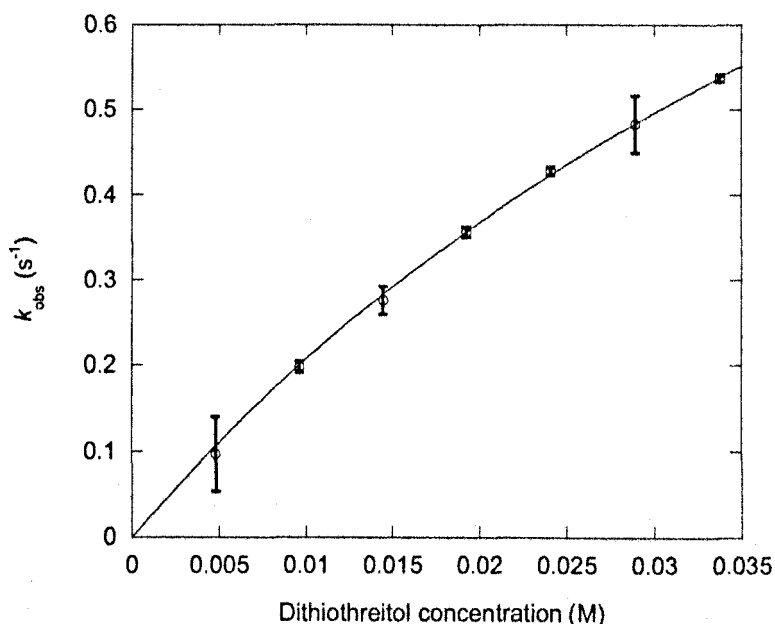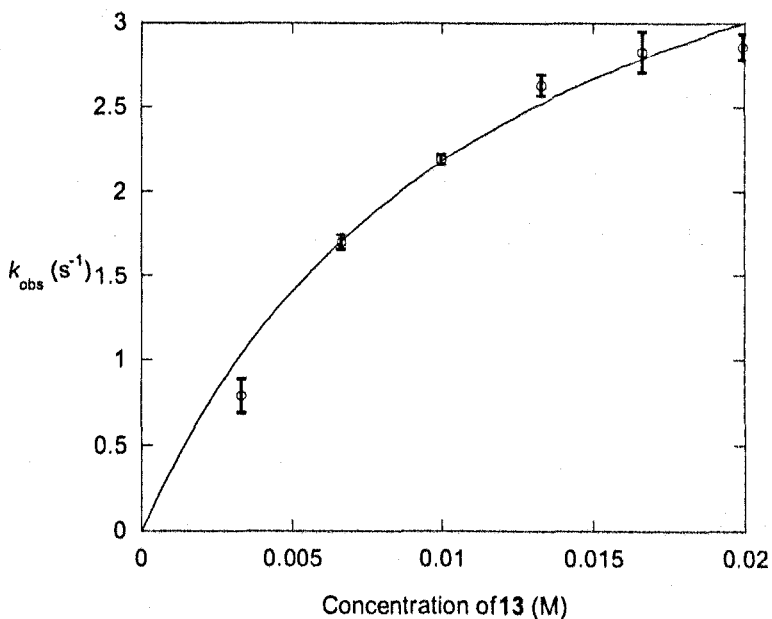
Figure 63. Data obtained for the first reaction (open circles). The fit (solid line) corresponds to a non reactive interaction between the reactant before the reaction occurs and gives a second order rate constant of $k = 400 \pm 50 \ \text{M}^{-1} \ \text{s}^{-1}$.
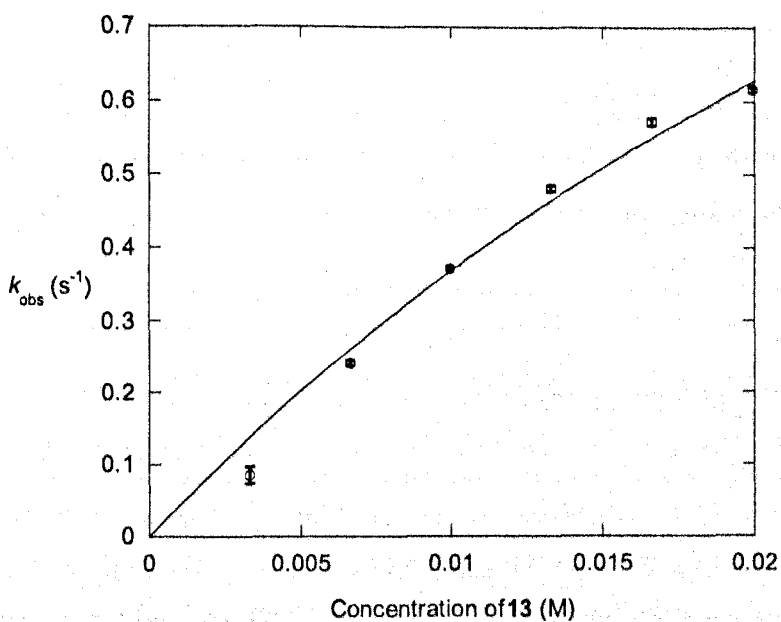
Figure 64. Data obtained for the second reaction (open circles). The fit (solid line) corresponds to a non reactive interaction between the reactant before the reaction occurs and gives a second order rate constant of $k = 45 \pm 3 \ \text{M}^{-1} \ \text{s}^{-1}$.

The first reaction is likely to involve cysteine ethyl ester hydrochloride **13** and 2,2'-dithiodipyridine **18** as an impurity due to the fact that in the fit the increase in absorbance related to this reaction accounts only for approximately 20 % of the total increase. Moreover the rates (400 ± 50 and 45 ± 3 M^{-1} s^{-1}) are similar to the ones obtained for the reaction between the cysteine ethyl ester hydrochloride **13** and 2,2'-dithiodipyridine **18** (900 ± 11 and 130 ± 2 M^{-1} s^{-1}), the second lower rate constant (130 ± 2 M^{-1} s^{-1}) representing the reaction between the intermediate asymmetric disulfide and cysteine ethyl ester hydrochloride **13**. The presence of the vesicles seems to slightly lower the rates of reaction when compared to the similar reactions in solution.

IV-2-6 Reaction of disulfide (7) embedded within vesicles with an excess of 2-ethoxycarbonylamino-3-mercapto-propionic acid (14)

This is the last experiment looking at the disulfide **7** embedded vesicles reacting with an excess of reductant. The reductant here is the synthesized water soluble thiol with an acid group instead of the amino group as the charged side group.

The vesicles containing the asymmetric disulfide with the cholesterol moiety are prepared as described before. The amount of disulfide is calibrated using an excess of dithiothreitol and was found to be 159 µM in the stock solution with a concentration of 4 mM of lipid.
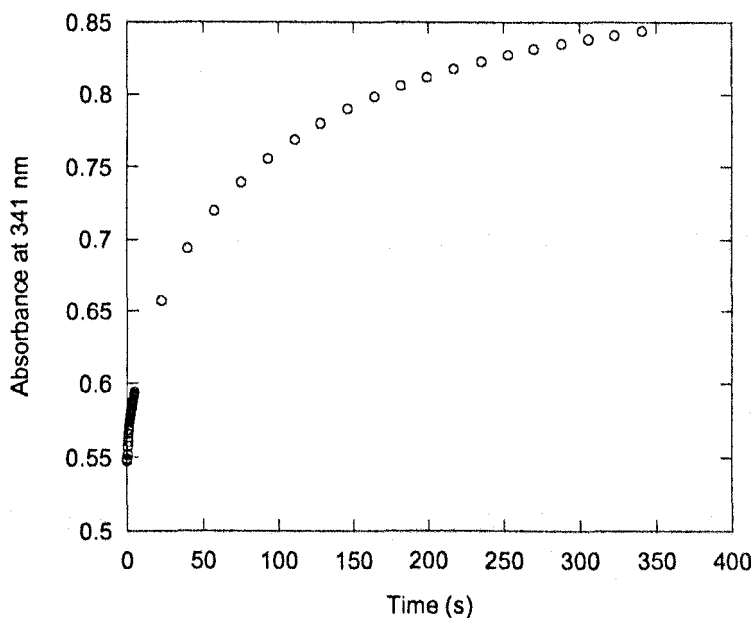
Figure 65. Increase in absorbance when 5.8 mM of **14** reacts with 20μM of **7** embedded within 0.5 mM of lipid.

No proper fit has been found for the reaction between the vesicle embedded disulfide and the reductant. Hence no second order rate constant was obtained. Nevertheless the time scale of the reaction gives us an indication about the speed of the reaction in the conditions used. It is clear that it is much slower, at least 20 times, than the identical reaction with the cysteine ethyl ester hydrochloride. This is probably due to the difference in pK_a between the two molecules, 7.45 for the cysteine ethyl ester hydrochloride and 9.6 for the reductant used in this experiment [60].

IV-2-7 First experiment to determine whether the thiol-disulfide exchange occurs intravesicularly

In the previous experiments we were trying to gain a better understanding of the reaction at the vesicular interface where one of the reactants is embedded within vesicles with the aim to compare it with the identical reaction in solution as determined in chapter 3. Now to continue further, we want to study the reaction between two molecules embedded within the vesicle membrane by synthesizing the thiol in situ by reduction of the embedded disulfide **7** with non membrane crossing phosphine **17**. Then

thiol **8** synthesized in situ should react with the disulfide remaining. After allowing enough time for the reaction to occur to completion, the remaining amount of disulfide is determined by adding membrane crossing reductant DTT **16**.

To a solution of 1 mM lipid with 50 μM of disulfide **7** embedded within was added a quarter of an equivalent of water soluble phosphine **17**. On completion of the reaction an excess of DTT **16** was added in order to determine how much of the disulfide was left. The data gathered are shown below on Figure 66. The reaction was followed at 341 nm which is the absorption maximum for the pyridinethiol that will be released from the reduction of the disulfide by PPh3 **17** and from the thiol-disulfide exchange at the interface. It is also followed at 450 nm as this is further away from the scattering of the vesicles, which diminishes with increasing wavelengths. The comparison between the two sets of data enables us to determine if the jumps in absorbance are due to a release of the pyridinethiol or not. If pyridinethiol is a product of the reaction, an increase in absorbance would only be seen at 341 nm. If however the jump is similar in size at both wavelengths, this means that the vesicles have been affected by the process they underwent, i.e. they have increased in size and their scattering have increased over the whole spectrum.
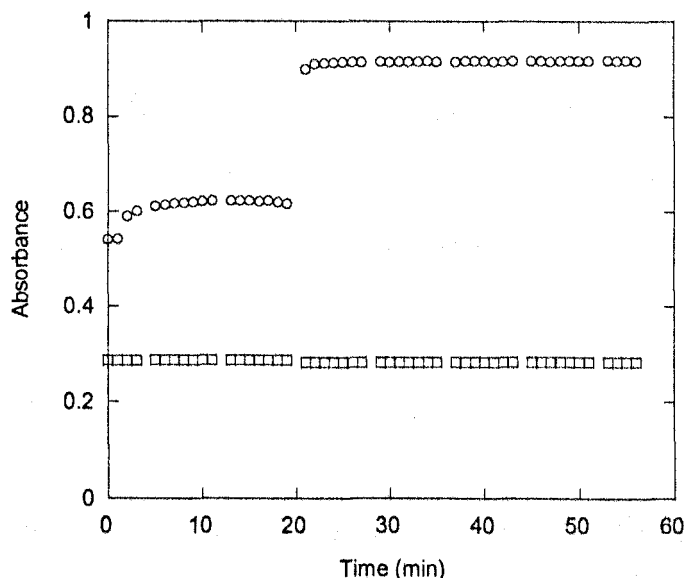
Figure 66. Evolution of the absorbance of a solution of 1 mM of lipid containing 50 μM of disulfide 7 when 12 μM of PPh3 is added (at t = 2 min), then an excess of DTT is added (at t = 20 min). The open squares and the open circles represent the reaction followed at 450 nm and 314 nm respectively.

The first increase in absorbance immediately following the addition of the water soluble phosphine as the limiting reagent corresponds to the release of 10 μM of pyridinethiol. The second jump which follows the addition of DTT in excess corresponds to the release of 37 μM of pyridinethiol. Hence the first jump accounts for 21 % of the total release of pyridinethiol and the second one for 78 %. This indicates that the addition of a quarter of an equivalent of water soluble phosphine only releases a quarter of an equivalent of the signaling molecule. Either the intravesicular reaction between the remaining disulfide on the outside and the thiol generated by the phosphine is slow or the reaction between the phosphine and the disulfide does not go to completion and is stopped at a non reactive species.

IV-2-8 Intravesicular experiments using sequential additions of limiting quantities of water soluble phosphine

The aim of this experiment is to determine if the intravesicular reaction between the thiol **8** generated by the disulfide **7** reduction by phosphine and the remaining disulfide **7** is fast. In order to determine this, vesicles containing disulfides were prepared as usual. The phosphine solution was calibrated using Ellman's reagent.

In order to determine what is happening at the interface when PPh3 is added, the aim of this experiment is to add a quarter of an equivalent of PPh3 (compared to the amount of disulfide at the start of the experiment) sequentially after each previous one has reacted completely. If the reaction between the thiol and disulfide occurs after the thiol has been synthesized in situ and considering that PPh3 does not cross the vesicle bilayer, nothing should happen when the second addition of phosphine is made.

To a solution of 1 mM lipid containing 50 µM of disulfide was added a quarter of equivalent of water soluble phosphine. The addition of the same amount of phosphine was repeated three times. A fifth addition was made with an excess of phosphine to check the amount of disulfide left.

The graph obtained is shown below.
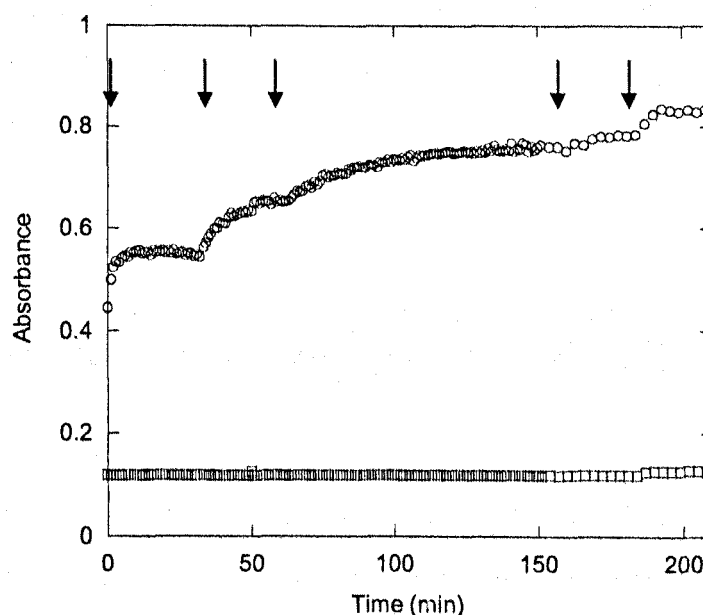
Figure 67. Evolution of the absorbance of a solution of 1 mM of lipid containing 50 μM of disulfide **7** when several additions of a quarter of an equivalent of phosphine are made. The open squares and the open circles represent the reaction followed at 600 nm and 341 nm respectively. The arrows represent the additions of phosphine.

250 μL of the disulfide containing vesicle solution was mixed with 750 μL MES buffer. The solution was scanned once then 0.5 μL of the phosphine solution was added. Subsequent additions of 0.5 μL of phosphine were made after each previous complete reaction.

The first three increases in absorbance are identical and corresponds respectively to 14 μM, 13 μM and 14 μM of disulfide. The fourth one however corresponds to only 4 μM of disulfide. The first two take 30 minutes to complete, the third one 100 minutes. The fourth one 24 minutes but there was still some disulfides as can be shown by the fifth addition of concentrated phosphine. This indicates that the phosphine's attack of the disulfide embedded within the inner membrane of the lipid vesicles is hindered by the membrane itself.

This experiment indicates that either the phosphine releases a thiol and the reaction between thiol and disulfide in the membrane is slow, or that the phosphonium intermediate that forms during the phosphine attack is not reactive. Moreover the fact that the phosphine added after all the outer layer disulfide should have reacted still caused an increase in absorbance seems to indicate that the disulfide can move between layers to become available for reaction.

IV-2-9 Disulfide (7) embedded vesicles reacting with quarter of an equivalent of phosphine (17), then with an excess of phosphine (17)

The aim of this experiment is to determine if the addition of a quarter of an equivalent of water soluble phosphine compared to the total disulfide 7 embedded in the vesicle will trigger the release of an equimolar amount of pyridinethiol (when compared to the amount of phosphine added) or double that amount.

This depends on the kinetics of the reaction at the vesicle interface between the disulfide still present and the thiol formed. This is shown on the following figure.
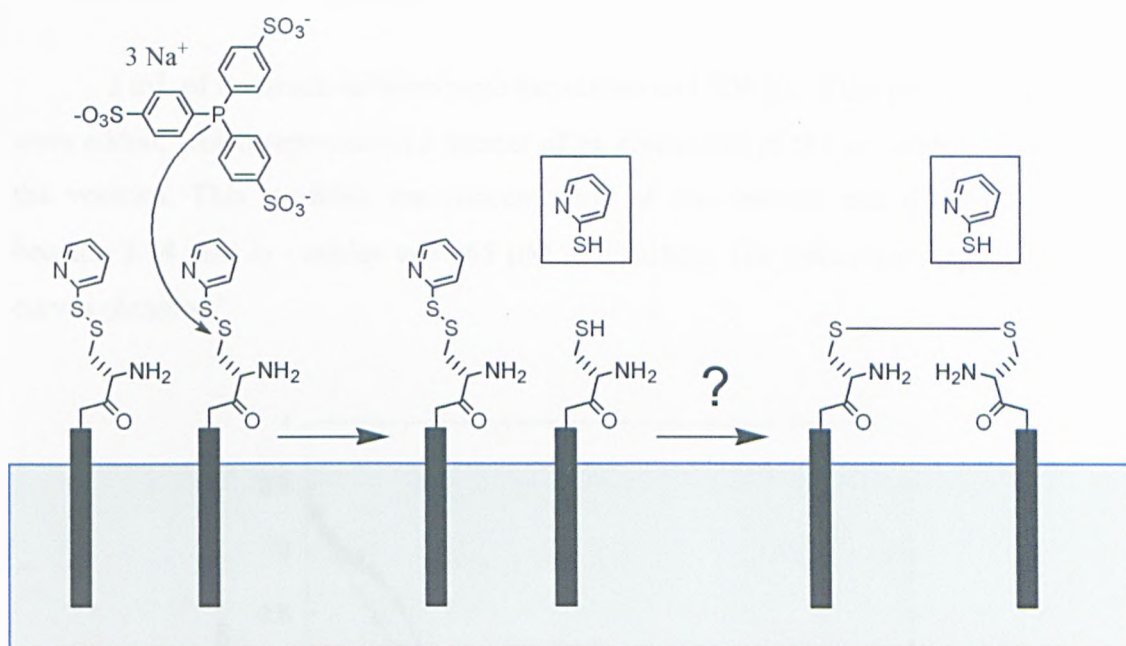
Figure 68. Events that happen at the vesicle interface when water soluble phosphine reacts with an embedded disulfide. The first reaction gives a pyridinethiol moiety. In case the intravesicular reaction between the disulfide left and the thiol produced is slow coinpared to the first one the subsequent reaction does not generate enough chromophore for rate constant measurement purposes in the time scales used. Hence only an equivalent of pyridinethiol is released. In case the intravesicular reaction is of a similar or superior rate the second reaction will occur and two equivalents of pyridinethiol will be obtained per water soluble phosphine.

A DTT solution was prepared by dissolving 21 mg in 0.2 mL of MES buffer to obtain a concentration of 690 mM. The water soluble phosphine solution was prepared by dissolving 61 mg in 15 mL of MES buffer and then diluting it ten times to obtain a solution of concentration 0.71 mM. The last solution was calibrated using an excess of a saturated Ellman's reagent solution in MES buffer. The phosphine solution was found to be 81% active, hence the real concentration is 0.57 mM.

Disulfide embedded vesicles were prepared as usual and calibrated using the DTT solution. The disulfide concentration was found to be 44 μM in the solution used for the calibration which is the fourth of the stock solution (1 mM lipid concentration). Hence the stock solution (4 mM lipid concentration) has a concentration of 176 μM in disulfide.

3 mL of the stock solution were then taken and 208 µL of the phosphine solution were added, which represented a quarter of an equivalent of the disulfide embedded in the vesicles. This modifies the concentration of the vesicles and disulfides, which become 3.74 mM in vesicles and 165 µM in disulfide. The following graph shows the curves obtained.
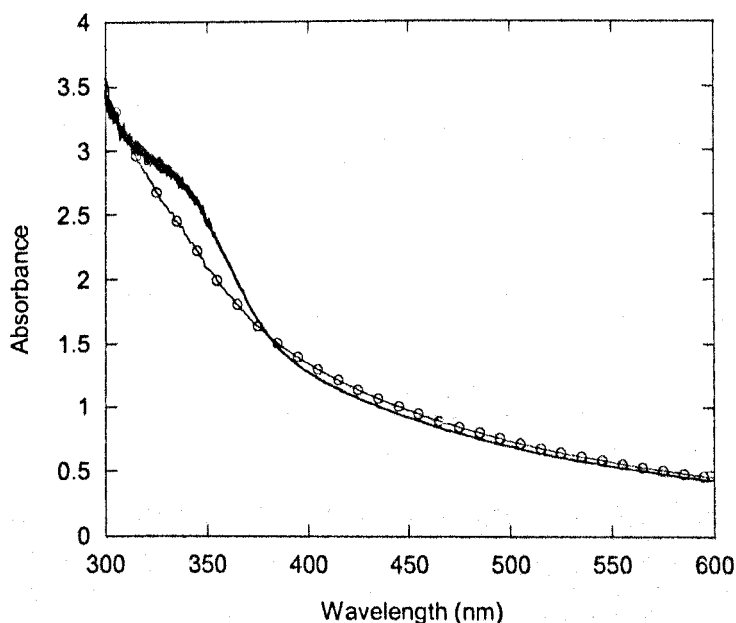
Figure 69. This graph represents the reaction between 3.74 mM vesicles with 165 µM disulfides embedded reacting with 37 µM of phosphine. The line with circles represents the absorption before the addition of phosphine. The increase in absorbance at 341 nm obtained is 0.42.

The obtained vesicle solution half reduced on the outer membrane, i.e. a quarter reduced compared to the total concentration of disulfide, was then introduced in a syringe of the stopped flow machine, the other two being filled with MES buffer and the stock phosphine solution (0.574 mM). The phosphine is not being able to cross the membrane, so if we see a reaction it should mean that there were some disulfide left outside and hence that the intravesicular reaction is slow. The following graph display the results obtained.
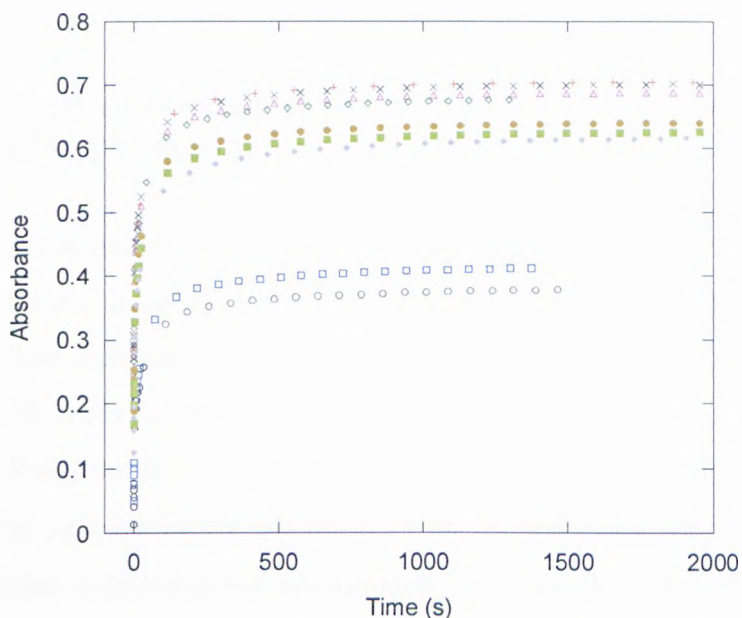
Figure 70. Results obtained for the reaction between the half reduced vesicles on the outer membrane and phosphine 17 in the stopped flow.

On Figure 70 each experiment represents the same concentration of disulfide embedded vesicles and phosphine. The experiments correspond to the mixture of identical volumes of the disulfide embedded vesicles solution, the MES buffer and the phosphine solution. The final concentrations of the vesicles solution and phosphine are respectively 55 μM of disulfide, a quarter or a half of which should have reacted after the first addition of phosphine, in 1.25 mM of lipid and 191 μM of phosphine.

For each experiment the increase in absorbance at 341 nm is much higher than what is expected, i.e. it is always considerably higher than the theoretical maximum: three quarter of the original quantity of disulfide at the start of the experiment. This is probably due to the charges on the phosphine, which may disrupt the vesicles when added in excess.

IV-2-10 Disulfide embedded in vesicles reacting with limiting amount of water soluble phosphine

We also carried out the following experiment in order to determine if the reaction of embedded disulfide **7** and embedded thiol **8** happens on the time scale we are looking at (less than one hour). Here as well thiol **8** is formed in situ by reaction of the disulfide with water soluble phosphine added as a limiting reagent. The amount of water soluble phosphine is increased while the amount of disulfide remains constant at 45 µM (amount determined by calibration with dithiothreitol). The range of water soluble phosphine concentrations (determined by weight) is 4 to 24 µM, which corresponds to 9% to 53% of the total disulfide present in the vesicles. Considering that the water soluble phosphine does not cross the membrane on the time scale used for the experiment, the amount of phosphine represents 18% to 106% of the disulfide present on the outside layer of the vesicles (the only ones accessible to the phosphine).

As is shown on Figure 68 above we want to find out whether the second reaction, between the embedded disulfide and embedded thiol, occurs. If it does not happen on the time scale used for the experiment, the jumps in absorbance at 341 nm due to the release of pyridinethiol will correspond to the concentration of phosphine added. If the thiol-disulfide reaction occurs the pyridinethiol jump will correspond to double the amount of the concentration of phosphine used.

The following graphs show the results obtained.
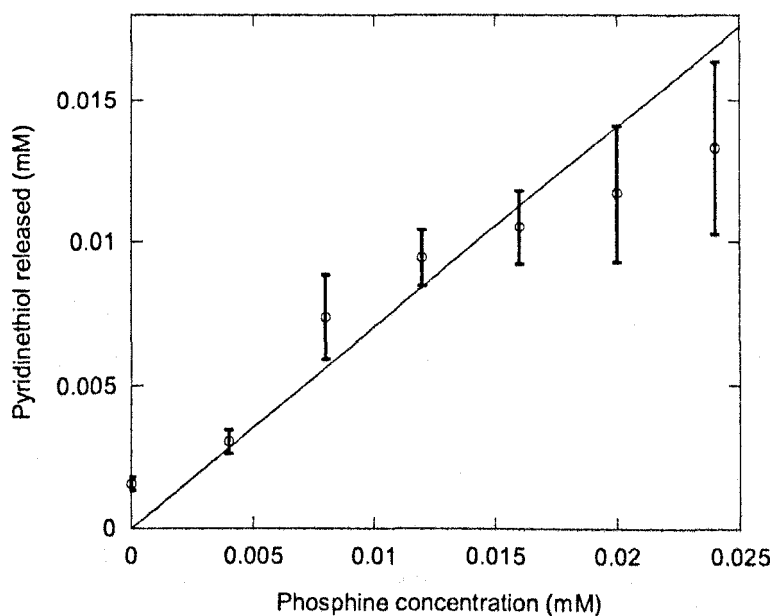
Figure 71. Relation between the concentration of pyridinethiol released versus the amount of phosphine used for the reaction. The line through the origin to which it is fitted gives a slope value of 0.7 ± 0.04.

When plotting the concentration of pyridinethiol versus the amount of phosphine used to react with the disulfide embedded a slope of 0.7 is obtained. This indicates that the reaction between the embedded thiol and the disulfide is not occurring in the conditions used for the experiment. Another explanation would be that the actual concentration of the phosphine in the experiment is lower than the one calculated by weight. However the discrepancy would have to be significant in order to disguise a slope of 2 that would validate the hypothesis of the intervesicular reaction between the embedded thiol and disulfide.

The difference between the addition of an excess of water soluble phosphine and an excess of dithiothreitol to the disulfide embedded vesicles was also investigated. The size of the absorbance jump and the shape of the curve is what interests us. The dithiothreitol should react directly with all the disulfide as it can cross the membrane.

Hence the shape should be a single exponential with the jump corresponding to the entire concentration of embedded disulfide. As regards the reaction involving the water soluble phosphine, the shape should be similar but the amount should be halved as the phosphine cannot cross the membrane. The following three graphs show the results obtained.
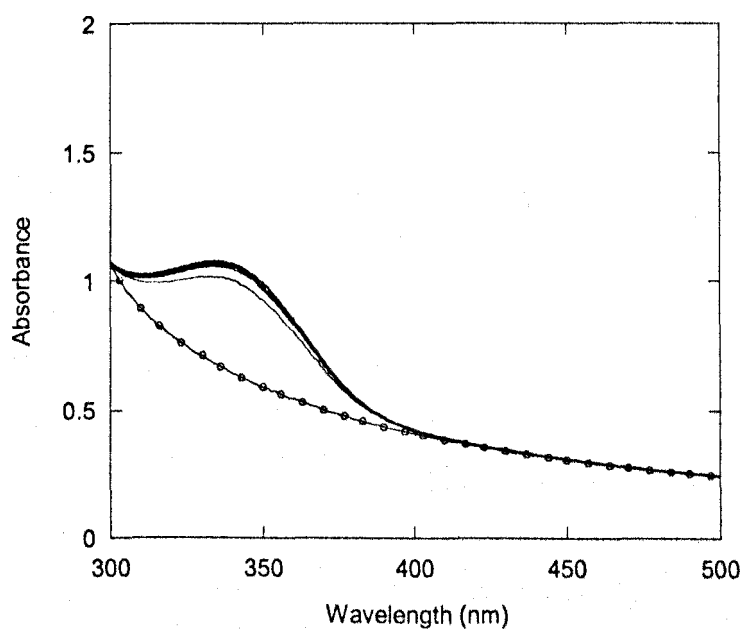
Figure 72. Result of the addition of dithiothreitol in excess to a solution of disulfide embedded vesicles. The time lapse between the spectras can be seen on Figure 74 (open circles).
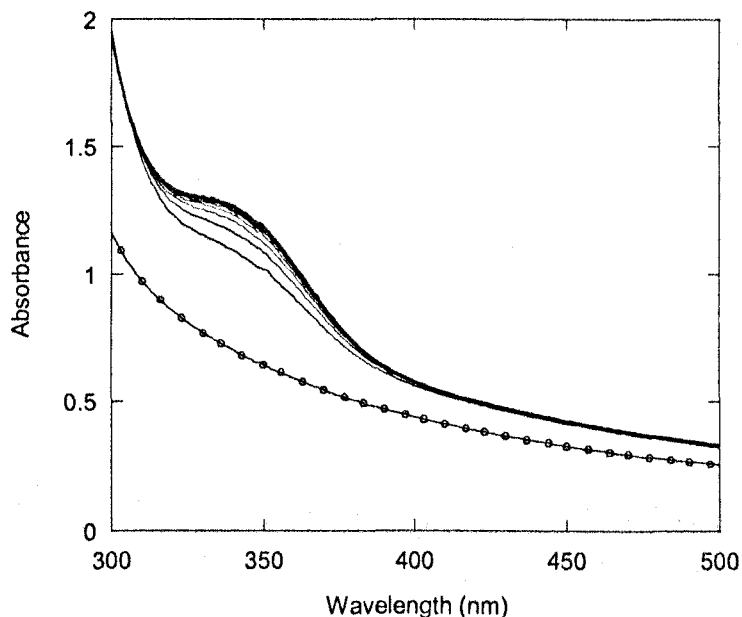
Figure 73. This graph shows the result of the addition of an excess of water soluble phosphine to a solution of disulfide embedded vesicles. The time lapse between the spectras can be seen on Figure 74 (open squares).
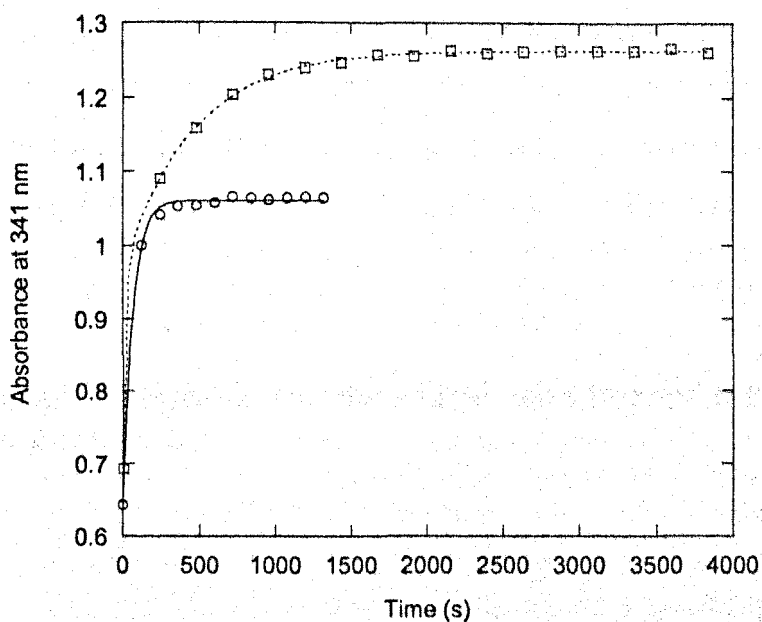
Figure 74. This graph represents the two kinetics at 341 nm for the addition of an excess of dithiothreitol in a solution of disulfide embedded vesicles (circles) and the addition of an excess of water soluble phosphine in a solution of disulfide embedded vesicles (squares). The solid line is a first order fit, whereas the dotted line is a two exponential fit, i.e. two consecutive reactions.

From the results obtained the difference between the two reductants is clear: the reaction involving the dithiothreitol is finished sooner than the phosphine one and it is a simple first order process as opposed to a more complex set of reactions for the phosphine. However Figure 74 shows that the absorbance jump caused by the introduction of phosphine in the vesicles solution is higher than expected. There are two likely explanations for this fact. The first is that the excess phosphine with all its charges disrupts the arrangements of vesicles and hence modifies the overall absorption, which is evidenced in Figure 73 where an increase over the whole range of wavelength can be observed. The second is that the complex processes involved are a first simple fast reaction on the outer layer of the vesicles and a subsequent much slower reaction. The first one is simple as we have previously seen the reaction of disulfide embedded vesicles with limiting amount of phosphine. There might have been intervesicular reaction between embedded thiol and embedded disulfide but this seems unlikely due to the excess of phosphine and the speed of the reduction of disulfide by phosphine as evidenced in chapter 3 for reactions in solutions. The second process could be the permeation of phosphine into the vesicles to react with the remaining disulfide, however this is not possible as the phosphine has been shown not to cross the membrane used even after 24 hours [51]. A more likely explanation is that unreacted disulfide crosses from the inner layer to the outer layer of the vesicle membrane, a process called flip flop.

IV-2-11 A simple experiment to determine whether the intravesicular reaction happens

The aim of this simple experiment is to determine whether the intravesicular reaction shown on Figure 109 above happens. To achieve this, a solution of disulfide 7 embedded vesicles is prepared. A quarter of an equivalent of non membrane crossing water soluble phosphine is subsequently added. As is shown on Figure 109 above, when a quarter of an equivalent of phosphine is added to the vesicle solution this leads to only half the disulfide contained in the outside vesicle layer to react. The thiol formed by the

reduction can then react intravesicularly with the remaining disulfide on the outside. In case this happens the phosphine added should trigger the release of half the total amount of pyridinethiol (the chromophore). In case the reaction is too slow only a quarter of the total amount of pyririnethiol will be released.

In this experiment the disulfide containing vesicle solution is prepared as described earlier. The amount of disulfide is calibrated using an excess of dithiothreitol and was found to be 183 µM in the stock solution with a concentration of 4 mM of lipid.

A solution of phosphine is prepared by dissolving a weighed amount in MES buffer. The solution is then calibrated with Ellman's reagent in order to determine its concentration. The concentration was found to be 11 mM.

The vesicle solution is then diluted four times to obtain a 1 mM vesicle solution containing 41 µM of disulfide. A small amount (less than 2 µL) of the phosphine solution is added to this solution to obtain a concentration of phosphine of 10 µM.
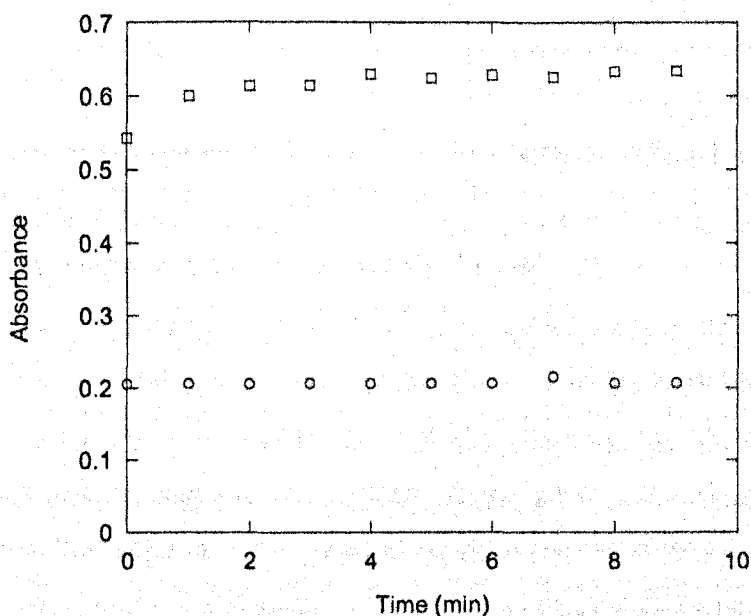

Figure 75. This graph shows the evolution of the absorbance at 341 nm (open squares) and 500 nm (open circles) when a solution of 1 mM vesicle containing 41 µM of disulfide reacts with 10 mM of phosphine.

Figure 75 shows the result obtained. The absorption jump is 0.091, which corresponds to a concentration of pyridinethiol of 11 µM, the absorption coefficient of pyridinethiol being 8220 M^{-1} cm^{-1}. The fact that the absorbance at 500 nm is not modified throughout the experiment indicates that the vesicles are not modified by the introduction of the limiting amount of phosphine. Hence it is clear from this experiment that the intravesicular reaction does not occur in the conditions used for the experiment.

IV-2-12 Determination of the end products

The aim of this experiment is to determine whether or not thiols **8** are present after the reduction of some of the disulfide **7** embedded in vesicles by phosphine. First a vesicle solution prepared as described on page 96 is reduced by a limiting amount of phosphine (a quarter of an equivalent) then Ellman's reagent is added to determine if thiols are present.

The amount of disulfide is calibrated using an excess of dithiothreitol and was found to be 188 µM in the stock solution with a concentration of 4 mM of vesicles.

A solution of phosphine is prepared by dissolving a weighed amount in MES buffer. The solution is then calibrated with Ellman's reagent in order to determine its concentration. The concentration was found to be 11 mM.

A solution of 1 mM of vesicles containing 42 µM of disulfide embedded is prepared by dilution. A small amount (less than 5 µL) of the prepared phosphine solution is added so as to obtain a concentration of phosphine of 10 µM. The reaction is followed between 250 and 600 nm. The appearance of pyridinethiol is followed at 341 nm. When the reduction of the disulfide is finished, as can be seen by the plateau at 341 nm after 4 minutes, 100 µL of a saturated Ellman's reagent solution in MES buffer is added to determine whether thiols are present.
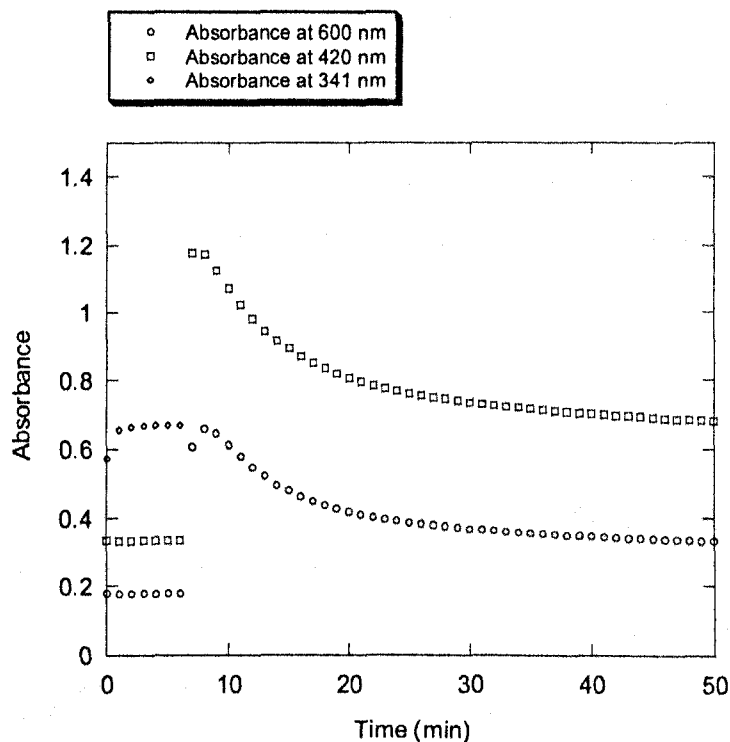
Figure 76. Evolution of the absorbance at 341 nm (open lozanges), 420 nm (open squares) and 600 nm (open circles) when a solution of 1 mM lipid containing 42 μM of disulfide reacts with a quarter of equivalent of phosphine (compared to the amount of disulfide), followed by the addition of an excess of Ellman's reagent. Upon addition of the excess of Ellman's reagent the absorption at 341 nm increases to approximately 3 and is therefore not shown.

An increase in absorbance can be observed over the whole range of wavelengths after the addition of Ellman's reagent (Figure 76). The addition of such a high quantity of solution should have lowered the absorbance at high wavelength due to the dilution. However, even at 600 nm, an increase in absorbance is occurring. After the initial jump the absorption steadily decreases. This is not conclusive as regards the presence of thiols in the solution because the increase is not confined to the wavelengths around 420 nm, the absorption maximum for the thionitrobenzoate ion (the thiol resulting from the reduction of Ellman's reagent). The excess of Ellman's reagent might have an effect similar to the one phosphine has on vesicles, due to the negative charge it bears on each aromatic ring.

IV-2-13 Intravesicular reaction and flip flop parallel experiments

Five 1 mL solutions containing 1 mM of lipid embedded with 50 μM of disulfide **7** were analysed in parallel, following the kinetics at two different wavelengths in order to see the effect on the signaling molecule (341 nm) and on the vesicles (450 nm).

At t=0 a quarter of an equivalent of water soluble phosphine was added in each of the five solutions. After the reaction was finished (about 30 minutes), an excess of concentrated water soluble phosphine was added in the first solution. After about 60 minutes the same excess of phosphine was added in the second solution. The same addition was repeated for the other three solutions at increased times, each new addition separated by approximately half an hour.
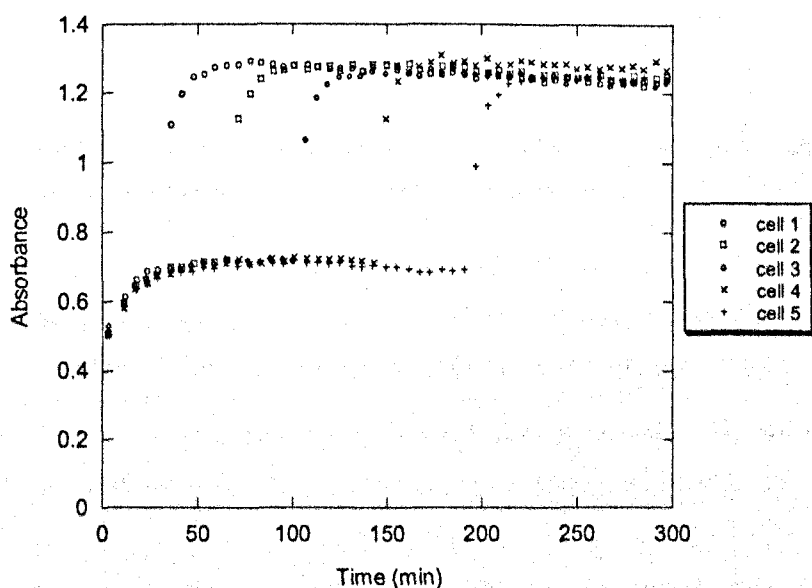
Figure 77. Evolution of the absorbance at 341 nm when five solutions of 1 mM of lipid containing 50 μM of disulfides reacts with a quarter of an equivalent of phosphine at the same time, then an excess of phosphine is added in each solution at different times.

The above shows the curves obtained at 341 nm. The following one shows the same experiments but followed at 450 nm further away from the absorbance peak of the signalling molecule and the scattering of the vesicles.
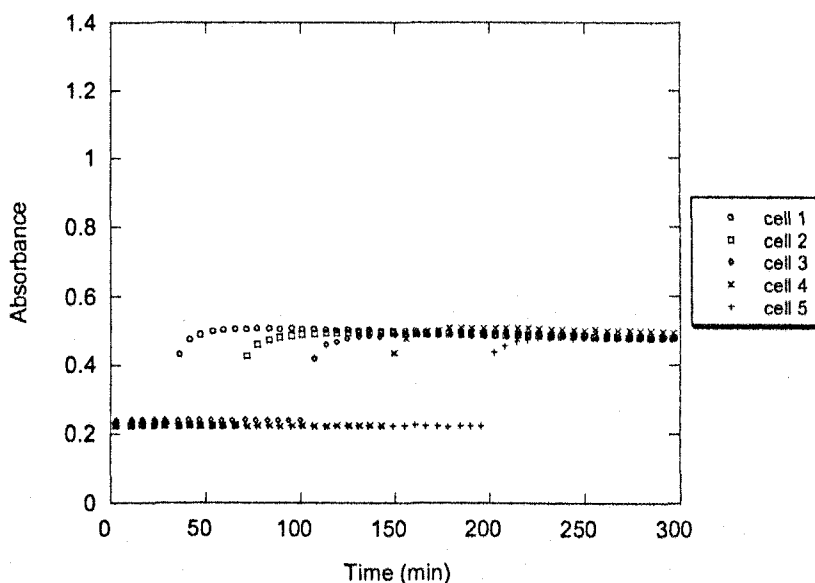
Figure 78. Evolution of the absorbance at 450 nm when five solutions of 1 mM of vesicles containing 50 μM of disulfides reacts with a quarter of an equivalent of phosphine at the same time, then an excess of phosphine is added in each solution at different times.

From the results shown on Figure 77 and 78, we can see that the addition of the quarter of an equivalent of phosphine has triggered an absorbance jump of 0.19, which corresponds to a release of 23 μM of pyridinethiol. However, only 12 μM of phosphine have been introduced in each cell, thus this means that the reduced thiol formed by reduction of the disulfide has reacted with the remaining disulfide since no jump in absorbance indicating a change in vesicle stability can be observed at 450 nm. This finding contradicts all previous results that indicated that no intravesicular thiol-disulfide exchange was taking place. This experiment being the only to tend to indicate that the intravesicular reaction occurs, no firm conclusion can be reached as to whether the reaction takes place or not.

As regards the second jump in absorbance after the addition of an excess of phosphine, no conclusions can be drawn from it since the absorbance at 450 nm shows a great increase. This proves that the vesicles are affected by the presence of a large amount of phosphine and the jump at 341 nm is only partly explained by the release of pyridinethiol.

IV-2-14 Flip flop experiment

This experiment is an attempt to determine the rate of flip flop for the asymmetric disulfide with a cholesterol moiety. Here disulfide 7 on the outside layer is reacted with the exact amount of phosphine then an excess of phosphine is added and the reduction of the disulfide embedded in the inside layer is observed as soon as it crosses the membrane.

In order to carry out this experiment the disulfide 7 embedded vesicles solution is prepared as described earlier. The amount of disulfide is calibrated using an excess of dithiothreitol and was found to be 184 μM in the stock solution with a concentration of 4 mM of vesicles.

Two phosphine solutions were prepared by weight and then calibrated against Ellman's reagent. The concentrations were found to be 52.2 mM and 9.5 mM. The two solutions were prepared in order to add the minimum amount necessary to obtain the desired concentration in phosphine so as to dilute the solution as little as possible.
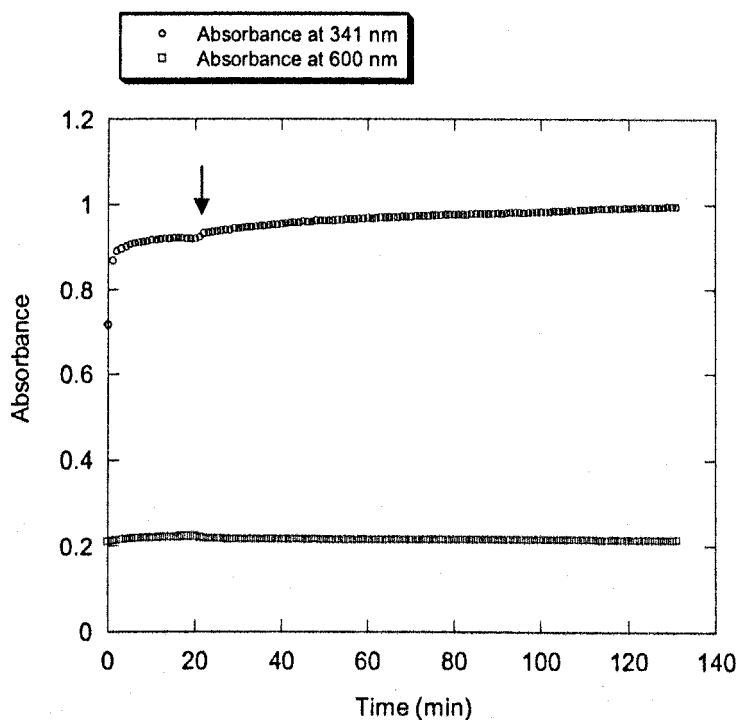
Figure 79. This graph represents the absorbance curves at 341 and 600 nm for the reaction of disulfide embedded vesicles (1 mM lipid containing 41 µM of disulfide) with the water soluble phosphine in two steps. The first jump in absorbance is due to 20 mM of phosphine added to reduce the outside disulfides. The second jump is due to an excess of phosphine added at the time indicated by the arrow.

The first jump identified on Figure 79 with a difference in absorbance of 0.204 corresponds to a 25 µM release of pyridinethiol, whose absorption coefficient at 341 nm is 8220 M^{-1} cm^{-1}. This is a bit more than to half the quantity (20 µM) of the total disulfide present at the start of the experiment, which is 41 µM. This could be due to the imprecision in the volume and the concentration of the solution of phosphine introduced. Another explanation is that the phosphine even in small quantity is capable of modifying the vesicles and hence their absorption. This seems unlikely since the absorption only increases in the 340 nm region and not over the whole range of wavelengths as can be seen in Figure 79 where no increase occurrs at 600 nm.

The second jump occurs after the addition of an excess of phosphine. Since in this case no increase in absorbance can be observed over the whole range of wavelengths as is evidenced by the flat absorption curve at 600 nm on Figure 79, the

increase at 341 nm cannot be explained by the effect of the phosphine on the vesicles. Since the phosphine cannot cross the membrane made of egg yolk phosphatidylcholine [51], the only explanation is the flip flop of the remaining disulfide from the inside layer to the outside layer. By considering that half the disulfide is left to react after the end of the first reaction and the disulfide reacts instantaneously with the excess of phosphine on the outside the speed of the flip flop process can be assessed.

In order to obtain an estimate of the flip flop rate, assuming that it is a first order process, we can evaluate it at a half time of approximately 100 minutes. The assumption that it is a first order process is reasonable since the process only involves overcoming the energy barrier that prevents molecules from flip flopping. This half life corresponds to a rate constant of approximately 10^{-4} s^{-1}, this rate constant is calculated as follows: $\ln2/t_{1/2}$ with $t_{1/2}$ = 100 minutes. This is comparable with the results reported earlier [3] in the introduction on page 4, where phospholipids flip flop is reported with a rate constant of 10^{-5} s^{-1}. This is consistent with our results, the discrepancy coming from the fact that the lipids used in this studies are cholesterol based and not phospholipids. However the medium is phospholipids for both results reported.

IV-3 Discussion and Conclusion:

The first conclusion that can be drawn from the experiments carried out at the interface of the vesicles is that the system, though simple in its description, is actually complex in its behaviour.

Nevertheless we managed to gain an understanding of the system and to solve a few questions, notably regarding the intravesicular reaction between the embedded disulfide and the embedded thiol synthesized in situ. Even though one experiment seems to indicate that it occurs, the vast majority lead to the opposite conclusion. The intravesicular thiol-disulfide exchange reaction does not occur under the conditions used for the study. The problem is that the full explanation for this fact has not been fully obtained. The fact that the embedded thiol and disulfide do not seem to react together could be due to the fact that the intermediate phosphonium formed by the attack on the disulfide is stable and not reactive (see Figure 68 on p93), hence no thiol is actually present in the system. Unfortunately the attempt to determine this fact by using Ellman's reagent was unsuccessful. Another possible explanation would be that the reaction is particularly slow at the conditions used and therefore cannot be detected in the time scale used here.

Those results appear to contradict results obtained from Regen *et al.* in various studies on Nearest Neighbour Recognition [68-73]. The aim of those studies is to determine the heterogeneity or homogeneity of a vesicle membrane constituted of a mixture of lipids [72]. They also investigate the effect of cholesterol [69], the effect of the head groups of phospholipids [73], the effect of the introduction of peptide in the bilayer [71], the effect of diluent [70], the effect of chirality [68] on general lipid mixing in vesicle membranes. The general method is to synthesize vesicles using a stoichiometric amount of symmetrical disulfides AA and BB (Figure 80 below) on their own, with additional cholesterol or other phospholipids. AA and BB are both formed by two phospholipids of equal carbon chain length linked by a disulfide linkage. When put together above the

liquid-crystalline phase transition temperature (T_m) of the highest melting dimmer and after addition of DTT the dimers react with thiols synthesized and at equilibrium form a mixture of homodimers (AA and BB) and heterodimer (AB) as shown on Figure 80 below. If the mixture at equilibrium is statistical (the ratio of AA to AB to BB is: 1:2:1) when starting from a stoichiometric ratio of AA and BB, i.e. a ratio of 1 to 1, the lipids are found to mix completely and no nearest-neighbor recognition takes place. Conversely if the mixture at equilibrium is not statistical, i.e. the ratio of AA to AB is less than 2, the mixture of lipids is deemed to have nearest-neighbor recognition. That is to say that the mixture is not homogeneous and possess lipid domains made primarily of a single lipid, therefore the statistical exchange between the homodimers cannot occur completely. To confirm the results obtain when starting from the stoichiometric mixture of AA and BB, another experiment is carried out starting from pure heterodimer AB.

homodimers   equilibrium dimer mixture   heterodimer
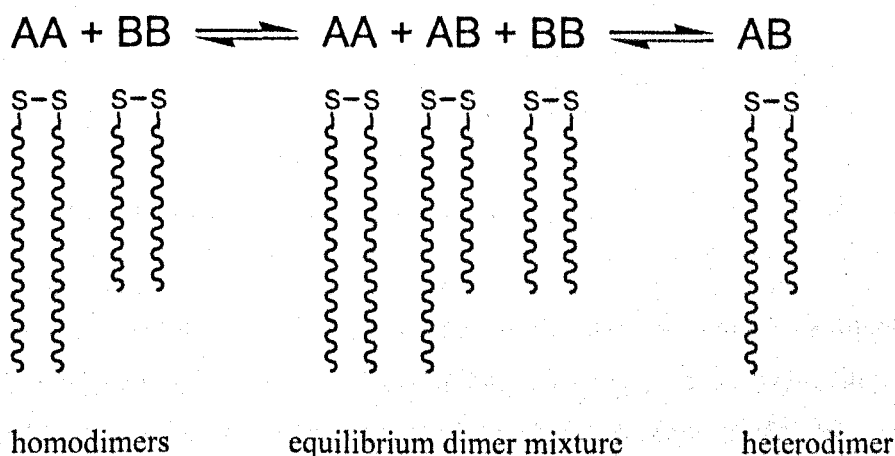
Figure 80. General method of Regen *et al.* studies on nearest-neighbor recognition. Two experiments are carried out, one starting from the stoichiometric mixture of AA and BB and another one starting from AB alone. The curvy lines represent *sn*-glycero-3-phosphocholine with 2 myristoyl moieties (14 carbons) for the short ones and 2 stearoyl moieties (18 carbons) for the long ones.

In those studies Regen *et al.* obtains exchange between disulfides in an efficient manner. However upon clear inspection some differences between both researches come to light. The main difference is the temperature at which the studies are carried out: 25°C for the present studies and 60°C for the ones carried out by Regen *et al.* In his studies Regen uses two disulfides embedded within vesicles reducing some of the

disulfides in situ to synthesize thiols and trigger thiol disulfide exchange reaction. It took 3 to 4 hours to reach the equilibrium in all cases reported by Regen et al. This is not a rapid reaction compared to the time scale we used on our studies and the temperature is 35°C higher in their studies than in the present one.

Due to the fact the reactions used in Regen et al. studies and the ones presented in this thesis are similar, let's assume that they both have a similar activation energy Ea. Fernandes et al. [65] have reported an average value of 15 kcal.mol^{-1} for the activation energy of the SN$_2$ attack of a thiolate on a disulfide. Using the Arrhenius equation $k = A \times e^{\left(-\frac{E_a}{RT}\right)}$, with E$_a$ the activation energy, A the pre-exponential factor, R the gas constant and T the temperature, we can therefore estimate the difference in rate constants between 25°C and 60°C. By taking k_1 the rate constant at T$_1$=298K and k_2 the rate constant at T$_2$=333K, $\ln\left(\frac{k_1}{k_2}\right) = \frac{E_a}{R} \times \left(\frac{1}{T_2} - \frac{1}{T_1}\right)$. As a result k_1 is 14 times lower than k_2, i.e. approximately one order of magnitude slower. This could explain why the reaction cannot be observed in our studies.

Moreover the molecules used by Regen et al. have a longer chemical link between the carbon chains and the disulfide than the chemical link between cholesterol and disulfide used here (Figure 81 below). The disulfide and relative thiol with the sn-glycero-3-phopshocholine link would therefore be more distant from the bilayer membrane and consequently more available for reaction than the one with the cysteine link.

In both studies, the experiments are carried out above the above the liquid-crystalline phase transition temperature (T$_m$) of the lipids constituting the membranes, 25°C for the EYPC and 60°C for the DMPC and DSPC. Therefore the difference cannot come from a restricted movement for the lipids due to the use of a gel phase instead of the liquid phase.

The reactive groups in the molecules used by Regen *et al.* have an increase availability compared to the ones used here. In addition a higher temperature is used in the experiments by Regen *et al.* Those two factors explain why there is a difference in observed reactivity between the present study and those reported by Regen *et al.* They reach an equilibrium at 60°C in 3 to 4 hours when reacting disulfides and thiols
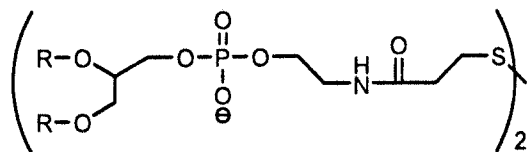
Molecules used by Regen *et al.*
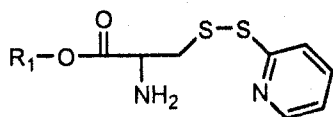
Molecules used in the present study

Figure 81. Molecules used in Regen *et al.* studies with R representing palmitic, stearic or myristic acids. R' represents cholesterol.

The flip flop of the disulfide has also been demonstrated and the rate of its process estimated as 10^{-4} s^{-1}.

The effect the presence of vesicles has on the reactivity of the disulfide towards a range of reductants (phosphine, cysteine ethyl ester hydrochloride, dithiothreitol and 2-ethoxycarbonylamino-3-mercapto-propionic acid) has also been assessed. Overall the vesicles do not affect the reactivity significantly. The second order rate constants obtained in vesicles are comparable to the ones in solution for the similar disulfides reacting with the same reductants. This assertion is valid because we use the total (macroscopic) concentration for the disulfide embedded in vesicles. The table below compares the rate constants for the water soluble disulfide and its membrane anchored analogue.

Table 4. This table gives the second order rate constants for the reaction in solution and in vesicles between the reductant shown on the left and the two disulfides.

All the rates are in $M^{-1} s^{-1}$	Water soluble disulfide **12**	Membrane anchored disulfide **7**
Phosphine **17**	320 ± 110	600 ± 150
Cysteine ethyl ester hydrochloride **13**	144 ± 2	45 ± 3
DTT **16**	29 ± 0.7	24 ± 2

In the next chapter, we will use the knowledge gained in chapter 3 and 4 to try and make vesicles containing complementary reactive groups (thiol and disulfide) react together.

Chapter V Intervesicular reactions

V-1 Aim and Design

The aim of this chapter is to demonstrate whether the knowledge gained in the previous chapters could be used to make a system that would mimic cell cell interaction. This would be achieved by allowing vesicles with complementary chemical groups, i.e. chemical groups that could react with each other, to come into contact and react. This has been achieved previously by Menger *et al.* [31, 74] and Constable *et al.* [48] most notably.

Menger *et al.* [31] used the molecules shown in Figure 17 above (page 26) to trigger intervesicular reaction. In the other studies mentioned [74], the hydroxamic acid containing lipid embedded within vesicles was identical to the one in Figure 17 whereas the ester was replaced with the one presented in the following Figure.
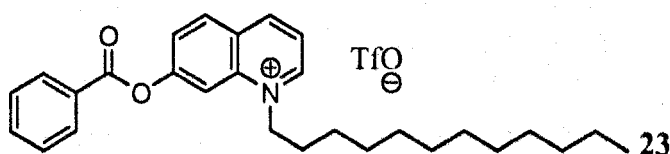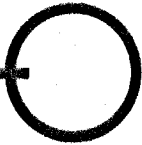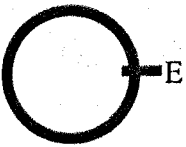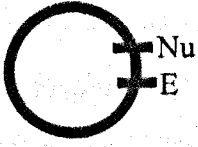

Figure 82. Molecule used as the ester in the intervesicular reactions studies by Menger *et al.* [74]

The complementary reactants were embedded within two different sets of vesicles and the reaction was followed by measuring the appearance of paranitrophenol in the case of the first study [31] or the appearance of the fluorescent hydroxyquinolinium ion lipid derivative in the second study [74]. In those two papers the intervesicular reactions were compared to intravesicular reactions. Reactions where reactant 1 which contains a lipid moiety was embedded within vesicles and the other reactant was a water soluble equivalent of reactant 2 were also investigated. Finally the rate of the reaction between the two water soluble equivalents of reactant 1 and 2 was

measured. The rates of those reactions were then compared to identify the influence of the vesicles on the rate and the possibility to obtain measurable intervesicular reactions. In the case of the study with the quinoline derivative **23**, no water soluble equivalent was used in the studies. **23** was used both embedded within vesicles and in solution as it was soluble enough in the buffer used (carbonate 50mM) at pH 9.0 to obtain a concentration of 20μM.

Different conclusions were reached in both studies by Menger *et al.*, i.e. the reactivity of the various situations studied did not give rise to a similar pattern of rate acceleration or deceleration.

Table 5. Results from Menger *et al.* studies[31, 74]. E and Nu represent the water soluble electrophile and nucleophile respectively, the latter being the hydroxamic acid derivative (Figure 17). The black rectangle represents the lipid moiety (cholesterol or carbon chain) that enables the molecules to embed within vesicles. The study involving quinoline derivative was carried out with an electrophile concentration of 20μM, the paranitrophenol study with an electrophile concentration of 100μM for the first two reactions and 50μM for the last three reactions.

	Reaction	Study with quinoline derivative ($t_{1/2}$ min)	Study with paranitrophenol derivative ($t_{1/2}$ min)
1	E Nu	0.21 (1mM Nu)	0.35 (1mM Nu)
2	E Nu	34 (1mM Nu) and 180 (0.1mM Nu)	7.7 (1mM Nu) and 38 (0.1mM Nu)
3	E Nu	0.75 (0.1mM Nu)	7 (0.lmM Nu)
4	E Nu	4.2 (0.1mM Nu)	120 (0.1mM Nu)
5	Nu E		Stage 1: 0.3 (0.1mM Nu) and stage 2: 6 (0.1mM Nu)

As can be seen from the table above, reactions involving only water soluble reactants have similar reaction rates. Overall, the classification of reaction types according to their reaction rate is as follows:

Vesicle-vesicle (intravesicular) ≈ Solution-solution > vesicle-solution > vesicle-vesicle (intervesicular)

The difference between the studies is that the intervesicular reaction rate for the study with the quinoline derivative is much higher than expected and more in line with the results obtained for intravesicular reaction in the study using paranitrophenol derivative. This is explained by the fact that in the paranitrophenol studies, for both the electrophile and nucleophile molecules, the hydrophilic moiety is a cholesterol unit which is strongly bound to the vesicle membrane due to its high hydrophobicity. However in the other study the quinoline derivative's hydrophobic moiety is a C_{12} carbon chain, see Figure 82 above. Therefore Menger *et al.* attribute the high reaction rate for intervesicular reactions to the fact that molecule **23** (the C_{12} quinoline derivative) "jumps" to the vesicle containing the hydroxamic acid when vesicles come into contact. The reaction rate observed therefore is the intravesicular reaction rate. Another point to note is that two reaction rates are reported for the intravesicular reaction in the studies with the paranitrophenol derivative. This is due to the fact that the vesicles are prepared at pH 3.0 and the pH is raised to 8.0 to trigger the reaction. Therefore upon increase in pH the hydroxamic acid is deprotonated to from the reactive species, the hydroxamate ion. The first stage corresponds to the intravesicular reaction on the outer layer of the vesicle. The second stage corresponds is limited either by the rate of transport of hydroxide ions through the membrane layer or the flip flop of the paranitrophenol molecule from the inner to the outer layer of the membrane.

The molecules used and the system designed by Constable *et al.* can be seen in Figure 21 on page 31 above. Essentially, they achieved a reversible interaction between vesicles, bringing them into contact by introduction of metal in the solution and disrupting those aggregates upon addition of metal chelating EDTA.

In order to carry out the intervesicular experiments the following molecules were used:
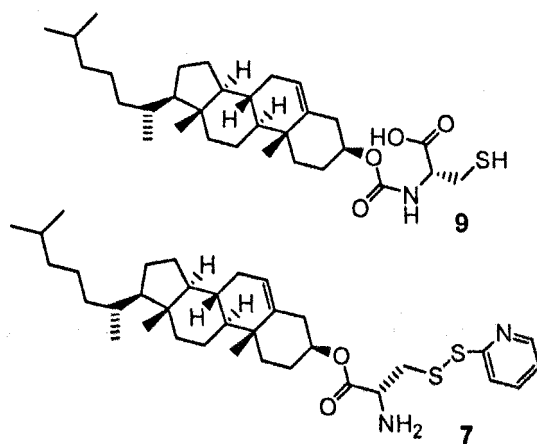
They both possess the cholesterol moiety which enables them to anchor in the lipid bilayer and hence to be embedded within the vesicles. When in the buffer solution they are both ionized, the thiol possesses a negative charge on the acid group and the disulfide a positive charge on the nitrogen. Disulfide **7** is used as the precursor to make thiol **8** shown below (Figure 84) in situ since this thiol was shown not to withstand the vesicles making process. The demonstration that thiol **8** does not withstand the vesicle making process was carried out by submitting a solution of lipids containing **8** to the process and titrate the remaining thiols with Ellman's reagent. None were found to be present.

The lipids used to make the vesicles and the process followed are identical to the ones described for the interface studies. Egg yolk phosphatidylcholine is used as the vesicle membrane lipid. A measured volume of the stock solution of phosphatidylcholine is mixed with a measured volume of the stock solution of the lipid to be embedded, i.e. thiol or disulfide. The solvent is then removed by blowing nitrogen on the solution then exposure to high vacuum for at least half an hour. The right amount

of MES buffer is then added and the resulting suspension is passed 25 times through 200nm polycarbonate filters.

V-2 Experiments results

V-2-1 Disulfide vesicles prepared in situ and purified by GPC

In this experiment we want to make vesicles with thiols **8** embedded by reducing the disulfides embedded in vesicles using DTT and passing the obtained vesicles through GPC. For this experiment disulfide embedded vesicles were prepared as usual except that the MES was at pH 3.6 as this should prevent the oxidation of thiol that will be formed as it is favored by basic pH. This is important as the thiol obtained by this method is the following:
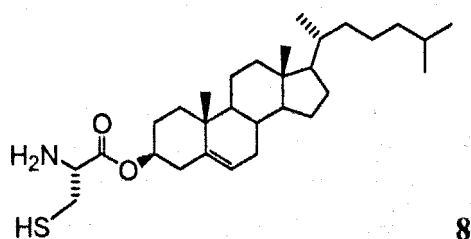
Figure 84. Thiol synthesized in situ from disulfide **7** using DTT as the reductant.

This molecule was shown not to withstand the vesicle making process. This experiment attempts to obtain vesicles containing **8** by another method.

In this experiment disulfide containing vesicles are prepared according to the described method. The amount of disulfide is calibrated using an excess of dithiothreitol and was found to be 164 µM in the stock solution with a concentration of 4 mM of lipid.

200 µL of a 6.5 mM DTT solution prepared by weight was added to 2 mL of the disulfide embedded vesicle solution. The following graph shows the result of this reaction (Figure 85).

The "reduced" vesicle solution was passed through a GPC column with a pH 3.6 MES buffer as the eluant. 2 mL of vesicles were obtained from the original volume of 2.2 mL. The two solutions, non reduced and reduced ones, were then brought back to pH 5.5 using a 0.1 N NaOH solution.

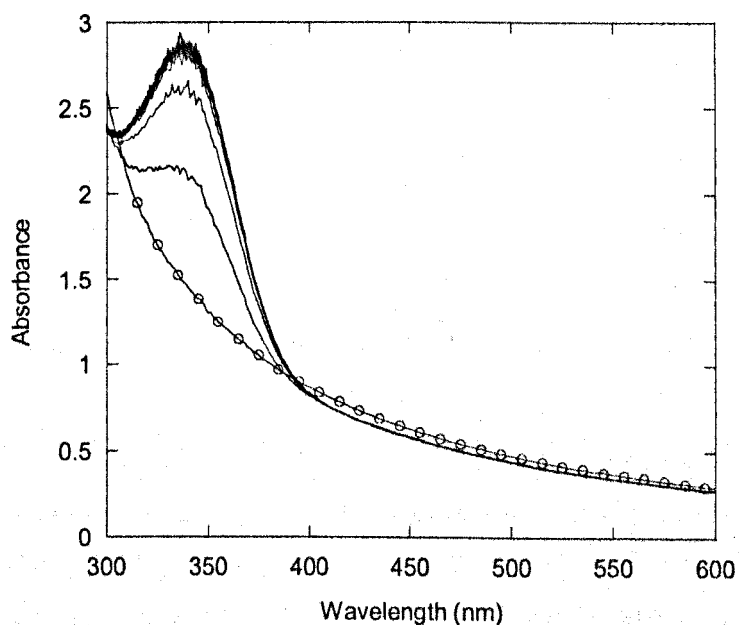**Figure 85.** Evolution of the absorbance when 200 µL of a 6.5 mM solution of DTT is added to a solution of disulfide embedded vesicles. The open circles indicate the first scan before the addition.

Then the "reduced" vesicle solution obtained from the GPC column was diluted twice and Ellman's reagent was added to determine the amount of thiol **8** present. The following graph gives the result obtained.
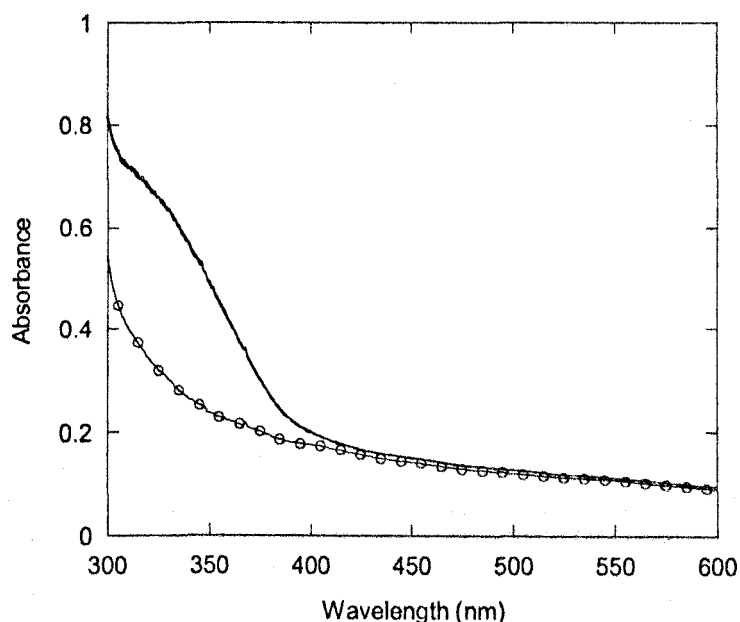
Figure 86. Evolution of the absorbance when 2 mL of a saturated Ellman's reagent solution is added to a solution of "reduced" vesicles. The open circles indicate the first scan before the addition.

Figure 86 shows that no thiols **8** seem to have survived the GPC column. No increase is observed around 420 nm, the absorption maximum of the thiol released after the thiol disulfide exchange with Ellman's reagent. The direct introduction of the thiol shown in Figure 84 before the vesicle making process has been shown in the laboratory not to be possible, since no response to an addition of Ellman's reagent was obtained when added to a solution of the thiol embedded in vesicles via the standard process (see the experimental section for a description of the method). The following experiments present alternatives to assess the intervesicular reaction between the thiol in Figure 84 and the corresponding disulfide.

V-2-2 Disulfide vesicles reduced with DTT reacting with disulfide vesicles

In this experiment disulfide **7** containing vesicles are prepared according to the described method. The amount of disulfide is calibrated using an excess of dithiothreitol and was found to be 184 µM in the stock solution with a concentration of 4 mM of vesicles.

Some vesicles are then completely reduced using an equivalent of DTT. The two sets of vesicles are then mixed in order to see the possible reaction between the thiol **8** containing vesicles and the disulfide **7** containing ones (Figure 87).
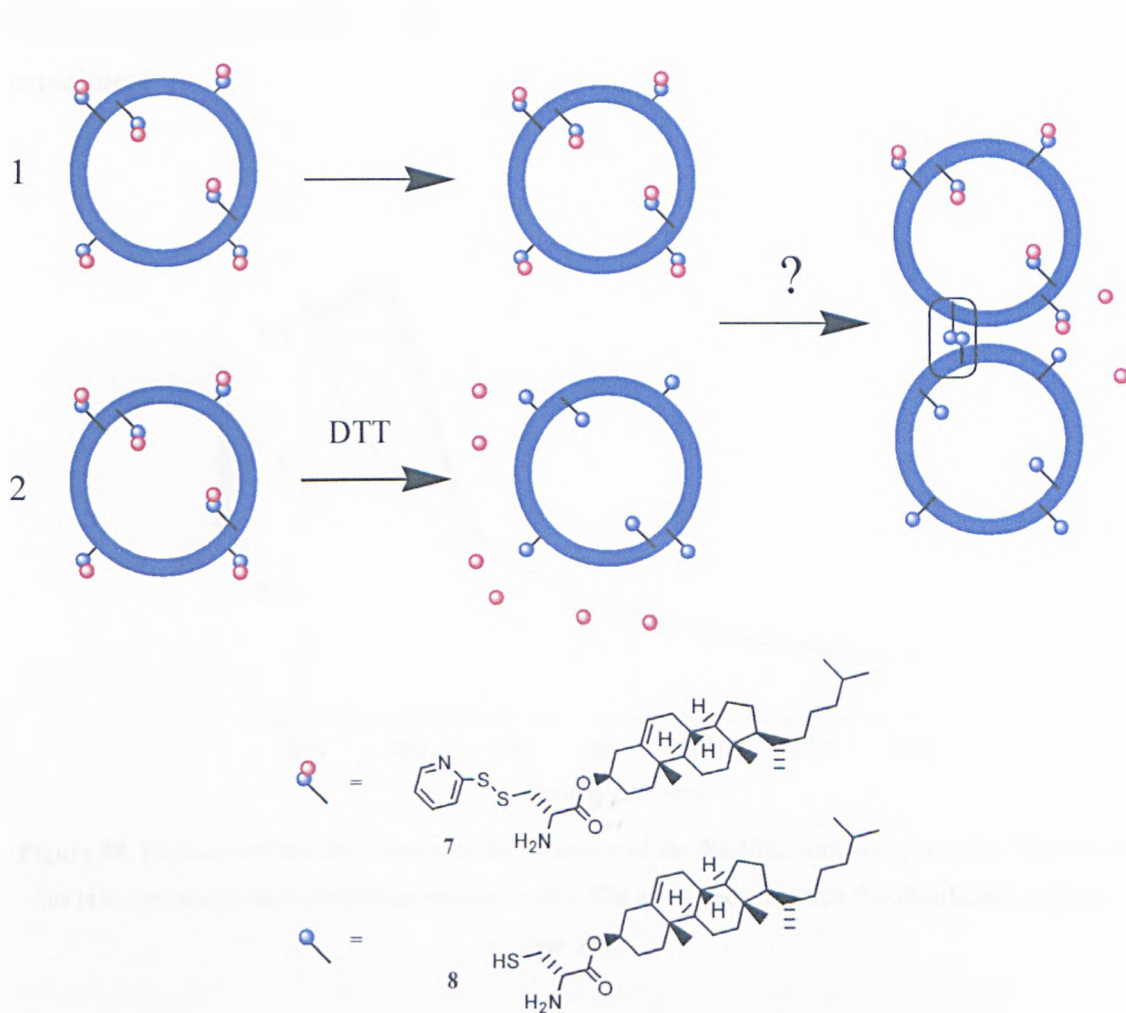
Figure 87. Design of the experiment. Two identical sets of vesicles are prepared (1 and 2), both containing the disulfide. One set (2) is completely reduced using dithiothreitol, then mixed with set 1. The absorption is followed between 300 and 600 nm to determine whether the thiol disulfide exchange occurs and whether the vesicles are affected by it.

A solution of 2 mM of vesicles containing 92 µM of disulfide was prepared by dilution. The volume of DTT solution added was enough to just reduce the entire quantity of disulfide present in the solution, i.e. 92 µM. The reaction was followed over the range of wavelengths from 300 to 600 nm in order to see the release of pyridinethiol at 341 nm and the effect on the vesicles if any. The following graph shows the reduction of the disulfide **7** vesicles in order to synthesise thiol **8** containing vesicles in situ. The amount of pyridinethiol released is 85 µM, as measured by the change in absorbance at 341 nm. This indicates that almost all the disulfide **7** present has been reduced, hence

the resulting vesicles can be considered as thiol **8** containing vesicles for the rest of the experiment.
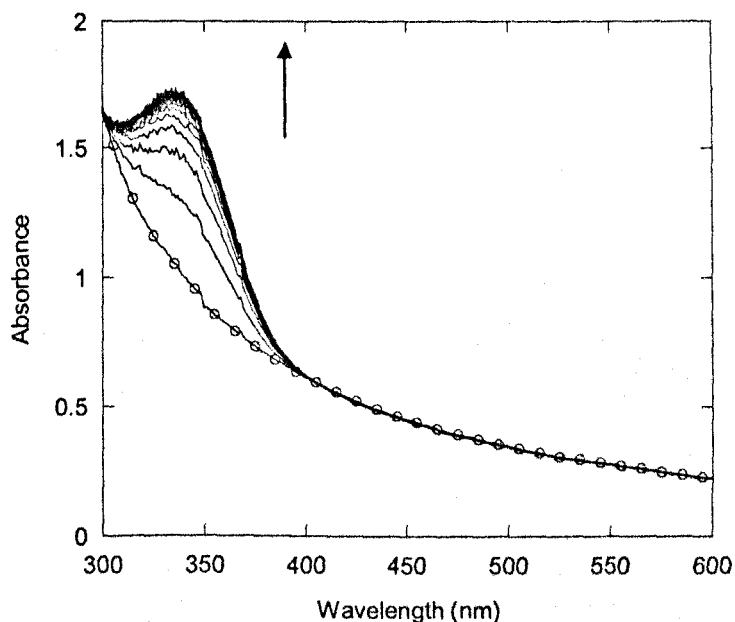
Figure 88. Evolution of the absorbance for the reduction of the disulfide containing vesicles. The aim of this is to synthesize thiol containing vesicles in situ. The arrow indicates that the absorbance increases over time.

The results of the intervesicular reaction experiments are shown in the graphs below. For the first experiment the thiol **8** containing vesicles solution is prepared as subsequently the disulfide **7** containing vesicles are added. For the second one the disulfide **7** containing vesicle solution is prepared and the thiol **8** embedded disulfide vesicles are added afterwards. The concentration of the mixture is 3 mM of lipid (1 mM from the disulfide **7** containing vesicles and 2 mM from the thiol **8** containing vesicles), 46 μM of disulfide and 92 μM of thiol for the experiment in Figure 89.

Figure 89. Evolution of the absorbance when the thiol vesicles (set 2 on Figure 87) are added to the disulfide vesicles (set 1 on Figure 87). The arrow indicates that the absorption increases with time.

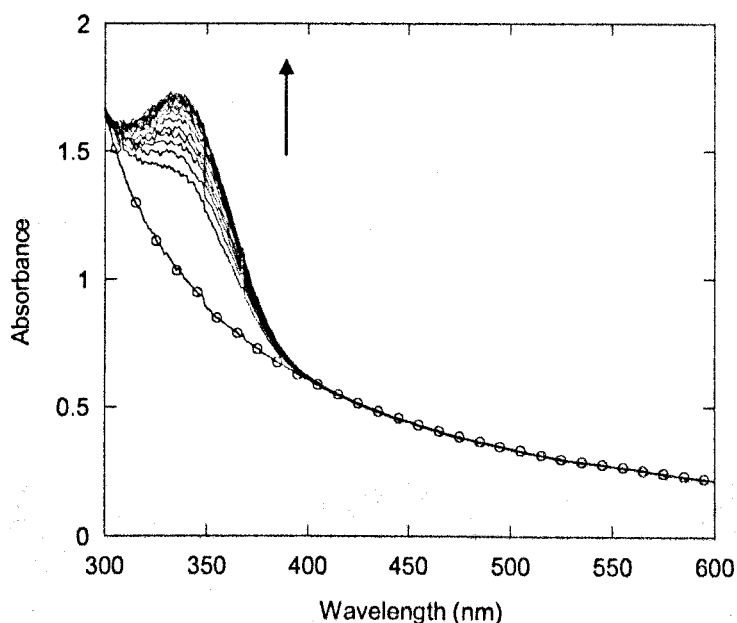The increase in absorbance at 341 nm after the addition of the disulfide **7** vesicles to the thiol **8** vesicles indicates that the thiol disulfide reaction occurs. However the absorbance is not modified over the whole range of wavelengths. This means that there is only a short interaction between the vesicles containing the different reagents and that the aggregate is not stable probably due to unfavorable interactions between the adjacent vesicles.

V-2-3 Reduced disulfide vesicles on the outside reacting with disulfide vesicles

In this experiment disulfide **7** containing vesicles are prepared according to the described method. The amount of disulfide is calibrated using an excess of dithiothreitol and was found to be 184 μM in the stock solution with a concentration of 4 mM of vesicles.

Some vesicles are then completely reduced on the outside using an equivalent of phosphine. The two sets of vesicles are then mixed in order to see the possible reaction

between the vesicles containing thiol **8** on the outside and the disulfide **7** containing ones (Figure 90).
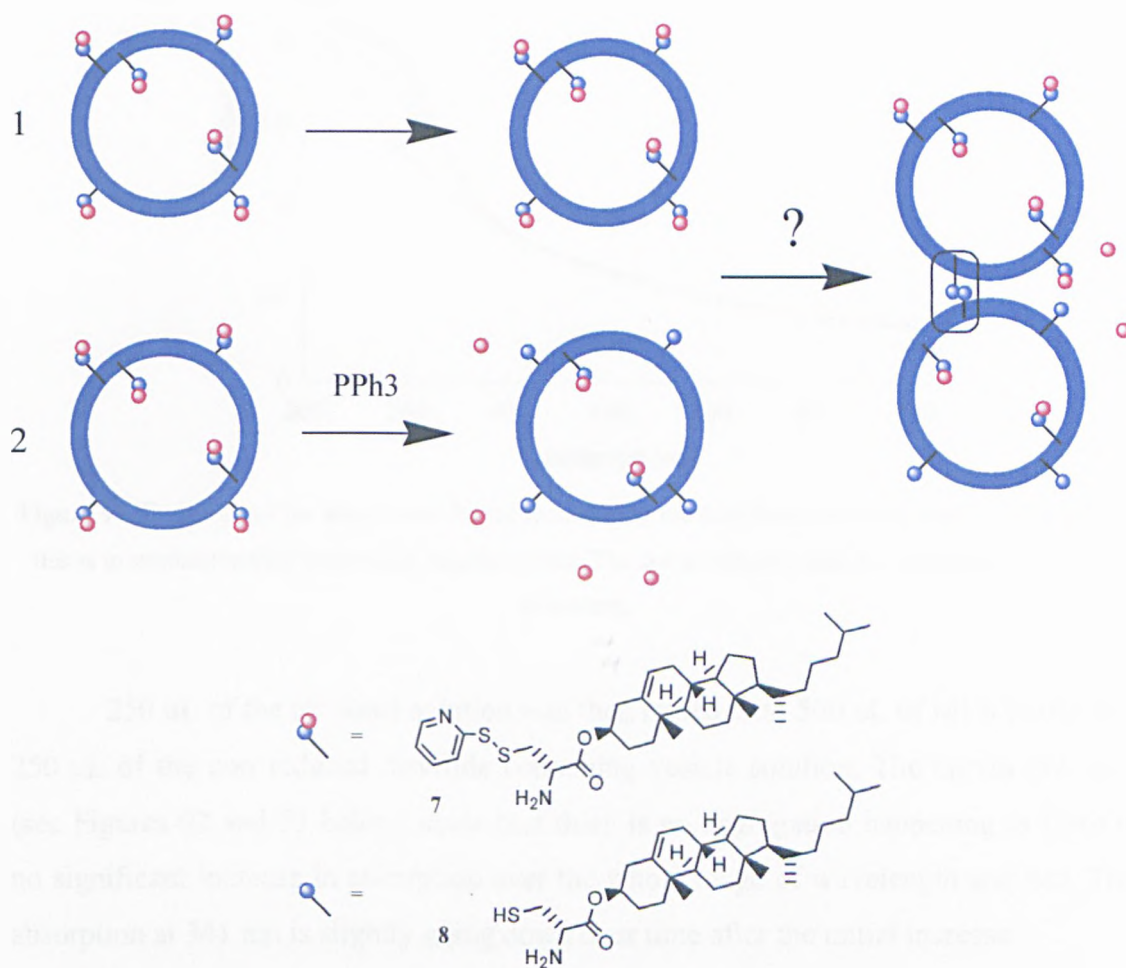
Figure 90. Design of the experiment. Two identical sets of vesicles are prepared (1 and 2), both containing the disulfide. One set (2) is completely reduced on the outside using phosphine, then mixed with set 1. The absorption is followed between 300 and 600 nm to determine whether the thiol disulfide exchange occurs and whether the vesicles are affected by it.

1 mL of the 200 µM disulfide **7** in 4 mM vesicle solution was mixed with 4 uL of the 24.8 mM (in fact 95 % pure so 23.6 mM) water soluble phosphine solution, which corresponds to 94 µM of phosphine. Hence 94 % of the outside disulfide is reduced to thiol. The reaction was followed in UV until its completion (see Figure 91 below).
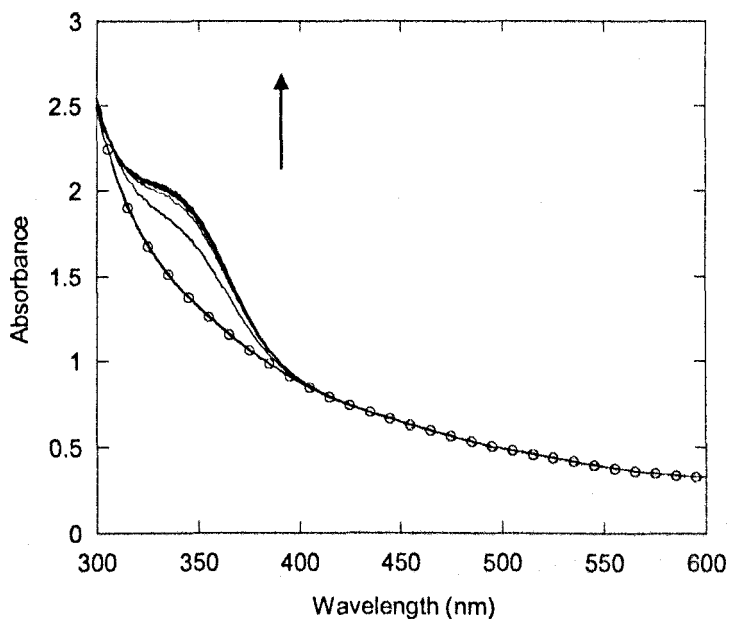
Figure 91. Evolution of the absorbance for the reduction of the disulfide containing vesicles. The aim of this is to synthesize thiol containing vesicles in situ. The arrow indicates that the absorbance increases over time.

250 uL of the obtained solution was then mixed with 500 uL of MES buffer and 250 uL of the non reduced disulfide containing vesicle solution. The curves obtained (see Figures 92 and 93 below) show that there is no aggregation happening as there is no significant increase in absorption over the whole range of wavelength scanned. The absorption at 341 nm is slightly going down over time after the initial increase.

Figure 92. Evolution of the absorbance when the disulfide vesicles (set 1 on Figure 90) are added to the vesicles reduced on the outside layer (set 1 on Figure 90).

Figure 93. Evolution of the absorbance for the previous graph at 341 and 600 nm.

This shows that the two sets of vesicles do not react together even though one set contains thiol **8** and the other disulfide **7**. The charge repulsion between the two positively charged sets of vesicles is likely to be preventing them from coming into contact long enough for the 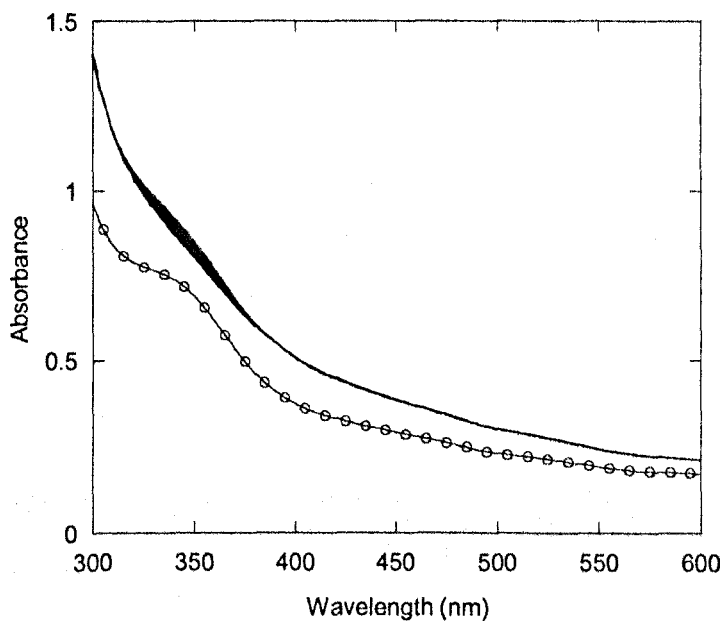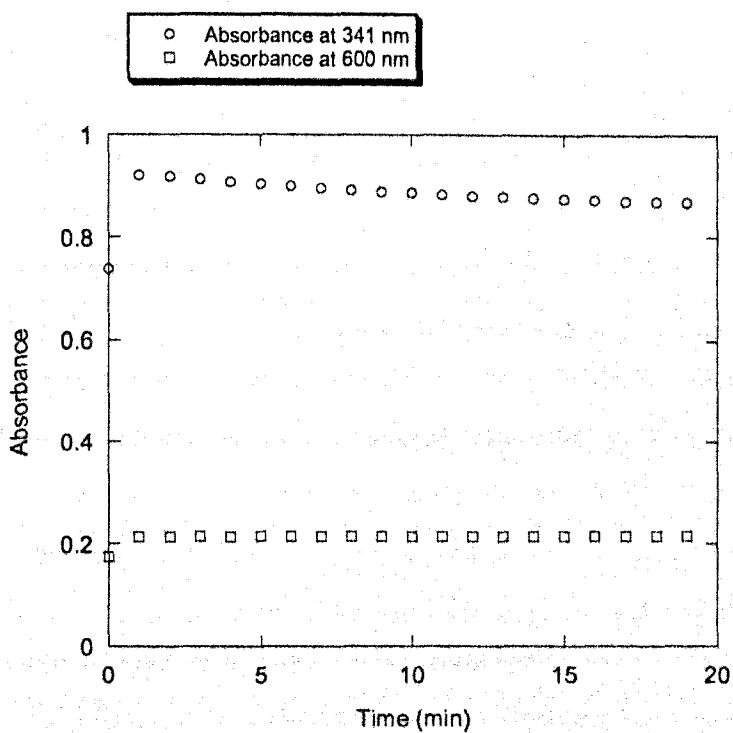reaction to occur. The other explanation for this is the stability of the phosphonium formed when the phosphine attacks the disulfide. If it is stable there is no thiol on the outside layer of the reduced vesicles for the disulfide to react with.

V-2-4 Control experiments for the interactions between vesicles

The aim of the following experiments is to determine whether vesicular aggregates are found upon mixture of vesicles containing disulfide **7** and vesicles containing thiol **9**. In each experiment, in order to determine the effect on the size of the vesicles, scans were collected over the range of wavelengths from 300 to 600 nm. From those scans, kinetic curves were derived at 341 nm, i.e. the maximum absorbance of pyridinethiol, and at 600 nm, further away from the scattering of the vesicles. A decrease or increase in absorbance at 600 nm would only be due to the decrease or increase in size of the vesicles respectively.

Before carrying out experiments with a set of vesicles containing disulfide **7** and another containing thiol **9**, the following control experiments are required. They will ensure that the increase or decrease in size is due to interaction between vesicles when both disulfide **7** and thiol **9** are present and no other interactions.

The control experiments required are:

1. Blank vesicles mixed with vesicles containing thiol **9**
2. Blank vesicles mixed with vesicles containing disulfide **7**
3. Vesicles containing thiol **9** mixed with vesicles containing thiol **9**
4. Vesicles containing disulfide **7** mixed with vesicles containing disulfide **7**

V-2-4-1 Blank vesicles and thiol containing vesicles

Figure 94. Evolution of the absorbance when 1 mM of thiol embedded vesicles is mixed with 1 M of blank vesicles. The open circles indicate the first scan before the addition of the thiol embedded vesicles and the arrow the direction of evolution.

Figures 94 and 95 show the results obtained when 250 µL of the thiol embedded vesicles was diluted with 500 µL of MES buffer. The first scan was taken and 250 µL of the blank vesicles solution was added. No significant change happened following the introduction of the second set of vesicles in the solution.

Figure 95. Evolution of the absorbance at 341 and 600 nm for the same mixture as Graph 93.

V-2-4-2 Blank vesicles and disulfide containing vesicles

Figure 96. Evolution of the absorbance when 1 mM of disulfide embedded vesicles is mixed with 1 mM of blank vesicles. The open circles indicate the first scan before the addition of the thiol embedded vesicles and the arrow the direction of evolution.

Figures 96 and 97 show the results obtained when 250 µL of the disulfide embedded vesicles was diluted with 500 µL of MES buffer. The first scan was taken and 250 µL of the blank vesicles solution was added. No significant change happened following the introduction of the second set of vesicles in the solution.

Figure 97. Evolution of the absorbance at 341 and 600 nm for the same mixture as Graph 95.
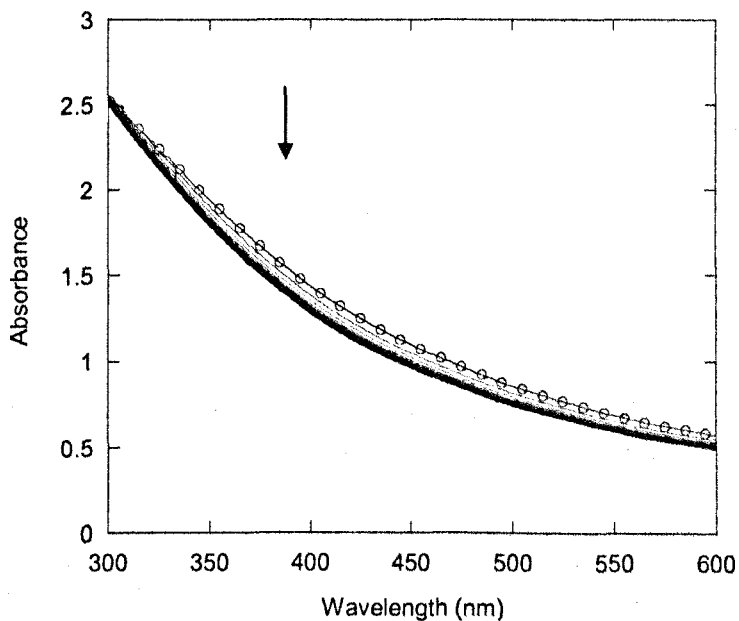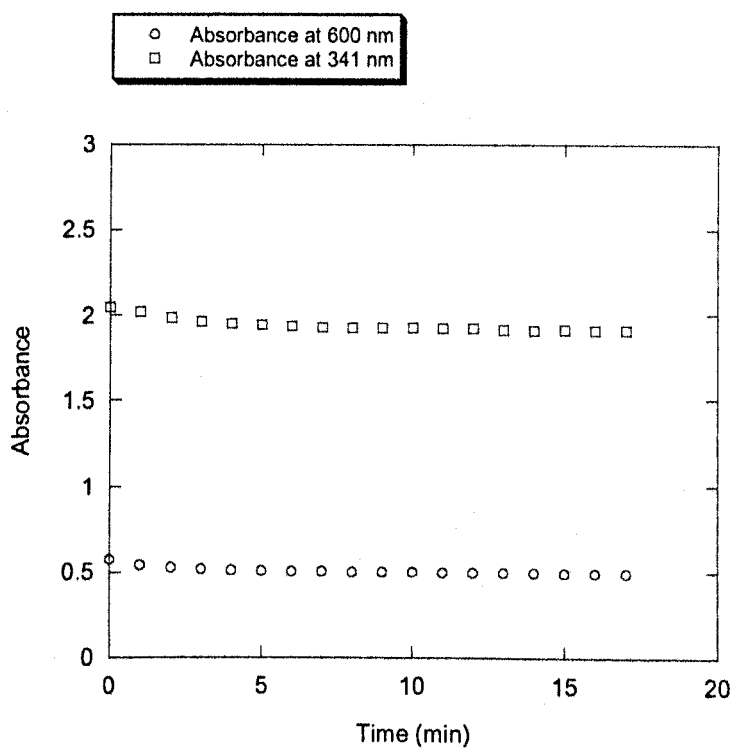
V-2-4-3 Thiol containing vesicles

Figure 98. Evolution of the absorbance when 1 mM of disulfide embedded vesicles is mixed with 1 mM of the same solution. The open circles indicate the first scan before the addition of the thiol embedded vesicles and the arrow the direction of evolution.

Figures 98 and 99 show the results obtained when 250 µL of the thiol embedded vesicles was diluted with 500 µL of MES buffer. The first scan was taken and 250 µL of the thiol embedded vesicles solution was added. An increase over the whole range of wavelengths can be observed.

Figure 99. Evolution of the absorbance at 341 and 600 nm for the same mixture as Graph 97.

V-2-4-4 Disulfide containing vesicles
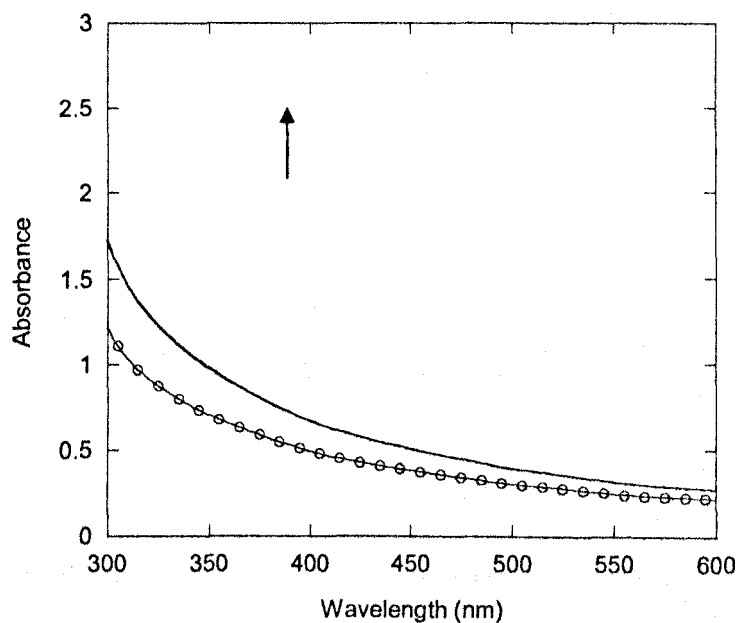
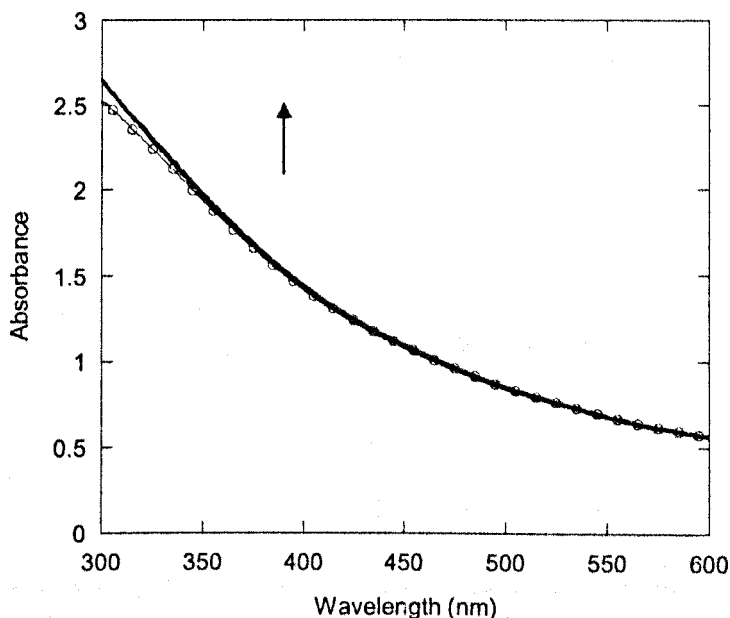**Figure 100.** Evolution of the absorbance when 1 mM of thiol embedded vesicles is mixed with 1 mM of the same solution. The open circles indicate the first scan before the addition of the thiol embedded vesicles and the arrow the direction of evolution.

Figures 100 and 101 show the results obtained when 250 μL of the disulfide embedded vesicles was diluted with 500 μL of MES buffer. The first scan was taken and 250 μL of the disulfide embedded vesicles solution was added. An increase over the whole range of wavelengths can be observed.
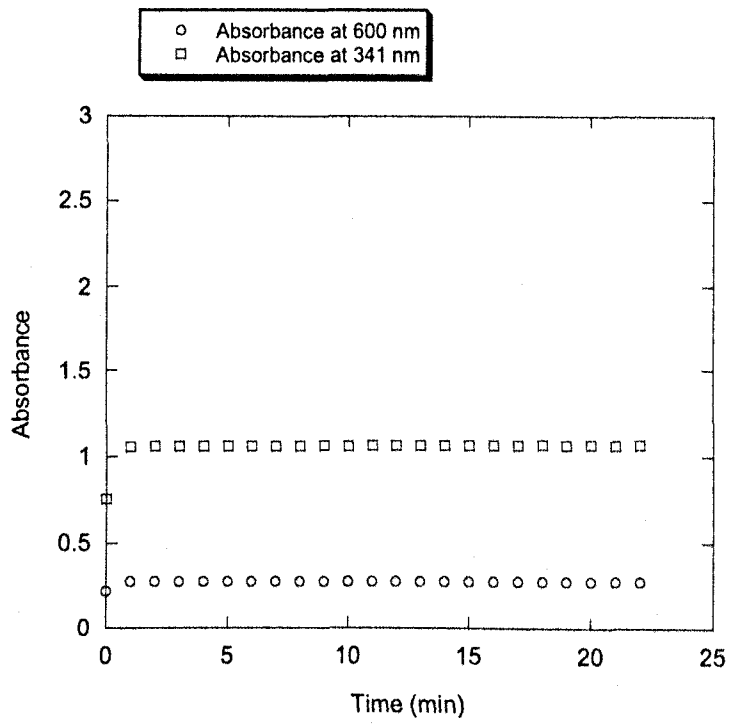
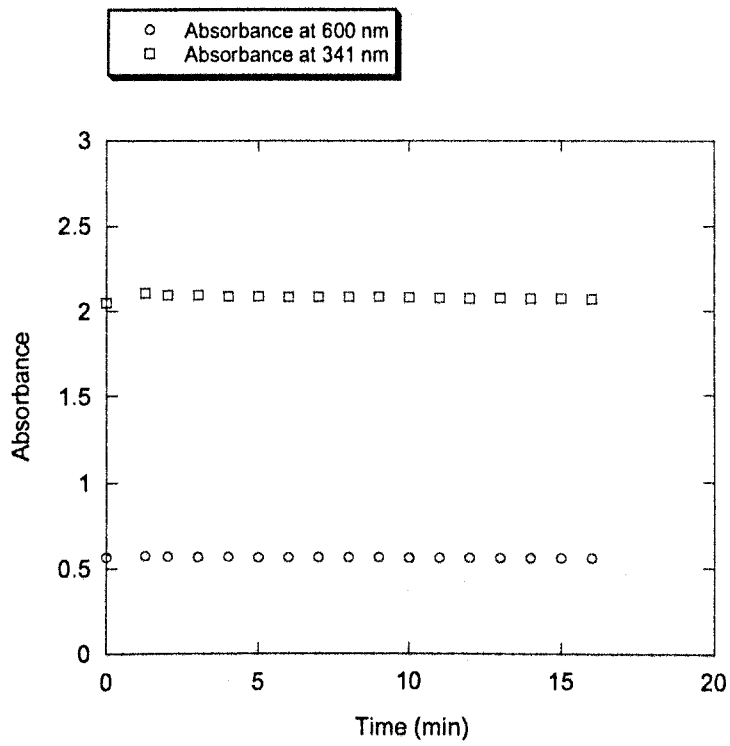**Figure 101.** Evolution of the absorbance at 341 and 600 nm for the same mixture as Graph 99.

V-2-4-5 Thiol containing vesicles and disulfide containing vesicles
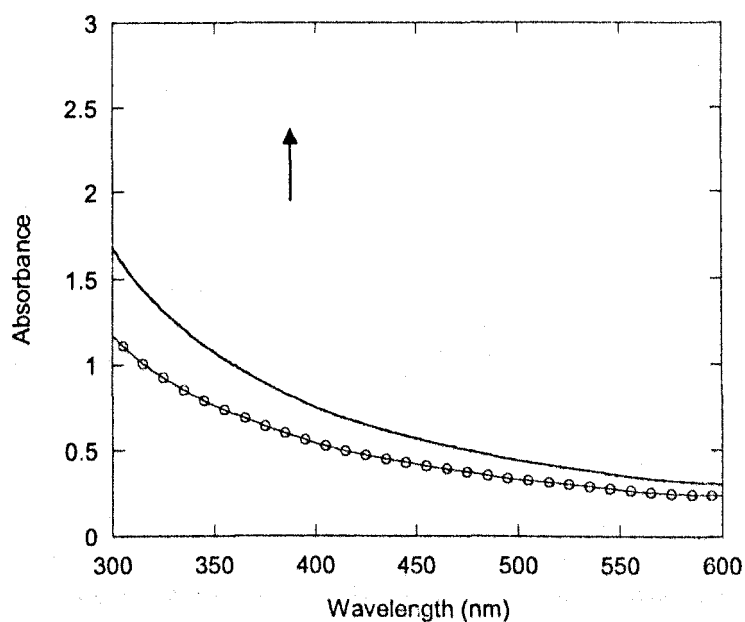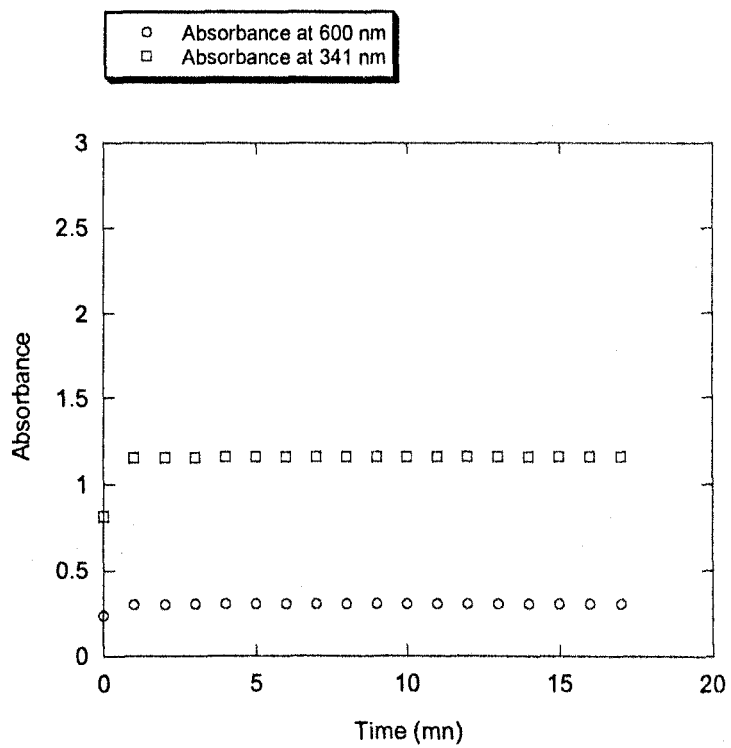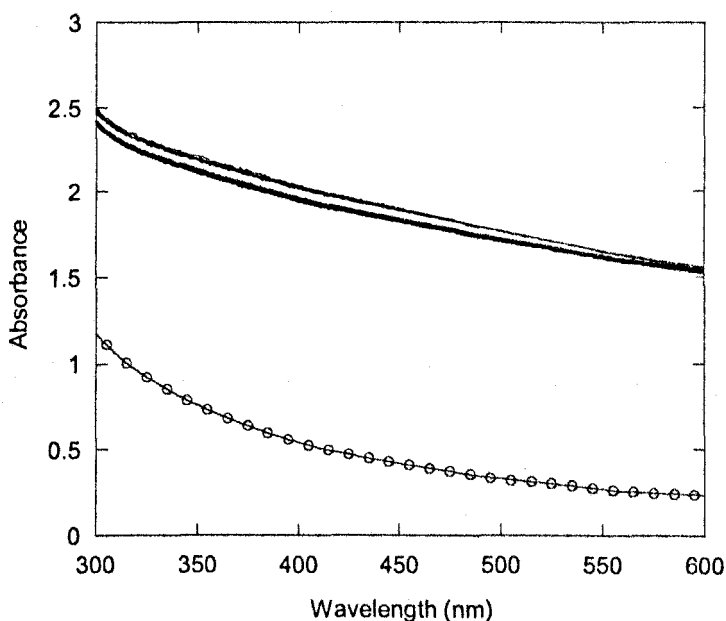

Figure 102. Evolution of the absorbance when a solution of 41 µM disulfide embedded in 1 mM vesicles is added to a solution of thiol embedded in 1 mM vesicles. The open circles indicate the first scan before the addition of the thiol embedded vesicles and the arrow the direction of evolution.

Figures 102 and 103 show the results obtained when 250 µL of the thiol embedded vesicles was diluted with 500 µL of MES buffer. The first scan was taken and 250 µL of the disulfide embedded vesicles solution was added. Compared to all other control studies carried out above, a significant increase over the whole range of wavelengths can be observed. This indicates that the average size of the vesicles has been greatly affected by the addition of the disulfide embedded vesicles.

Two different and probably concurrent effects could explain this increase in size. First the vesicles could react intervesicularly and form clusters of vesicles which would scatter light with a greater intensity than the original vesicles. The second one is the electrostatic attraction between the two sets of vesicles. One set of vesicles bears disulfides **7** with a positively charged amino group, whereas the other set bears thiol **9**

with a negatively charged acid group. The following experiments describe the attempts made to characterize the vesicles obtained when the two sets of vesicles are mixed together.
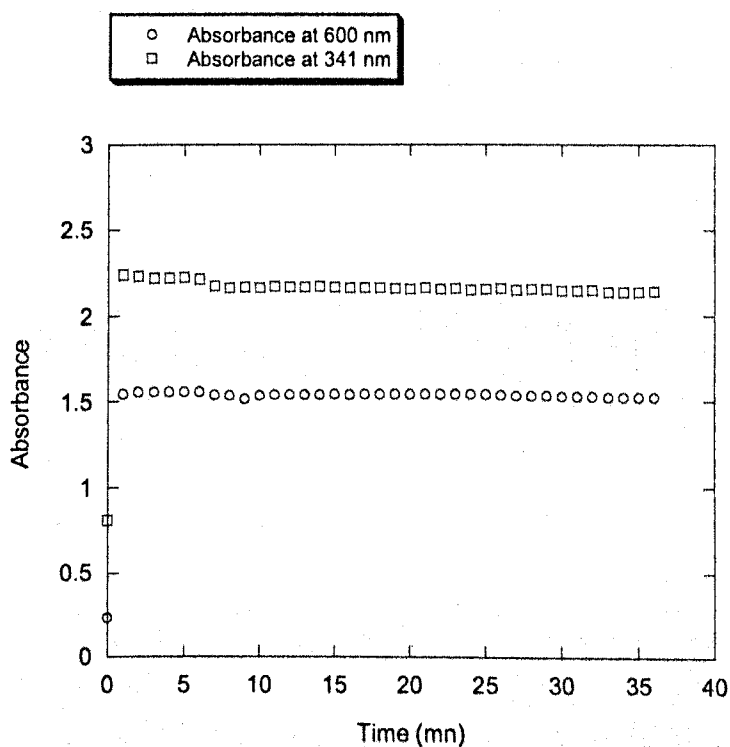
Figure 103. Evolution of the absorbance at 341 and 600 nm for the same mixture as Graph 101.

V-2-5 TEM Microscopy

The thiol **9** embedded vesicles solution (52 mM of **9** embedded in 2 mM of lipid), the disulfide **7** embedded vesicles one (90 μM of **7** embedded in 2 mM of lipid) and the solution obtained by mixing the two solution in one to one ratio and diluting twice to obtain an overall concentration of 2 mM for the lipids were all analysed using TEM microscopy. This was done in order to determine if there was a change at the microscopic level when both solutions were mixed. The results obtained are shown on Figures 104, 105 and 106 below. See the experimental section for further details on the technique.
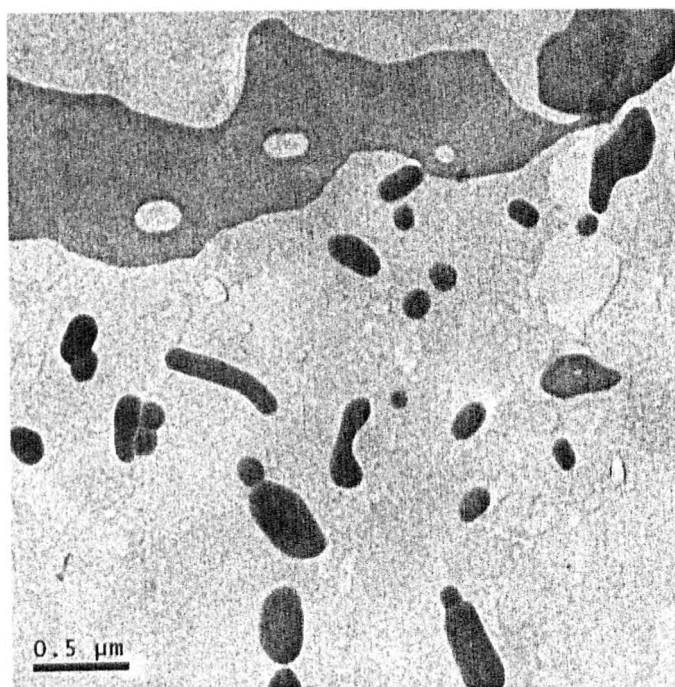
Figure 104. TEM microscopy image of the disulfide embedded vesicles solution (scale 1 cm = 0.5 μm).
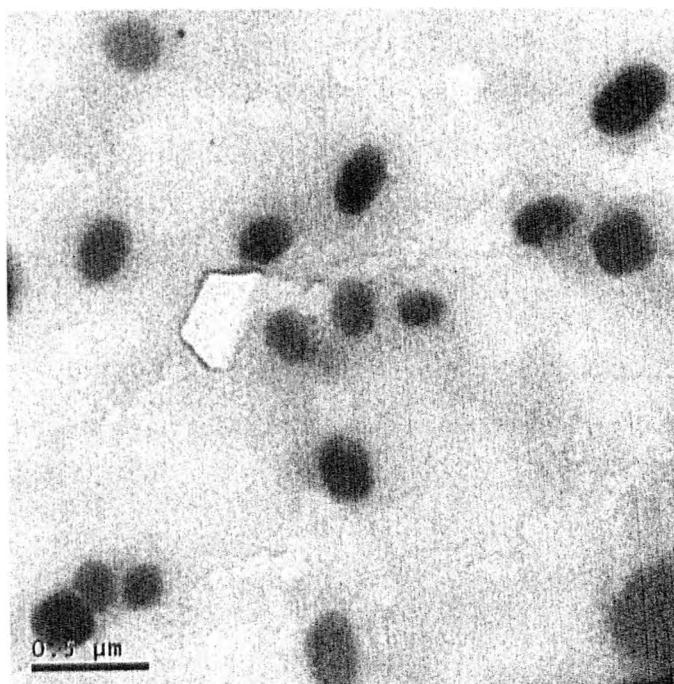
Figure 105. TEM microscopy image of the thiol embedded vesicles solution (scale 1 cm = 0.5 μm).
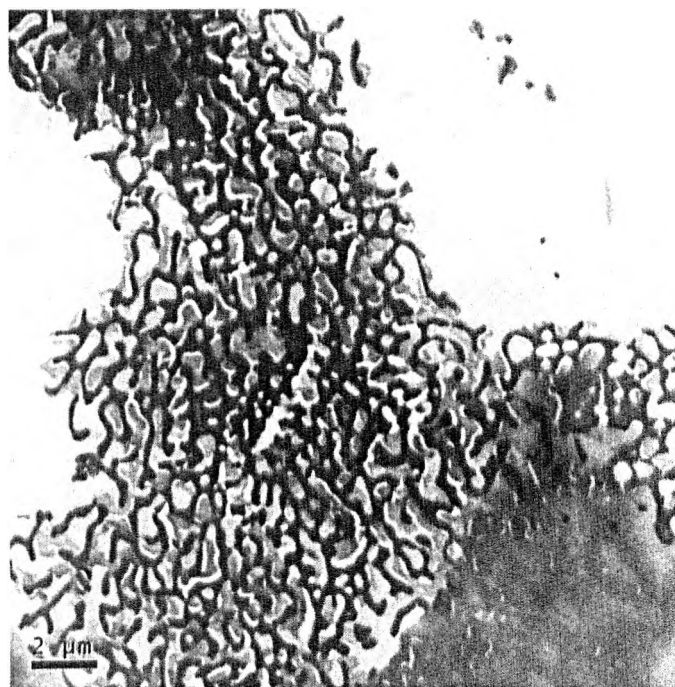
Figure 106. TEM microscopy image of the aggregates obtained upon mixture of vesicles containing thiol **9** and vesicles containing disulfide **7** (scale: 1 cm = 2 µm).

From the pictures taken, it is clear that an aggregate is formed when the two sets of vesicles are mixed together. This result confirms the results in the previous experience where a significant increase in absorbance was observed over the whole range of wavelengths when the two sets of vesicles were mixed together.

Nevertheless on its own this experiment cannot be conclusive on the formation of the vesicles since the aggregates seen on the images could simply be precipitated salts from the solution (MES).

V-2-6 Visual Appearance

Another experiment carried out to confirm that the mixture of the two sets of vesicles was producing aggregates when mixed together was to take pictures of the individual thiol **9** containing and disulfide **7** containing vesicle solutions as well as the solution resulting from their equimolar mixture. The concentrations of each solution are identical to the ones from the previous experiment. Pictures of three vials next to each other, each containing one of the three mentioned solutions, were taken at different times to determine if there was any change occurring (Figures 107 to 110).
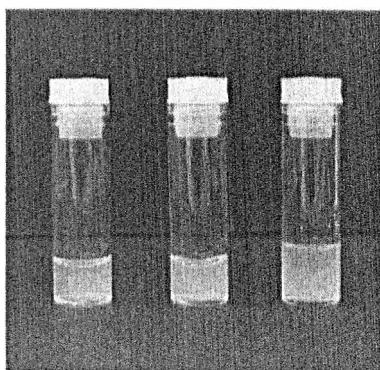
Figure 107. Picture of the three solutions, from left to right: thiol embedded vesicles solution, disulfide embedded vesicles solution and equimolar mixture of both solutions at t = 0 min after mixing.
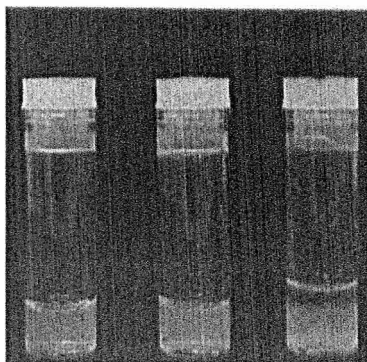
Figure 108. Picture of the three solutions, from left to right: thiol embedded vesicles solution, disulfide embedded vesicles solution and equimolar mixture of both solutions at t = 3 hours.
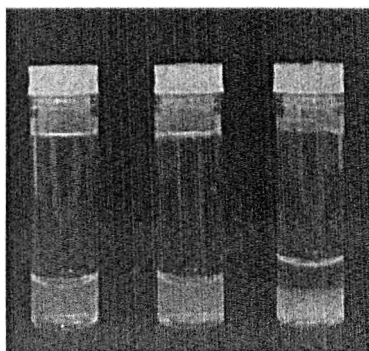
Figure 109. Picture of the three solutions, from left to right: thiol embedded vesicles solution, disulfide embedded vesicles solution and equimolar mixture of both solutions at t = 5 hours.
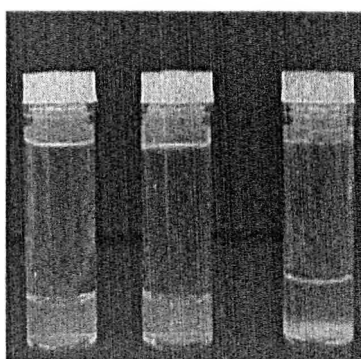
Figure 110. Picture of the three solutions, from left to right: thiol embedded vesicles solution, disulfide embedded vesicles solution and equimolar mixture of both solutions at t = 25 hours.

The pictures clearly show that the only solution for which there is sedimentation is the solution containing the mixture of both thiol and disulfide containing vesicles solutions. This indicates that the aggregates formed upon mixture of the two vesicles solutions are very large and their dispersion in water is not stable. Therefore they sediment with time as opposed to the other vesicles containing solutions that do not over the identical period of time.

V-2-7 Measurement of vesicle charge: Zeta potential

The first experiment carried out in order to try and understand the rationale for the formation of the reported aggregates (see experiments V-2-4, V-2-5 and V-2-6 respectively on pages 125,135 and 138 above), was the measurement of the Zeta potential of the charged vesicles. This potential represents the amount of charges present at the outer layer of the vesicular membrane. The measurement of the charges at the outer layer of the vesicles containing thiol **9** and of the vesicles containing disulfide **7** will enable us to determine the influence of charge on the aggregation of the vesicles. See the experimental section for further details on the technique.

The Zeta potential has been measured over time for the thiol **9** embedded vesicles (52 mM of **9** embedded in 2 mM of lipid), the disulfide **7** embedded ones (90 μM of **7** embedded in 2 mM of lipid) and for a solution obtained by mixing the two solution in one to one ratio and diluting twice to obtain an overall concentration of 2 mM for the lipids. The results obtained are shown below on Figures 111, 112 and 113 for the thiol **9** vesicles, disulfide **7** vesicles and the equimolar mixture of both set of vesicles respectively.
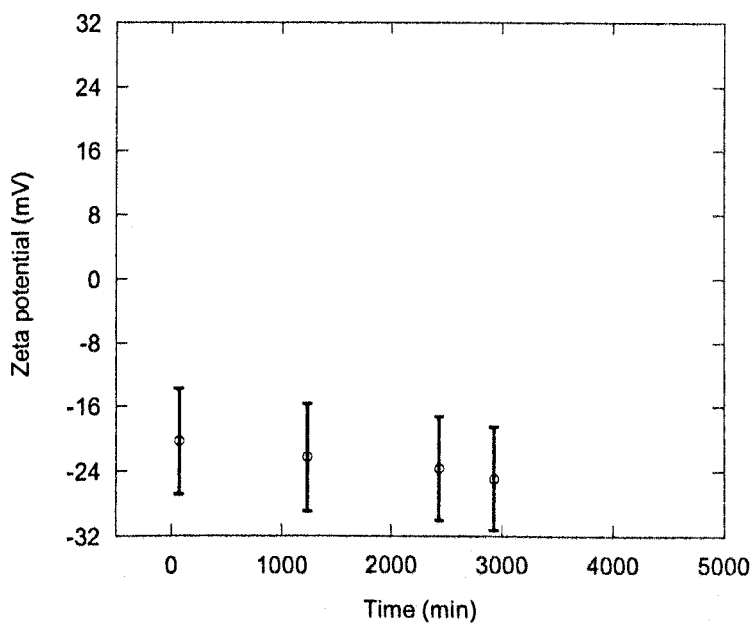
Figure 111. Evolution of the zeta potential of the thiol embedded vesicles. The error bars represent the standard deviation given by the apparatus used to measure the potential.
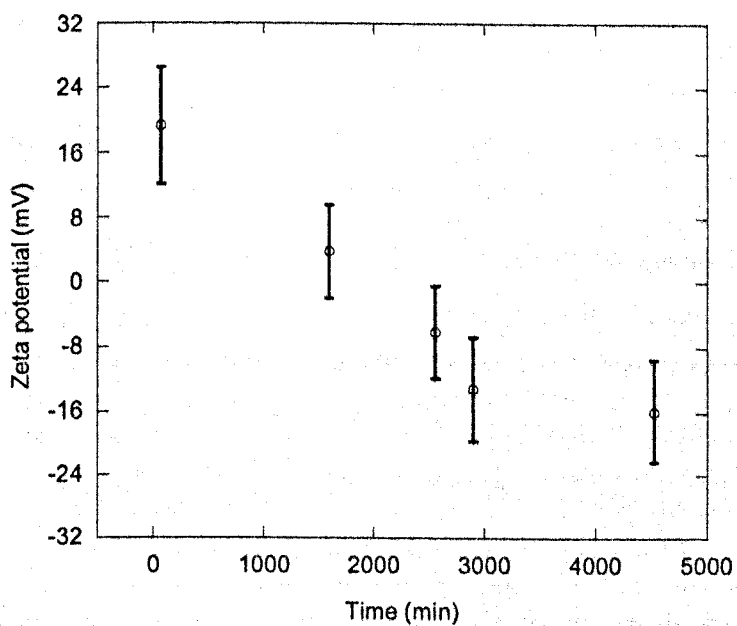
Figure 112. Evolution of the zeta potential of disulfide embedded vesicles. The error bars represent the standard deviation given by the apparatus used to measure the potential.

145
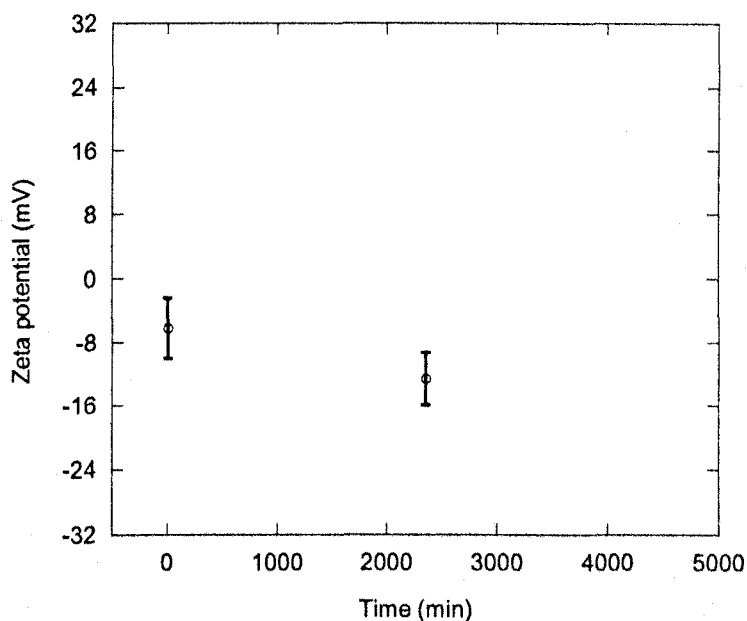
Figure 113. Evolution of the charges of the mixture of thiol embedded and disulfide embedded vesicles. The error bars represent the standard deviation given by the apparatus used to measure the potential.

From the results obtained, we can see that the negative charges on the disulfide **7** containing vesicles do not appear to be stable over time whereas the negative charges on the thiol **9** embedded vesicles are. The increase in absorbance as shown on Figure 103 page 139 above was found not to happen when 2 days old disulfide **7** containing vesicles were used in the experiment. This is confirmed by the charges measurements, since the charges on the outside layer of the disulfide containing vesicles becomes negative over time. Hence both sets of vesicles are negatively charged when 2 days old disulfide containing vesicles are mixed with thiol containing vesicles. The electrostatic repulsion is likely to be the explanation why no aggregates are formed in this case.

V-2-8 Dynamic Light Scattering

In order to confirm whether the vesicles sizes were modified when the disulfide embedded vesicles were mixed with the thiol embedded vesicles, the vesicles size for each individual vesicle solution and that of the mixture was measured using dynamic light scattering. This technique measures the difference in light intensity caused by the diffraction of light by the brownian motion of particles in solution. It then deducts the size of the particles using the Stokes-Einstein equation. See the experimental section for more details on this technique and how measures were taken.

The concentrations for each solution are identical to the two previous experiments. Blank vesicles were also prepared and their size was measured. See the experimental section for further details on the technique.

Table 6. Vesicle size measured by DLS.

	Vesicle size (in nm)	Polydispersity
Blank vesicles solution	190 ± 10	0.15
Thiol 9 containing vesicles solution	166 ± 0.9	0.17
Disulfide 7 containing vesicles solution	165 ± 1.1	0.13
Mixture of thiol and disulfide containing vesicles solutions	208 ± 15	0.27

The results obtained seem to contradict the previous experiments, since the size of the vesicle mixture solution does not appear to be significantly different from the sizes of the vesicles from the three other solutions. This might be explained by the fact that the detection limit of the DLS is 5 µm; hence the aggregates are probably not detected by this method. Moreover in order to carry out the measurements, the solutions

are diluted and this might disrupt the aggregates, which would explain why the size measured for the vesicles in the mixture is close to the ones for the other vesicles.

V-2-9 Experiment to determine the end products of the reaction between vesicles containing thiol 9 with vesicles containing disulfide 8

The aim of this experiment is to study the evolution of the absorbance of the mixture obtained from mixing a set of vesicles containing thiols 9 with another set of vesicles containing disulfides 7. Dithiothreitol is added to determine if disulfides 7 are still present in the mixture.

200 µM of thiol 9 was embedded within 4 mM of egg yolk phosphatidylcholine vesicles to obtain the first set of vesicles. 200 µM of disulfide 7 was also embedded within 4 mM phosphatidylcholine vesicles to obtain the second set of vesicles. Both concentrations of thiol 9 and disulfide 7 have been determined using Ellman's reagent and dithiothreitol respectively. The concentrations were found to be 75 µM of thiol in 4 mM of vesicles and 175 µM of disulfide in 4 mM of vesicles.

The following graph shows the evolution of the absorbance of the mixture of the two types of vesicles over time. The first part of the graph corresponds to the change over time without any other chemical entering the system. The second part with a sharper decrease corresponds to the response of the system after the addition of an excess of DTT to the suspension.
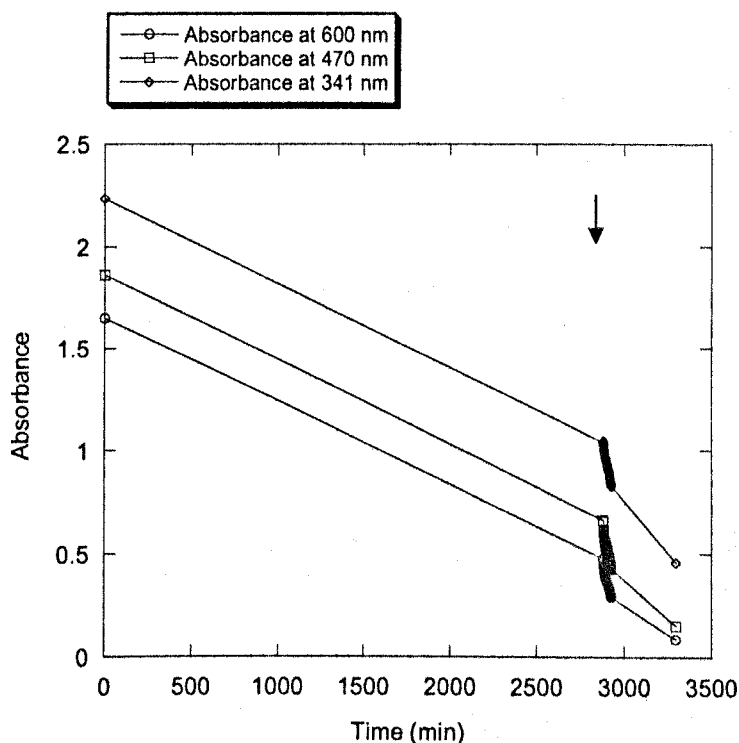
Figure 114. Evolution of the absorption of the thiol embedded and disulfide embedded vesicles at three different wavelengths (341, 470 and 600 nm). All the data collected are shown and the arrow indicates the time when dithiothreitol in excess has been introduced in the solution.

The introduction of the reductant does not trigger any release of pyridinethiol, which would indicate the presence of remaining disulfides and would be observed at 341 nm. A decrease in absorbance is occurring before the addition of the reductant but the decrease is significantly sharper after the addition. The slow decrease could be due to a rearrangement of the disulfide formed at the interface between the two vesicles, one containing thiols and another one containing disulfides (see Figure 115 below).
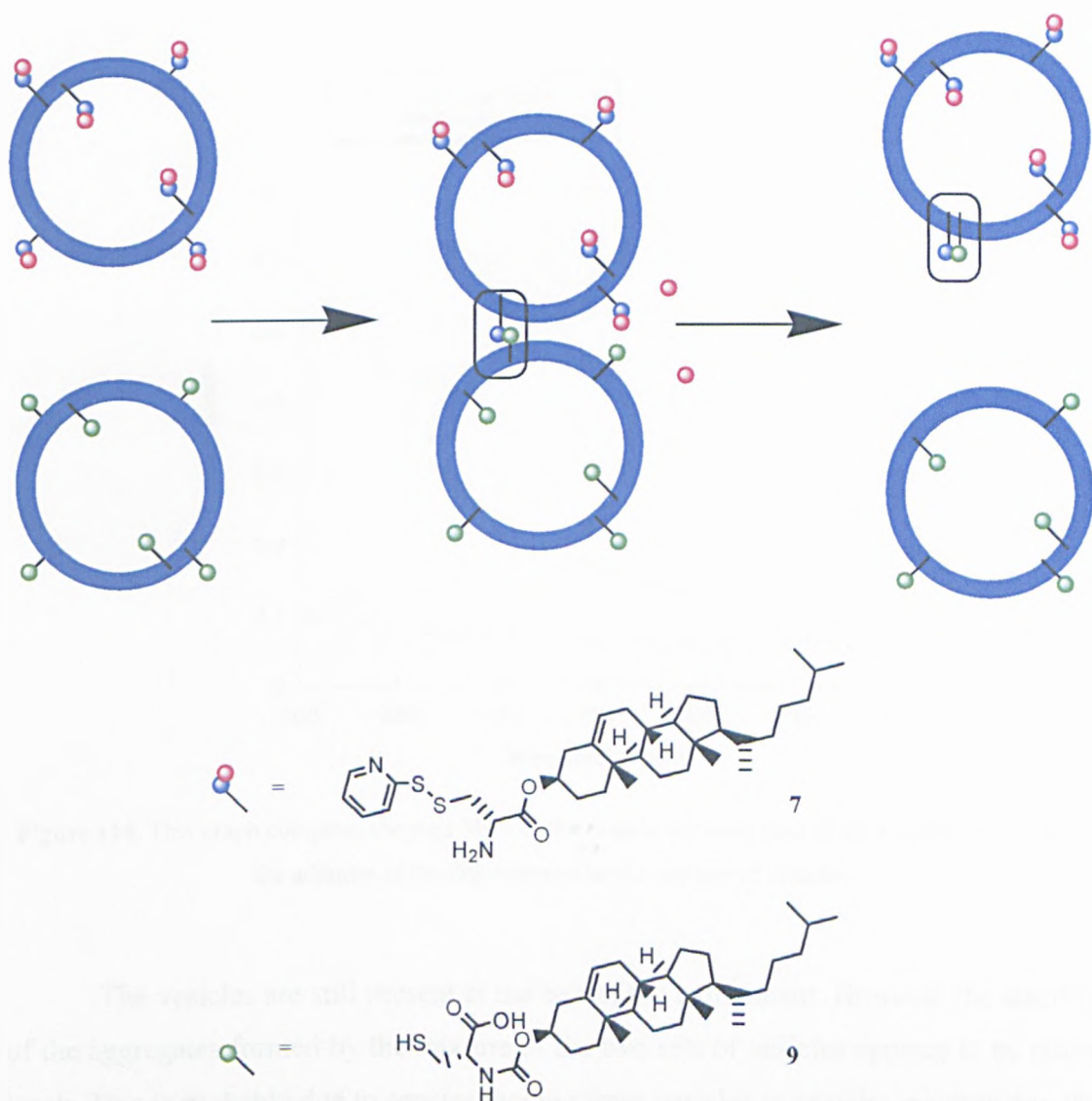
Figure 115. Possible explanation for the slow decrease of the absorbance after the two sets of vesicles have been mixed. One set contains the thiol shown and the other one the disulfide. When mixed together they react intervesicularly and a subsequent rearrangement of the molecules disrupts the aggregate.

The fact that the introduction of dithiothreitol accentuates the decrease in absorbance without possessing any charges seems to indicate that disulfides are formed between the vesicles and act as a bridge in addition to the coulombic attraction. The absorbance at the end of the experiment is back to an absorbance pattern that clearly indicates that vesicles are still present. The pure MES buffer has an absorbance between 0.056 and 0.1 in the 600 to 300 nm wavelengths range and the final scan shown below is absorbing much more than this in the shorter wavelengths.

150
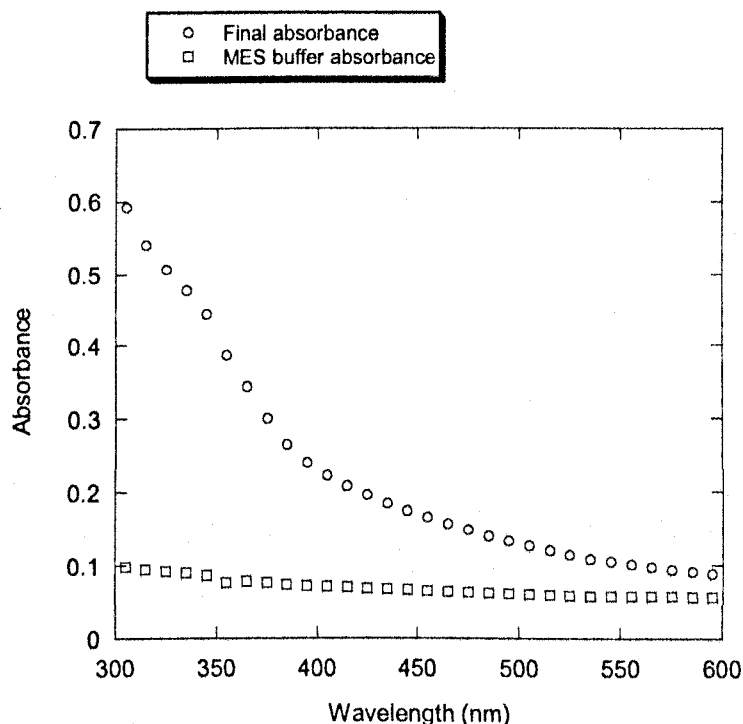
Figure 116. This graph compares the pure MES buffer scan to the final scan of the experiment, i.e. after the addition of the dithiothreitol to the mixture of vesicles.

The vesicles are still present at the end of the experiment. However the stability of the aggregates formed by the mixture of the two sets of vesicles appears to be rather weak. This is probably due to species moving from vesicles to vesicles, neutralizing the charges and forcing the aggregate to disrupt itself eventually. The contact between the vesicles is also not favorable due to the short length interactions happening when two vesicles are in close contact. All those factors can explain the relative instability of the aggregates formed.

V-2-10 Aggregate disruption using a charged polymer

200 μM of thiol **9** was embedded within 4 mM of egg yolk phosphatidylcholine vesicles to obtain the first set of vesicles. 200 μM of disulfide **7** was also embedded within 4 mM phosphatidylcholine vesicles to obtain the second set of vesicles. Both

concentrations of thiol **9** and disulfide **7** have been determined using Ellman's reagent and dithiothreitol respectively. The concentrations were found to be 50 μM of thiol in 4 mM of lipid and 184 μM of disulfide in 4 mM of lipid.

250 μL of the thiol containing vesicle solution was mixed with 500 μL of MES buffer and 250 μL of the disulfide containing vesicle solution. The solution was scanned between 300 and 600 nm every two minutes. Between 6 and 8 minutes 1.7 μL of a MES buffer solution of a water soluble positively charged polymer (4.6 mg.mL^{-1}) was added to the vesicle solution. The water soluble positively charged polymer used is PDMA (Poly[2-(dimethylamino)ethyl methacrylate]), with a molecular weight of 7400 g.mol^{-1}. I added more polymer (1.7 μL each time) after 14 minutes and after 16 minutes. I shook the solution after 36 minutes. I finally added 10 μL of polymer after 40 minutes.
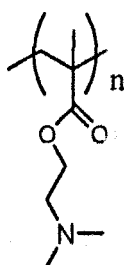
Figure 117. Structure of the PDMA polymer (average n= 47).
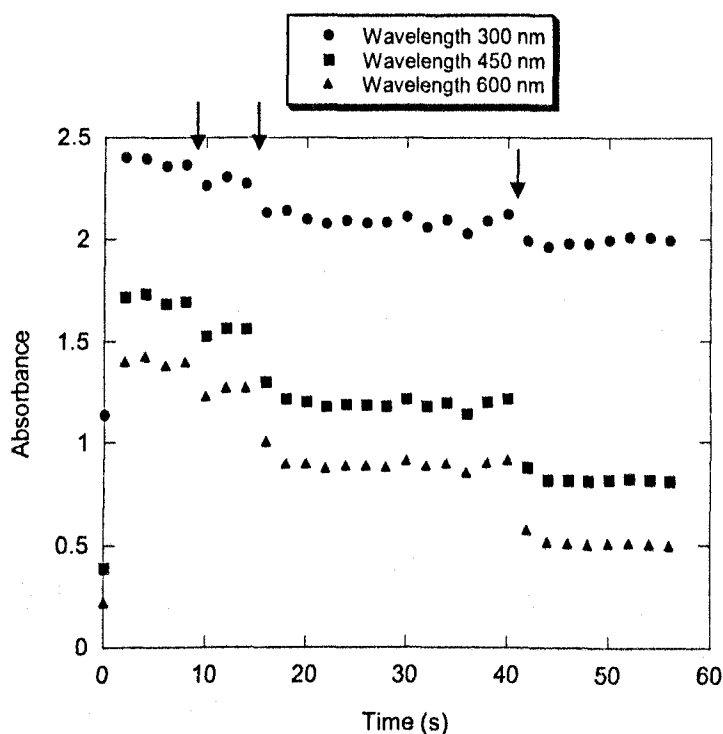
Figure 118. Evolution of the absorbance of a mixture of a set of thiol containing vesicles and a set of disulfide containing vesicles after the additions of a charged polymer. The absorbance is followed at three wavelengths (300, 450 and 600 nm). The arrows indicate the additions of polymer.

The addition of charged polymer affects the vesicles as we can observe a decrease in absorbance after each addition whereas the solution is relatively stable when no more polymer is added.

This indicates that there is a charge effect involved in the aggregation of the vesicles of opposite charges, thiol **9** having a side chain charged negatively due to the acid group and disulfide **7** having a side chain charged positively due to the amino group.

V-3 Discussion

What is first apparent when analysing the results obtained in our studies is that the system used, though reasonably simple at first glance, is in fact rather difficult to work with. This was mainly due to the difficulty faced when trying to incorporate thiol 7 within vesicles. This was done in the first experiment described (V-2-1 page 119). Following this failed attempt, we tried to synthesise thiol 7 in situ by reducing already incorporated disulfide 8 either with DTT (V-2-2 page 122) or with water soluble phosphine (V-2-3 page 125). The "reduced" vesicles were then mixed with disulfide 8 containing vesicles to determine whether a reaction could be observed between both sets of vesicles. In the case of the vesicles that were reduced using DTT, a reaction was observed between the two sets of vesicles; however it was not the case when phosphine was used as the reducing agent.

Despite the fact that reaction occurred between the two sets of vesicles when DTT was used as the in situ reagent to synthesise thiol 7 from disulfide 8 already embedded within vesicles, no aggregation of vesicles was observed.

Thiol 9 was then used as a replacement for thiol 7 since it was more stable to the vesicle making process. In addition charges interaction between the positively charged disulfide 8 and the negatively charged 9 could favour the reaction and aggregation of the vesicles.

The aggregation of the vesicles when using thiol 9 and disulfide 7 in different sets of vesicles was demonstrated in the control experiments V-2-4 on page 129. It was found that the only mixture of vesicles that triggered a significant increase in absorbance over the whole range of wavelengths 300-600nm was the mixture of vesicles containing thiol 9 with vesicles containing disulfide 7. The increase in absorbance was superior to 1 across the whole wavelengths. Only the formation of vesicular aggregates can explain an indiscriminate increase over the whole range of wavelengths observed.

In order to determine whether the aggregation was due to the reaction between thiol **9** and disulfide **7** and the formation of intervesicular disulfide bonds as a result and to confirm the formation of aggregates, the following experiments were carried out.

First each set of vesicles is observed using TEM microscopy (V-2-5 page 139), i.e. the one containing thiol **9** and the one containing disulfide **7**. The mixture of both sets of vesicles was observed as well to assess whether aggregates are made by aggregation of vesicles, fusion or other mechanisms. Unfortunately this experiment is not conclusive since the images obtained for the three solutions observed could just be images of precipitated salt (MES) since it is in high concentration compared to the lipid (ratio of 25:1).

The following experiment confirmed that the only solution that had aggregates was the solution formed by mixing vesicles containing thiol **9** with vesicles containing **7**. This was achieved by observing the sedimentation over time of a solution of vesicles containing thiol **9**, another of vesicles containing disulfide **7** and a third one which contained a mixture of both previous solutions (V-2-6 page 142). Only the latter showed sedimentation of the aggregates over a period of 25 hours whereas the other two solutions remained uniform over the same period of time.

The outer charges of the vesicles containing thiol **9**, vesicles containing disulfide **7** and solution made from a mixture of both were measured using Zeta potential (V-2-7 page 144). The change of the charge over time was also assessed. It was found that over time the charge of vesicles containing disulfide **7** changed from a positive outer charge to a negative one. The vesicles containing thiol **9** had a stable negative outer charge. Only two measurements have been made of the outer charge of the solution containing both sets of vesicles, therefore no definitive conclusion can be reliably drawn from the data for this solution. Nevertheless it appears that the overall negative outer charge is increasing over time. From this experiment it has been demonstrated on the one hand that the vesicles containing thiol **9** are negatively charged on the outer layer, this is

likely to be due to the charged carboxyl group on the reactive cysteine moiety. On the other hand it was found that the vesicles containing disulfide 7 are positively charged in the outer layer, this is likely to be due to the charged amino group on the reactive cysteine moiety. However this positive outer charge is decreasing over time until it becomes negative after approximately 33 hours and consequently increases its negative outer charge. No explanation could be found for this phenomenon. Nevertheless it was clear that on the time scales used for the reaction experiments between vesicles, i.e. a few hours, the change in charges would not be an issue.

The last experiment carried out to assess whether aggregates are formed was to measure the size of vesicles in solution using Dynamic Light Scattering (V-2-8 page 147). This technique measures the difference in light intensity caused by the diffraction of light by the brownian motion of particles in solution. It then deducts the size of the particles using the Stokes-Einstein equation. First the size of vesicles containing no thiol or disulfide was measured, then the size of vesicles containing thiol 9, followed by the size of vesicles containing disulfide 7. Finally the size of vesicles in a solution made by mixing a solution of vesicles containing thiol 9 and a solution of vesicles containing disulfide 7 was measured. The results do not indicate a significant increase in size upon mixing. However this might be due to the fact that this technique is limited in the size that it can measure to approximately 5 μm. As a result the aggregates are not detected.

From the above described experiments reasonably clear evidence that aggregates are formed has been obtained. It also appears that so far the main explanation for the formation is the electrostatic interaction between the oppositely charged vesicles. Some experiments were not conclusive but the detection limits of the techniques used or apparatus explain why no additional conclusive evidence was collected. The only unexplained fact is the decrease in charge of the vesicles containing disulfide 7 over time.

Therefore the next step was to confirm whether or not reactions occurred between thiols and disulfides embedded within different vesicles. In order to achieve

this, the last two experiments were carried out. We tried to determine what the end product was after a solution of vesicles containing thiol 9 was mixed with a solution of vesicles containing disulfide 7. Essentially we tried to assess how much of disulfide 7 remained at the end of the experiment. This was done since if we obtain the same quantity at the end than what was embedded within vesicles at the start of the experiment it would mean that the aggregate form only due to electrostatic interactions. Finally we tried to disrupt the aggregates with a water soluble polymer in the last experiment. If we can achieve this with a small amount of polymer that would indicate that no disulfide bridge brought the vesicles into aggregates.

In the first of the last two experiments (V-2-9 page 148 and V-2-10 page 151), we found that reaction between both sets of vesicles seem to have occurred since no disulfide remains to react with a large excess of DTT. This indicates that the formation of the aggregate triggers a reaction between the thiol and disulfide. Another indication of this fact that stems from the experiment is that the absorbance of the solution decreases over the whole range of wavelengths followed when the DTT is added. This is linked to the disruption of the aggregate. Therefore it appears that DTT has reduced the disulfide bonds that were holding the aggregate together. The decrease is significantly steeper after the addition of DTT than prior to it. This previous less sharp decrease could be due to the rearrangement of molecules between vesicles, i.e. disulfides formed between vesicles would migrate to a single one. This would also cause a disruption of the aggregates but would be slower than the disulfide reduction by DTT, not only due to the fact that the disulfide link between vesicles would be removed but also since charges would become equilibrated between vesicles. The equilibration would come from the fact that oppositely charged moieties of the newly formed disulfides would be in the same vesicles.

Finally the aggregates were disrupted with a water soluble positively charged polymer. Each addition of charged polymer to the solutions containing the aggregates decreased the overall absorbance over the whole range of wavelengths studies (300-600nm). Therefore this last experiment confirmed the fact that the aggregates are

formed partly due to the electrostatic interactions between the oppositely charged sets of vesicles.

Overall therefore we have demonstrated that our system enables the formation of vesicular aggregates via electrostatic interaction between the oppositely charged vesicles and formation of disulfide links between vesicles. The aggregates appear to be stable over at least a 24 hours period. Afterwards some probable molecular rearrangement between vesicles appears to disrupt the aggregate. Those findings are in line with other research in the field, most notably by Menger et al. [75-77] when he studied the adhesion of oppositely charged vesicles. However in his research no chemical reaction was occurring.

In the research that most resembles the present study [76], he obtained adhesion of giant vesicles using oppositely charged lipids embedded within two different giant vesicles. His adhesion was maintained during 30 minutes, consequently the vesicles drifted apart. This observation was explained by reorganisation of the lipids from a vesicle to another at the zone of contact between the vesicles, hence making them both neutral. As a result they drifted apart due to the loss of the electrostatic interactions. The vesicles we are using are different since they are of much lower size, nevertheless the reorganisation would be expected to occur at a similar rate. Therefore the stability of our aggregates over a period of 24 hours appear to indicate that in addition to the electrostatic interactions between oppositely charged vesicles, a chemical link must exist. This is in line with the fact that reactions appear to occur between thiol 9 in vesicles and disulfide 7 in others.

In another study [77] Menger et al. reported that the electrostatic adhesion of oppositely charged vesicles could be controlled by coating the outer layer of vesicles with charged polymer, therefore confirming the effect of the outer layer charge on the interaction between vesicles.

Chapter VI Conclusion

Thanks to the solution studies carried out in chapter 3, a much better understanding of the different thiol-disulfide reactions involved in the system as well as the reduction of disulfide by water soluble phosphine PPh3 was obtained. Rate constants were calculated for each reaction investigated and the mechanisms were confirmed by the data. However the mechanism and the rate constant for the oxidation of the different thiols using ferricyanide could not be determined.

The incorporation of one of the two reactants in vesicles and its effect on the rate of the thiol-disulfide exchange was then studied in chapter 4. The effect was shown to be minor, the rate constant being only slightly decreased by the presence of the vesicles.

The intravesicular reaction between the membrane anchored thiol 8 synthesized in situ by reduction with PPh3 and the membrane anchored disulfide did not occur, only when the thiol was synthesised in situ with DTT did thiol disulfide exchange occurred. This is the key reaction of the system since the fact that it was reported not to occur for the vesicles membrane spanning thiols and disulfides in the system designed by Barton et al.[21] was the basis of their experiment. It seems that the findings of this research are in disagreement with their findings. Even though the molecules in this present study are different from the molecules in Barton et al.'s study[21], they bear the same groups and are anchored to the vesicle via a cholesterol unit as well. However the fact that on one occasion the embedded thiols 8 and disulfides 7 seem to have not reacted indicate that this reaction still requires more research to be fully characterized.

Some experiments carried out in chapter 4 suggested that the embedded disulfide 7 was switching between the inner layer of the vesicle to the outer layer. The rate for this process was 10^{-4} s^{-1}. This value is an estimation of the rate of the process under the conditions used for the experiment; nevertheless even if the value is

inaccurate this indicates that the flip flop of the disulfide **7** is comparable to all the rates measured.

The last part of this research covered various attempts made to obtain an intervesicular reaction between two sets of vesicles bearing complementary reactive groups, one set containing thiols and the other disulfides. The synthesis of the thiol **8** in situ by reduction with the PPh3 or DTT was making it difficult to determine whether the intervesicular thiol-disulfide exchange reaction was occurring. The thiol **8** had to be synthesized in situ since it did not withstand the vesicle making process. Hence thiol **9** which was shown to remain largely active as thiol after the vesicle making process was used instead of thiol **8.** This new thiol could then be incorporated before the vesicles were extruded. The mixing of thiol **9** containing vesicles and disulfide **7** containing vesicles was found to generate vesicles aggregates due to the electrostatic interactions between the opposite charges on the side groups of the reactive species. Using different techniques and experiments, it was also found that reaction occurs between vesicles and thus disulfide links strengthen the aggregates formed.

Finally it is clear that further research on the behaviour of molecules inserted in vesicles and on intervesicular reactions is required to obtain a better understanding of the processes involved. Nevertheless this research has shown that aggregates of vesicles can be made using electrostatic interactions combined with chemical reactions for improved stability.

Experimental

Materials

All chemicals except the ones synthesized (see below), were obtained from Sigma Aldrich Chemical Co. and used without further purification.

The PDMA polymer was a gift from Dr Damien Dupin.

Synthesis of cholest-5-en-3β-yl S-(pyridine-2-thiol)-L-cysteinate (7)
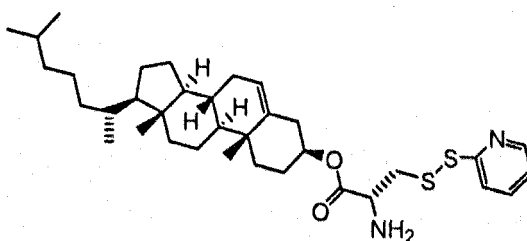
0.24 g (0.25 mmol) of **10** were dissolved in 6.4 mL of DCM. A solution of 0.44 g (2.9 mmol) of DTT in 1:1 water:methanol mixture was then added. The heterogeneous solution was stirred under argon overnight. The solvents were removed under reduced pressure and the residue was dissolved in 50 mL of chloroform. The organic solution was washed three times with 25 mL of water. It was dried over anhydrous sodium sulphate and filtered. 0.949 g (4.31 mmol) of 2,2'-dithiodipyridine dissolved in 10 mL of methanol were added to this solution. The obtained mixture was stirred under argon for 50 minutes. The solvents were removed under reduced pressure and the residue was dissolved in approximately 100 mL of chloroform. The organic solution was then washed four times with 100 mL of saturated NaHCO₃ solution and once with 100 mL of brine. It was then dried over anhydrous magnesium sulphate,

filtered and the solvent removed under reduced pressure. The crude product was then purified by column chromatography on silica gel eluting with 95:5 DCM:methanol (R_f=0.15).

0.11 g (36%) of **7** was obtained as an oil.
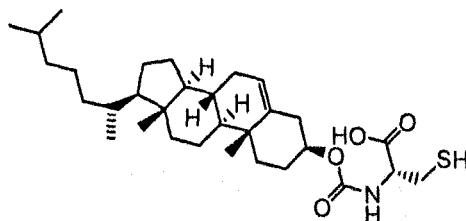
^{1}H NMR 250 MHz (CDCl$_3$): δ 0.5 – 2.3 (45H, broad multiplet, aliphatic cholesterol protons), 2.99 (1H, dd, 8 Hz, 13 Hz, CH_aH$_b$S), 3.23 (1H, dd, 4 Hz, 13 Hz, CH$_a$$H_b$S), 3.75 (1H, dd, 4 Hz, 8 Hz, CH-N), 4.63 (1H, m, HC-O-C=O), 5.34 (1H, d, 4Hz, HC=C), 7.10 (1H, m, aromatic proton), 7.64 (2H, m, aromatic proton), 8.49 (1H, m, proton in ortho to the nitrogen).

^{13}C NMR 62.9 MHz (CDCl$_3$): δ 11.85, 18.72, 19.30, 21.02, 22.56, 22.81, 23.82, 24.27, 27.66, 28.00, 28.21, 29.69, 31.83, 31.90, 35.78, 36.18, 36.55, 36.90, 37.95, 39.51, 39.71, 42.30, 44.31, 49.99, 53.76, 56.13, 56.67, 75.21, 120.12, 120.91, 121.08, 122.91, 136.97, 139.34, 149.80, 172.88.

Mass Spec ES$^+$: 599 (MH$^+$).

Accurate Mass Spec: 599.3687 for MH$^+$ (calculated mass for MH$^+$: 599.3705).

This synthesis follows the method previously described by Timothy Potter in his PhD thesis [78].

Synthesis of 2-[cholest-5-en-3β-yloxycarbonylamino]-3-mercapto-propionic acid (9)

300 mg of **22** (0.39 mmol) were dissolved in 10 mL of DCM, 10 mL of TFA was added, the solution was stirred 2 minutes before 0.4 mL of TIS were added. The solution was then evaporated under reduced pressure. The crude product was then purified by chromatography on silica, eluting with DCM first in order to remove impurities, then with 9:1 DCM:methanol in order to collect the product (R_f=0.3 eluting with 9:1 DCM:methanol).

190 mg (91%) of **9** was obtained as a white solid.

TOF Mass Spec ES⁺: 556 (MNa⁺), no peak around 1100 (no disulfide).

Accurate Mass Spec: 556.3442 for MNa⁺ (calculated mass for MNa⁺: 556.3437).

This synthesis follows the method previously described by Timothy Potter in his PhD thesis [78].

Synthesis of di(cholest-5-en-3β-yl) L-cysteinate (10)

0.93 g (1.11 mmol) of **20** were dissolved in 13 mL of DCM. 40 mL of TFA were added dropwise, followed by TIS until the dark orange colour turned to pale pink. The solution was stirred for two minutes afterwards. The solvents were removed under *reduced pressure; the residue was dissolved in approximately 100 mL of chloroform.* This solution was washed twice with 100 mL of saturated NaHCO₃ solution and once with 100 mL of brine. It was dried on anhydrous sodium sulphate, filtered and the solvent was removed under reduced pressure. The crude product was purified by column chromatography on silica gel eluting with 9:1 DCM:methanol (R_f=0.33).

0.24 g (44%) of **10** was obtained as a slightly brown solid.

¹H NMR 250 MHz (CDCl₃): δ 0.5 – 2.3 (45H, broad multiplet, aliphatic cholesterol protons), 2.86 (1H, dd, 8 Hz, 13 Hz, C*H*ₐHᵦS), 3.08 (1H, dd, 5 Hz, 13 Hz, CHₐ*H*ᵦS), 3.71 (1H, dd, 5 Hz, 8 Hz, C*H*-N), 4.60 (1H, m, *H*C-O-C=O), 5.31 (1H, d, 4Hz, *H*C=C).
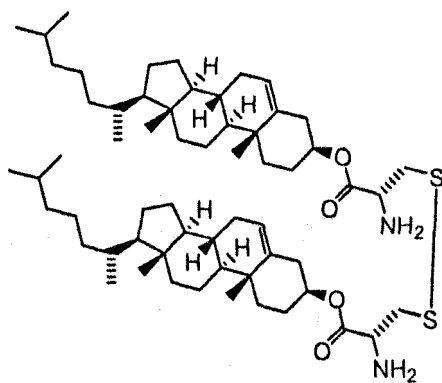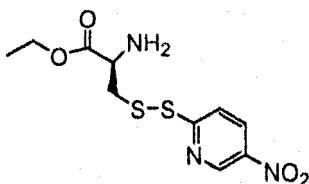
¹³C NMR 62.9 MHz (CDCl₃): δ 11.85, 12.29, 17.69, 18.71, 19.31, 21.03, 22.55, 22.80, 23.83, 24.27, 27.72, 28.00, 28.21, 31.84, 31.90, 35.78, 36.18, 36.57, 36.92, 38.04, 39.51, 39.72, 42.31, 43.95, 49.99, 53.80, 56.14, 56.68, 75.20, 173.11.

Mass Spec ES⁺: 978 (MH⁺).

Accurate Mass Spec: 977.7182 for MH⁺ (calculated mass for MH⁺: 977.7203).

This synthesis follows the method previously described by Timothy Potter in his PhD thesis [78].

Synthesis of S-(4-nitro-pyridine-2-thiol)-L-cysteine ethyl ester (11)

0.61 g (3.3 mmol) of cysteine ethyl ester hydrochloride were dissolved in approximately 30 mL of deionized water. The solution was brought to pH 8.2 using 1N NaOH solution in deionized water. The solution was then extracted three times with 40 mL of chloroform. The organic layer was then dried over anhydrous sodium sulphate, filtered and the solvent was removed under reduced pressure. The oil obtained was dissolved in 40 mL of methanol. 2.03 g (6.5 mmol) of 2,2'-dithiobis(5-nitropyridine) in 30 mL of DCM were added and the solution was stirred under argon for 25 minutes. The solvent was then removed under reduced pressure. The mixture was dissolved in chloroform and then washed three times with 200 mL of saturated NaHCO₃ solution and once with brine. The organic layer was then dried over anhydrous sodium sulphate, filtered and the solvent was removed under reduced pressure. The crude product was purified by column chromatography on silica gel eluting with 95:5 DCM:methanol (R_f=0.15).

0.24 g (24%) of **11** was obtained as an oil.

^{1}H NMR 250 MHz (CDCl$_3$): δ 1.24 (3H, t, 7 Hz, C*H₃*-C-O), 3.03 (1H, dd, 8 Hz, 14 Hz, C*Hₐ*H$_b$S), 3.23 (1H, dd, 5 Hz, 14 Hz, CHₐ*H$_b$*S), 3.72 (1H, dd, 5 Hz, 8 Hz, C*H*-N), 4.16 (2H, q, 7 Hz, C-C*H₂*-O), 7.86 (1H, d, 9 Hz, C*H*-C(S)=N), 8.38 (1H, dd, 3Hz, 9 Hz, C*H*-C-NO$_2$), 9.26 (1H, d, 2 Hz, N-C*H*-C-NO$_2$).

^{13}C NMR 62.9 MHz (CDCl$_3$): δ 14.15, 44.16, 53.71, 61.60, 119.61, 131.61, 142.19, 145.17, 167.97, 173.22.

Mass Spec ES$^+$: 304 (MH$^+$).

Accurate Mass Spec: 304.0423 for MH$^+$ (calculated mass for MH$^+$: 304.0426).

This synthesis follows the method previously described by Timothy Potter in his PhD thesis [78].

Synthesis of S-(pyridine-2-thiol)-L-cysteine ethyl ester (12)

0.47 g (2.5 mmol) of cysteine ethyl ester hydrochloride were dissolved in approximately 30 mL of deionized water. The solution was brought to pH 8.2 using 1N NaOH solution in deionized water. The solution was then extracted three times with 40 mL of chloroform. The organic layer was then dried over anhydrous sodium sulphate, filtered and the solvent was removed under reduced pressure. The oil obtained was dissolved in 35 mL of absolute ethanol. 1.41 g (6.4 mmol) of 2,2'-dithiodipyridine were added and the solution was stirred under argon for 45 minutes. The solvent was then removed under reduced pressure. The mixture was dissolved in chloroform and then washed five times with 100 mL of saturated NaHCO$_3$ solution and once with brine. The

organic layer was then dried over anhydrous sodium sulphate, filtered and the solvent was removed under reduced pressure. The crude product was purified by column chromatography on silica gel eluting with 95:5 DCM:methanol (R_f=0.15).

0.23 g (35%) of **12** was obtained as an oil.

^{1}H NMR 250 MHz (CDCl$_3$): δ 1.22 (3H, t, 7 Hz, C*H$_3$*-C-O), 2.95 (1H, dd, 8 Hz, 13 Hz, C*H$_a$*H$_b$S), 3.21 (1H, dd, 4 Hz, 13 Hz, CH$_a$*H$_b$*S), 3.75 (1H, dd, 4 Hz, 8 Hz, C*H*-N), 4.14 (2H, q, 7 Hz, C-C*H$_2$*-O), 7.08 (1H, m, aromatic proton), 7.61 (2H, m, aromatic proton), 8.46 (1H, m, proton in ortho to the nitrogen).

^{13}C NMR 62.9 MHz (CDCl$_3$): δ 14.55, 44.36, 53.97, 61.84, 120.51, 121.36, 137.42, 150.21, 159.66, 173.89.

Mass Spec EI$^+$: 258 (M$^+$).

Accurate Mass Spec: 258.0496 for M$^+$ (calculated mass for M$^+$: 258.0496).

This synthesis follows the method previously described by Timothy Potter in his PhD thesis [78].

Synthesis of 2-ethoxycarbonylamino-3-mercapto-propionic acid (14)

0.50 g (1.3 mmol) of **15** were dissolved in 50 mL of water. 1.74 g (3.1 mmol) of 3,3',3''-phosphinidyne-tris(benzenesulfonic acid) trisodium salt were added to the solution that was then stirred for an hour under argon. The solution was washed three

times with 50 mL of ethylacetate. The organic layer was dried over anhydrous magnesium sulphate, filtered and the solvent was removed under reduces pressure.

0.40 g (78%) of **14** was obtained as an oil.

^{1}**H NMR 250 MHz (CDCl$_3$):** δ 1.26 (3H, t, 7 Hz, C*H$_3$*-C-O), 2.05 (1H,), 3.00 (1H, dd, 9 Hz, 14 Hz, C*H$_a$*H$_b$S), 3.30 (1H, dd, 4 Hz, 14 Hz, CH$_a$*H$_b$*S), 4.09 (1H, q, 7 Hz, C*H*-N), 4.52 (2H, dd, 4 Hz, 9 Hz, C-C*H$_2$*-O).

^{13}**C NMR 62.9 MHz (CDCl$_3$):** δ 14.59, 27.15, 55.05, 61.84, 156.39, 174.27.

This synthesis follows the method used by Crankshaw *et al.* [79].

Synthesis of 3-(2-carboxy-2-ethoxycarbonylamino-ethyldisulfanyl)-2-ethoxycarbonylamino-propionic acid (15)

6 g (25.0 mmol) of cystine were added to a solution made of 2.02 g (50.5 mmol) of NaOH dissolved in 25 mL of water. The whole solution was kept at 0°C using an ice bath. A solution of 3.4 g (32.1 mmol) of Na$_2$CO$_3$ in 50 mL of water was added drop wise to the cystine solution followed by the addition of 13 mL (132 mmol) of ethylchloroformate added drop wise as well. The solution was stirred and kept at 0°C and at pH 8-9 for 40 minutes, following this treatment it was stirred at room temperature for 2 hours. Afterwards, the solution was acidified to pH 1 using a 1:1 water:concentrated HCl solution. The product was then extracted in 3 times 100 mL of ethyl acetate. The organic layer was dried over anhydrous magnesium sulphate, filtered and the solvent was removed under reduced pressure.
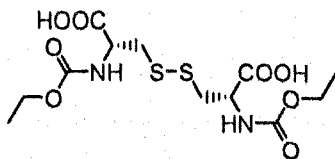
7.76 g (81%) of **15** was obtained as colourless grease.

¹H NMR 250 MHz (D₂O): δ 1.21 (3H, t, 7 Hz, C*H₃*-C-O), 3.00 (1H, dd, 9 Hz, 14 Hz, C*Hₐ*HᵦS), 3.30 (1H, dd, 4 Hz, 14 Hz, CHₐ*Hᵦ*S), 4.09 (1H, q, 7 Hz, C*H*-N), 4.52 (2H, dd, 4 Hz, 9 Hz, C-C*H₂*-O).

¹³C NMR 62.9 MHz (D₂O): δ 13.87, 39.21, 53.22, 62.32, 174.58.

Mass Spec ES⁺: 385 (MH⁺).

Accurate Mass Spec: 385.0734 for MH⁺ (calculated mass for MH⁺: 385.0739).

This synthesis follows the method used by Nadel *et al.* [80].

Synthesis of cholest-5-en-3β-yl N-α-Boc-S-trityl-L-cysteinate (20)

2.40 g (5.2 mmol) of N-α-Boc-S-trityl-cysteine were dissolved in 60 mL of DCM. 1.44 g (11.8 mmol) of DMAP, 0.97 g (8.22 mmol) of DCC and 5.43 g (14.0 mmol) of cholesterol were added to the solution in that order. The mixture was stirred at room temperature for three days. The solution was washed 3 times with 150 mL of 0.1N HCl solution, dried over anhydrous magnesium sulphate, filtered and the solvent was

removed under reduced pressure. The crude product was purified by column chromatography on silica gel eluting with DCM ($R_f = 0.5$ eluting with DCM).

3.50 g (81 %) of **20** was obtained as a white solid.

^{1}H NMR 250 MHz (CDCl$_3$): δ 0.5 – 2.3 (52H, broad multiplet, aliphatic cholesterol protons and (CH_3)$_3$- protons), 2.5 – 2.6 (2H, m, CH_2STrt), 4.25 (1H, m, O=C-N-CH), 4.6 (1H, m, HC-O-C=O), 5.1 (1H, d, 8Hz, NH proton), 5.4 (1H, d, 4Hz, HC=C), 7.2 – 7.6 (15H, m, aromatic protons).

^{13}C NMR 62.9 MHz (CDCl$_3$): δ 11.87, 18.72, 19.33, 21.03, 22.57, 22.83, 23.83, 24.29, 27.63, 28.02, 28.23, 28.32, 31.85, 34.34, 35.80, 36.18, 36.57, 36.88, 37.84, 39.52, 39.71, 42.31, 49.98, 56.13, 56.67, 66.62, 75.41, 122.92, 126.81, 127.98, 129.51, 139.39, 144.35, 170.12.

Mass Spec ES$^+$: 855 (MNa$^+$).

Accurate Mass Spec: 854.5146 for MNa$^+$ (calculated mass for MNa$^+$: 854.5158).

This synthesis follows the method previously described by Timothy Potter in his PhD thesis [78].

Synthesis of carbonic acid cholest-5-en-3β-yl ester 4-nitro-phenyl ester (21)

1 g of cholesterol (2.6 mmol) was dissolved in 20 mL of DCM, 0.7 mL (5 mmol) of triethylamine was added followed by 1.07 g (5.3 mmol) of 4-nitrophenyl chloroformate dissolved in 10 mL of DCM added dropwise to the stirred solution. The reaction was stirred under argon overnight. It was then washed 3 times with 100 mL of saturated NaHCO₃, 2 times with 100 mL of deionised water then once with 100 mL of brine. The DCM solution was dried over anhydrous magnesium sulphate, filtered and the solvent was removed under reduced pressure. The crude product was purified by column chromatography on silica gel (around 100 g) eluting with 3:2 DCM:hexane to collect the product (R_f=0.6).

1.17 g (81%) of **21** was obtained as a white solid.

^{1}H NMR 250 MHz (CDCl₃): δ 0.6-2.6 (43H, broad multiplet, aliphatic cholesterol protons), 4.60 (1H, m, *H*C-O-C=O), 5.42 (1H, d, 5 Hz, *H*C=C), 7.37 (2H, m, O-C-C*H*-C-C-NO₂), 8.27 (2H, m, O-C-C-C*H*-C-NO₂).

The reaction was based on the methodology from Lingard *et al.* [81].

Synthesis of 2-[cholest-5-en-3β-yloxycarbonylamino]-3-tritylsulfanyl-propionic acid (22)

138 mg of **21** (0.25 mmol) were dissolved in 6 mL of dry DCM and added dropwise to a 5 mL dry DCM solution of 110 mg of S-Trt-cysteine (0.3 mmol) and 80 μL of triethylamine (0.55 mmol). The solution was stirred under argon for five days. The mixture was then washed 3 times with 100 mL of cold 40% brine then twice with 100 mL of cold saturated Na_2CO_3. The DCM solution was then dried over anhydrous sodium sulphate, filtered and the solvent evaporated under reduced pressure. The crude product was purified by column chromatography on silica gel (13 g) eluting with 95:5 DCM:methanol to collect the product (R_f=0.1).

82 mg (42%) of **22** was obtained as a white solid.

^{1}H NMR 250 MHz (CDCl$_3$): δ 0.5-2.3 (40H, broad multiplet, aliphatic cholesterol protons), 2.55 (2H, broad peak, CH_2-S), 4.0 (1H, broad peak, O=C-N-CH), 4.3 (1H, broad peak, HC-O-C=O), 5.05 (1H, broad peak, NH proton), 5.3 (1H, broad peak, HC=C), 7.1-7.3 (15H, broad multiplet, aromatic protons).

^{13}C NMR 62.9 MHz (CDCl$_3$): δ 11.88, 18.76, 19.37, 21.09, 22.59, 22.84, 23.94, 24.33, 28.03, 28.29, 31.88, 35.86, 36.25, 36.51, 36.89, 38.52, 39.54, 39.77, 42.33, 49.93, 56.23, 56.68, 107.42, 122.50, 126.74, 127.99, 129.57, 139.82, 144.53.

TOF Mass Spec ES⁻: 775 (M(-H)⁻)

Accurate Mass Spec: 774.4576 for M(-H)⁻ (calculated mass for M(-H)⁻: 774.4556).

Preparation of vesicles

Egg yolk L-α-phosphatidylcholine (type XVI-E 99% (TLC), Sigma P3556) was dissolved in HPLC grade chloroform. Quantities of lipid were used such as to give a final lipid concentration of 2 mM in all cases. A chloroform solution of the thiol or disulfide to be incorporated was added to the lipid solution, such as to give a final concentration of 50 μM. The lipid was deposited as a thin film by removal of the solvent under reduced pressure, and then put under high vacuum for half an hour. Buffer (MES, pH 5.5) was added to the flask to give a suspension. The mixture was shaken and sometimes vortexed if required until all of the lipid had become detached from the side of the flask. 1 mL suspension was passed 19 times through a 200 nm polycarbonate filter in an Avestin Liposofast™ extrusion apparatus, to give unilamellar vesicles.

Acquisition of kinetic data using stopped flow apparatus

The stopped flow apparatus used was a SFM-300 stopped flow with a MOS-450 sprectrometer from Bio-Logic SA (France), the program to command the apparatus and record the data was Bio-Kine v4.25. The kinetic fits on the data gathered using the stopped flow instrument were computed using the Kaleidagraph program. The two solutions of the reactants whose reaction was studied by stopped flow were prepared by weight in MES buffer at pH 5.5. Those two solutions are then entered into syringes 1 and 3 of the stopped flow apparatus (see Figure 119 below for a scheme of the

apparatus), syringe 2 containing pure MES buffer at pH 5.5. Syringe 1 was filled with the reactant in excess and syringe 3 with the limiting reactant.

Then using the program to command the stopped flow apparatus, the ratio of volumes from the three different syringes were varied so as to obtain traces at different concentrations of the reactant in excess with a constant concentration of the limiting reactant. This was achieved by adding a constant volume coming from syringes 1 and 2 with different ratios of buffer to reactant 1 to a constant volume of syringe 3 containing the limiting reactant.

Figure 119. Scheme of the stopped flow apparatus.

Images of the vesicles by TEM

The samples were prepared by evaporating one drop of a very dilute solution (typically < 10 µM) to be analysed on a copper based TEM grid. No staining was done on the samples analysed. The sample analysis was carried out by Andreas Schmit.

Characterisation of the vesicles charges using Zeta potential measurements

Zeta potentials were calculated from measured electrophoretic mobilities using a Malvern Zetasizer Nano ZS instrument. Measurements were performed as the solution pH of a dilute dispersion of the nanocomposite particles was varied. The solutions to be analysed were used as prepared. Zeta potentials were averaged over twenty runs. In order to minimise electric double layer effects, the dispersion was diluted using MES buffer with an identical concentration to the one used when preparing vesicles.

Figure 120. Electric double layer.

Much colloidal dispersion in aqueous media carry an electric charge and, in the case of the vesicles used in this research, this is due to the ionisation of surface groups. The development of net charge at the particle surface affects the distribution of ions in

the surrounding interfacial region, resulting in an increased concentration of counter-ions close to the surface, which is known as t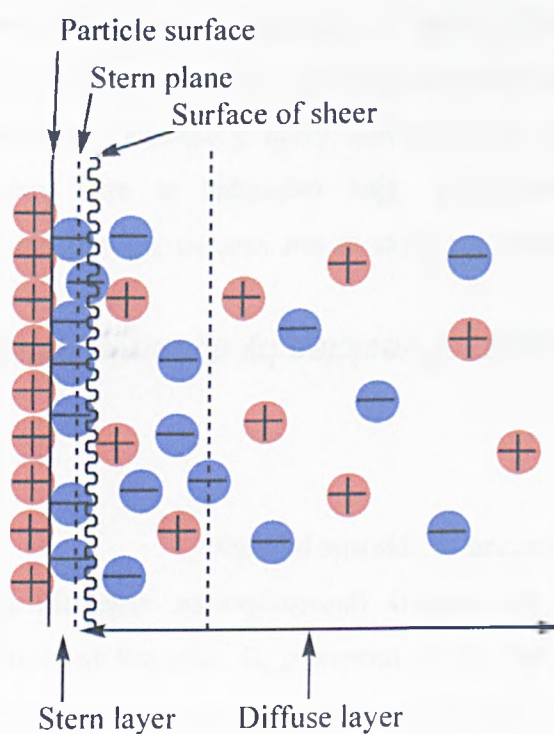he electric double layer[82]. This layer exists as two parts: the inner region (Stern layer) where the ions are strongly bound, and the outer (diffuse) region where the ions are less strongly associated. Within the diffuse layer there is a notional boundary, and when the particle moves, the ions within the boundary move with it and those beyond it do not. The potential at the boundary is the zeta potential, and this is measured by applying an electric field across the electrolyte and analysing the velocity (electrophoretic mobility) of the particles as they move towards the electrode of opposite polarity.

Characterisation of vesicles by dynamic light scattering

To measure the sizes of our vesicles the technique of dynamic light scattering (DLS) was employed. This technique is also known as *Photon Correlation Spectroscopy* or *Quasi-Elastic Light Scattering*. Measurements were made at 20 °C using a Malvern Zetasizer Nano ZS instrument, equipped with a digital correlator and a solid state laser (125 mW, $\lambda = 532$ nm). Scattered light was detected at a fixed angle of 90° and the mean hydrodynamic particle diameter was calculated from the quadratic fitting of the correlation function over 20-30 minutes. All measurements were performed on dilute dispersions (typically < 10 μM), filtered with a 200nm size pore.

DLS is a technique that analyses the random 3D light diffraction pattern caused by Brownian motion of the dispersed colloidal particles. This random motion is assessed by measuring the rate at which the intensity of the scattered light fluctuates with time, and is defined by the translational diffusion coefficient, D. The hydrodynamic particle radius (R_H) is related to D by the Stokes-Einstein equation (Equation below), which is valid only for dilute, isolated monodisperse spheres. The value for R_H can then be used to determine d_z, which is related approximately to the intensity-average particle diameter d_i ($2R_H = d_i \sim d_z$).

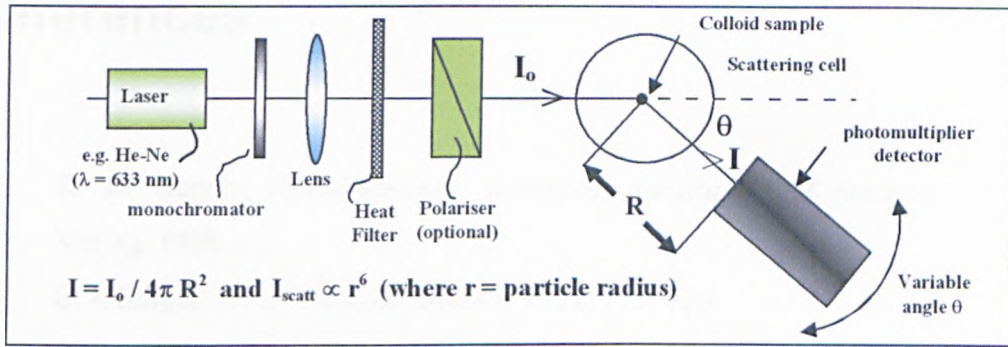**Figure 121.** Schematic representation of the DLS instrument set-up.

Stokes-Einstein Equation

$$D = \frac{kT}{6\pi.\eta.R_H}$$

k is Boltzman's constant (J K^{-1})

η is the solution viscosity (N s m^{-2})

T is the absolute temperature (K)

References

[1]   R. B. Gennis, *Biomembranes: molecular structure and function*, Springer-Verlag, **1989**.

[2]   S. J. Singer, G. L. Nicolson, *Science* **1972**, *175*, 720.

[3]   J. B. Finean, *Membranes and their cellular functions*, Third ed., Blackwell Scientific Publications, **1984**.

[4]   J. T. Hancock, *Cell signalling*, Second ed., Oxford University Press, **2005**.

[5]   M. Antonietti, S. Forster, *Advanced Materials* **2003**, *15*, 1323.

[6]   C. H. Tung, L. Z. Wu, L. P. Zhang, B. Chen, *Accounts of Chemical Research* **2003**, *36*, 39.

[7]   C. H. Tung, L. Z. Wu, L. P. Zhang, H. R. Li, X. Y. Yi, K. S. Ming, Z. Y. Yuan, J. Q. Guan, H. W. Wang, Y. M. Ying, X. H. Xu, *Pure and Applied Chemistry* **2000**, *72*, 2289.

[8]   T. Rispens, J. Engberts, *Organic Letters* **2001**, *3*, 941.

[9]   T. Lian, R. J. Y. Ho, *Journal of Pharmaceutical Sciences* **2001**, *90*, 667.

[10]   W. M. Leevy, G. M. Donato, R. Ferdani, W. E. Goldman, P. H. Schlesinger, G. W. Gokel, *Journal of the American Chemical Society* **2002**, *124*, 9022.

[11]   S. Shawaphun, V. Janout, S. L. Regen, *Journal of the American Chemical Society* **1999**, *121*, 5860.

[12]   M. Kirch, J.-M. Lehn, *Angew. Chem. Int. Ed.* **1975**, *14*, 555.

[13]   K. Ng, D. W. Pack, D. Y. Sasaki, F. H. Arnold, *Langmuir* **1995**, *11*, 4048.

[14]   D. W. Pack, G. H. Chen, K. M. Maloney, C. T. Chen, F. H. Arnold, *Journal of the American Chemical Society* **1997**, *119*, 2479.

[15]   X. D. Song, J. Nolan, B. I. Swanson, *Journal of the American Chemical Society* **1998**, *120*, 4873.

[16]   D. Y. Sasaki, T. A. Waggoner, J. A. Last, T. M. Alam, *Langmuir* **2002**, *18*, 3714.

[17]   S. Kolusheva, T. Shahal, R. Jelinek, *Journal of the American Chemical Society* **2000**, *122*, 776.

[18]   J. J. Pan, D. Charych, *Langmuir* **1997**, *13*, 1365.

[19] S. Y. Okada, R. Jelinek, D. Charych, *Angew. Chem. Int. Ed.* **1999**, *38*, 655.

[20] S.-i. Kugimiya, T. Lazrak, M. Blanchard-Desce, J.-M. Lehn, *Chemical Communications* **1991**, 1179.

[21] P. Barton, C. A. Hunter, T. J. Potter, S. J. Webb, N. H. Williams, *Angew. Chem. Int. Ed.* **2002**, *41*, 3878.

[22] G. O. Bizzigotti, *J. Org. Chem.* **1983**, *48*, 2598.

[23] R. A. Moss, T. F. Hendrickson, G. O. Bizzigotti, *Journal of the American Chemical Society* **1986**, *108*, 5520.

[24] R. A. Moss, S. Swarup, *J. Org. Chem.* **1988**, *53*, 5860.

[25] L. Garcia-Rio, P. Herves, J. C. Mejuto, J. Perez-Juste, P. Rodriguez-Dafonte, *New Journal of Chemistry* **2003**, *27*, 372.

[26] J. H. Fendler, W. L. Hinze, *Journal of the American Chemical Society* **1981**, *103*, 5439.

[27] C. Matos, H. Chaimovich, J. Lima, I. M. Cuccovia, S. Reis, *Journal of Pharmaceutical Sciences* **2001**, *90*, 298.

[28] I. M. Cuccovia, F. H. Quina, H. Chaimovich, *Tetrahedron* **1982**, *38*, 917.

[29] M. K. Kawamuro, H. Chaimovich, E. B. Abuin, E. A. Lissi, I. M. Cuccovia, *Journal of Physical Chemistry* **1991**, *95*, 1458.

[30] T. Kunitake, T. Sakamoto, *Journal of the American Chemical Association* **1978**, *100*, 4615.

[31] F. M. Menger, V. A. Azov, *Journal of the American Chemical Society* **2000**, *122*, 6492.

[32] F. M. Menger, K. D. Gabrielson, *Angewandte Chemie International Edition* **1995**, *34*, 2091.

[33] F. M. Menger, S. J. Lee, *Langmuir* **1995**, *11*, 3685.

[34] F. M. Menger, K. D. Gabrielson, *Journal of the American Chemical Society* **1994**, *116*, 1567.

[35] F. M. Menger, N. Balachander, *Journal of the American Chemical Society* **1992**, *114*, 5862.

[36] F. M. Menger, M. I. Angelova, *Accounts of Chemical Research* **1998**, *31*, 789.

[37] F. M. Menger, J. S. Keiper, *Current Opinion in Chemical Biology* **1998**, *2*, 726.

[38]   L. A. M. Rupert, D. Hoekstra, J. Engberts, *Journal of the American Chemical Society* **1985**, *107*, 2628.

[39]   F. M. Menger, K. Gabrielson, *Journal of the American Chemical Society* **1994**, *116*, 1567.

[40]   T. Oberholzer, M. Albrizio, P. L. Luisi, *Chemistry and Biology* **1995**, *2*, 677.

[41]   A. Fischer, A. Franco, T. Oberholzer, *Chembiochem* **2002**, *3*, 409.

[42]   T. Oberholzer, K. H. Nierhaus, P. L. Luisi, *Biochemical and Biophysical Research Communications* **1999**, *261*, 238.

[43]   W. Yu, K. Sato, M. Wakabayashi, T. Nakaishi, E. P. Ko-Mitamura, Y. Shima, I. Urabe, T. Yomo, *Journal of Bioscience and Bioengineering* **2001**, *92*, 590.

[44]   V. Marchi-Artzner, L. Jullien, T. Gulik-Krzywicki, J.-M. Lehn, *Chemical Communications* **1997**, 117.

[45]   V. Marchi-Artzner, T. Gulik-Krzywicki, M.-A. Guedeau-Boudeville, C. Gosse, J. M. Sanderson, J.-C. Dedieu, J.-M. Lehn, *ChemPhysChem* **2001**, *2*, 367.

[46]   S. Chiruvolu, S. Walker, J. Israelachvili, F. Schmitt, D. Leckband, J. Zasadzinski, *Science* **1994**, *264*, 1753.

[47]   Z. Sideratou, D. Tsiourvas, C. M. Paleos, A. Tsortos, G. Nounesis, *Langmuir* **2000**, *16*, 9186.

[48]   E. C. Constable, W. Meier, C. Nardin, S. Mundwiler, *Chem. Comm.* **1999**, 1483.

[49]   V. Marchi-Artzner, L. Jullien, L. Belloni, D. Raison, L. Lacombe, J.-M. Lehn, *Journal of Physical Chemistry* **1996**, *100*, 13844.

[50]   F. M. Menger, J. S. Keiper, S. J. Lee, *Langmuir* **1997**, *13*, 4614.

[51]   G. Battaglia, A. J. Ryan, S. Tomas, *Langmuir* **2006**, *22*, 4910.

[52]   L. E. Overman, D. Matzinger, E. M. Oconnor, J. D. Overman, *Journal of the American Chemical Society* **1974**, *96*, 6081.

[53]   G. J. Bridgart, M. W. Fuller, I. R. Wilson, *Journal of the Chemical Society-Dalton Transactions* **1973**, 1274.

[54]   G. J. Bridgart, I. R. Wilson, *Journal of the Chemical Society-Dalton Transactions* **1973**, 1281.

[55]   R. C. Kapoor, R. K. Chohan, B. P. Sinha, *Journal of Physical Chemistry* **1971**, *75*, 2036.

[56]   R. C. Kapoor, Kachhwah.Op, B. P. Sinha, *Journal of Physical Chemistry* **1969**, *73*, 1627.

[57]   E. J. Meehan, I. M. Kolthoff, H. Kakiuchi, *Journal of Physical Chemistry* **1962**, *66*, 1238.

[58]   G. Stochel, P. Martinez, R. Vaneldik, *Journal of Inorganic Biochemistry* **1994**, *54*, 131.

[59]   D. M. E. Reuben, T. C. Bruice, *Journal of the Chemical Society-Chemical Communications* **1974**, 113.

[60]   H. M. S. Patel, D. L. H. Williams, *Journal of the Chemical Society. Perkin Transactions 2* **1990**, 37.

[61]   G. M. Whitesides, J. Houk, M. A. K. Patterson, *J. Org. Chem.* **1983**, *48*, 112.

[62]   J. L. Kice, G. E. Ekman, *J. Org. Chem.* **1975**, *40*, 711.

[63]   Y. H. Khim, L. Field, *J. Org. Chem.* **1972**, *37*, 2714.

[64]   M. Narisada, Y. Terui, M. Yamakawa, F. Watanabe, M. Ohtani, H. Miyazaki, *J. Org. Chem.* **1985**, *50*, 2794.

[65]   P. A. Fernandes, M. J. Ramos, *Chemistry-a European Journal* **2004**, *10*, 257.

[66]   G. M. Whitesides, J. E. Lilburn, R. P. Szajewski, *J. Org. Chem.* **1977**, *42*, 332.

[67]   D. J. Hupe, D. Wu, *J. Org. Chem.* **1980**, *45*, 3100.

[68]   M. Inagaki, M. Shibakami, S. L. Regen, *Journal of the American Chemical Society* **1997**, *119*, 7161.

[69]   S. M. Krisovitch, S. L. Regen, *Journal of the American Chemical Society* **1993**, *115*, 1198.

[70]   M. Shibakami, M. Inagaki, S. L. Regen, *Journal of the American Chemical Society* **1997**, *119*, 12354.

[71]   M. Shibakami, M. Inagaki, S. L. Regen, *Journal of the American Chemical Society* **1998**, *120*, 3758.

[72]   S. J. Vigmond, T. Dewa, S. L. Regen, *Journal of the American Chemical Society* **1995**, *117*, 7838.

[73]   M. Uragami, T. Dewa, M. Inagaki, R. A. Hendel, S. L. Regen, *Journal of the American Chemical Society* **1997**, *119*, 3797.

[74] F. M. Menger, K. L. Caran, V. A. Seredyuk, *Angew. Chem. Int. Ed.* **2001**, *40*, 3905.

[75] F. M. Menger, H. L. Zhang, *Journal of the American Chemical Society* **2006**, *128*, 1414.

[76] F. M. Menger, V. A. Seredyuk, *Journal of the American Chemical Society* **2003**, *125*, 11800.

[77] F. M. Menger, V. A. Seredyuk, A. A. Yaroslavov, *Angew. Chem. Int. Ed.* **2002**, *41*, 1350.

[78] T. J. Potter, University of Sheffield (Sheffield), **2002**.

[79] D. L. Crankshaw, L. I. Berkeley, J. F. Cohen, F. N. Shirota, H. T. Nagasawa, *Journal of Biochemical and Molecular Toxicology* **2002**, *16*, 235.

[80] A. Nadel, J. Palinkas, *J. Heterocycl. Chem.* **2000**, *37*, 1463.

[81] I. Lingard, G. Bhalay, M. Bradley, *Synlett* **2003**, *12*, 1791.

[82] D. J. Shaw, *Introduction to Colloid and Surface Chemistry*, 4th ed., Butterworth-Heinemann, **1992**.

Appendix

Estimation of the second order rate constant for reactions with low interactions between reactants.

The equation used to fit the data obtained is the following with A and B the two reactants, B being in excess:

$$k_{obs} = \frac{k \times [B]}{K + [B]}$$

In order to compare the rate constants of reactions with low interactions between reactants with the other ones, the rate constant for low interaction reactions was estimated as k/K. It is the value of the derivative of k_{obs} against the concentration of B at [B] equals zero. This corresponds to the hypothetic situation where no low interaction would occur due to the fact that no reactant B is in solution.

The derivation is as follows:

$$\frac{dk_{obs}}{d[B]} = \frac{d\left(\frac{k \times [B]}{K + [B]}\right)}{d[B]}$$

$$\frac{d\left(\frac{k \times [B]}{K + [B]}\right)}{d[B]} = \frac{k}{K + [B]} - \frac{k \times [B]}{(K + [B])^2}$$

$$\frac{k}{K + [B]} - \frac{k \times [B]}{(K + [B])^2} = \frac{k \times (K + [B]) - k \times [B]}{(K + [B])^2}$$

$$\frac{k \times (K + [B]) - k \times [B]}{(K + [B])^2} = \frac{k \times K}{(K + [B])^2}$$

Therefore at [B]=0, $\left(\dfrac{dk_{obs}}{d[B]}\right)_0 = \dfrac{k}{K}$.

Estimation of the error of the second order rate constant for reactions with low interactions between reactants.

In order to evaluate the error of k/K, i.e. the second order rate, as shown in chapter 3 for the rates of reaction where the equation similar to the Michaelis-Menten equation is used to characterise some reactions, the following method was used.

Using Δk and ΔK represents the error in each value, the error of k/K was calculated by

$$\left(\sqrt{\left(\frac{\Delta k}{k}\right)^2 + \left(\frac{\Delta K}{K}\right)^2}\right) \times \frac{k}{K}.$$